ISSN 0917-1185

ANNUAL REPORT OF NATIONAL INSTITUTE FOR FUSION SCIENCE

April 2018 – March 2019

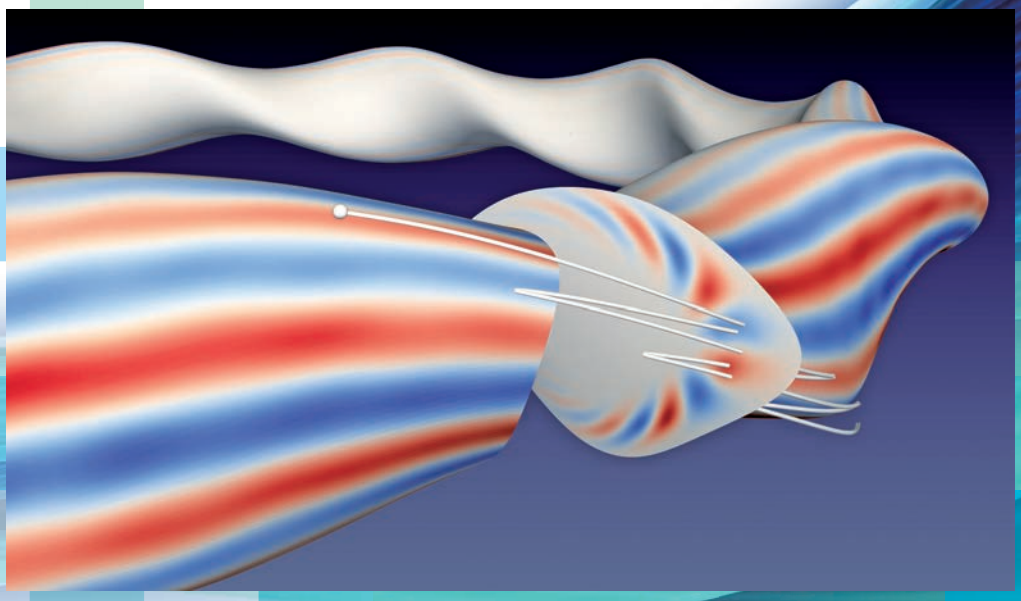

NATIONAL INSTITUTE FOR FUSION SCIENCE
TOKI CITY, JAPAN

Front Cover Caption: Fluctuations of electron pressure due to a ballooning mode and orbits of trapped ions in LHD.

Printer: Arakawa Printing Co., Ltd.
2-16-38 Chiyoa, Naka-ku, Nagoya-shi 460-0012, JAPAN
Phone: +81-52-262-1006, Facsimile: +81-52-262-2296

Printed in Japan, ISSN 0917-1185

ANNUAL REPORT OF NATIONAL INSTITUTE FOR FUSION SCIENCE

April 2018 – March 2019

December 2019

Inter-University Research Institute Corporation
National Institutes of Natural Sciences

NATIONAL INSTITUTE FOR FUSION SCIENCE

Address : Oroshi-cho, Toki-shi, Gifu-ken 509-5292, JAPAN
Phone : +81-572-58-2222
Facsimile : +81-572-58-2601
Homepage on internet : URL = http://www.nifs.ac.jp/

Contents

National Institute for Fusion Science
April 2018 – March 2019

The most inevitable issue for mankind in this century is energy security. Energy resources alternative to fossil fuels are indispensable for a sustainable society, since there is expanding demand for energy on a global scale due to the explosive population growth and economic development concentrated in developing countries. In addition, the increase in greenhouse gases such as carbon dioxide due to the continued use of fossil fuels and the depletion of fuel resources will become serious issues.

The realization of nuclear fusion energy can resolve the serious environmental and energy crisis which humans are now facing. The fuels for fusion can be obtained from seawater, therefore fusion energy is virtually inexhaustible. Furthermore, the fusion reaction does not emit carbon dioxide, thus fusion energy can be the ultimate clean energy. Fusion research around the world has progressed year by year based on the steady progress of basic science and advanced technology. On the other hand, critical scientific and technological issues which must be resolved to put this energy resource in our hands remain.

In order to promote the scientific and engineering research towards the realization of fusion energy, National Institute for Fusion Science (NIFS) conducts three major projects, the Large Helical Device (LHD) Project, the Numerical Simulation Reactor Research Project and the Fusion Engineering Research Project. These three pillars collaborate and stimulate each other to contribute to the progress of the comprehensive fusion science. In addition to the three major projects mentioned above, NIFS also supports interdisciplinary and basic research, and promotes the coordinated research for ITER-BA cooperation, laser cooperation and academic-industrial cooperation.

This annual report summarizes achievements of research activities concerning the fusion research at NIFS from April 2018 to March 2019. NIFS is an inter-university research organization which conducts collaboration research programs under three frameworks, i.e., General Collaboration Research, LHD Collaboration Research and Bilateral Collaboration Research. More than 500 collaborating research topics were proposed by collaborators in universities or institutes across the country. Proposals from abroad were also included.

Finally, I would like to emphasize one more important role of NIFS, the development of human resources. NIFS is pouring energy into education for graduate students who will realize fusion power generation and our society. For this purpose, NIFS provides the advanced education system through the Graduate University for Advanced Studies (Sokendai). Educational collaboration with partner universities across the nation is also conducted by accepting their graduate students to NIFS.

Yasuhiko Takeiri
Director-General
National Institute for Fusion Science

1. Large Helical Device (LHD) Project

The Large Helical Device (LHD) project conducts fusion-grade confinement research in a steady-state machine to elucidate important research issues in physics and engineering for the helical-type fusion reactor.

The LHD is one of the largest helical devices, with major and averaged minor radii of 3.6 – 4.0 m and 0.6 m, respectively. A double helical coil and three pairs of poloidal coils are all superconducting, by which maximum magnetic field strength at the plasma center is 3 T. For plasma heating, three negative-ion-based 180 – 190 keV neutral beams with total heating power of 8 – 16 MW are injected tangentially to the plasma.

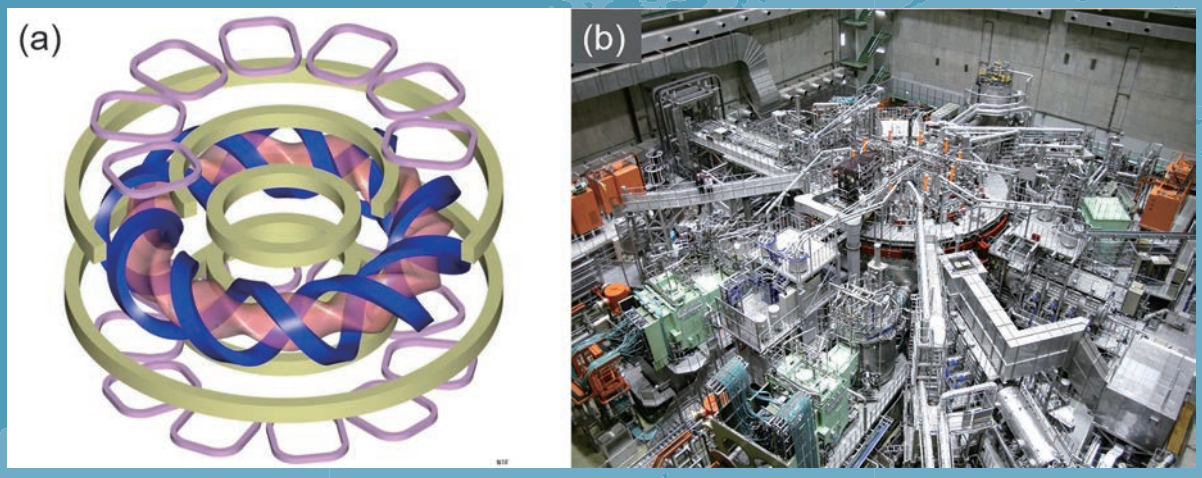

Fig. 1 (a) Coil configuration of LHD. Superconducting helical coils (blue), poloidal coils (yellow) and normal conducting RMP coils, together with plasma. (b) LHD torus hall.

Two positive-ion-based 40 – 80 keV neutral beams with total heating power of 6 – 18 MW are also injected perpendicular to the plasma. In addition, electron cyclotron resonance heating with total heating power of ~ 5.5 MW is also available. For fuelling, LHD is equipped with four gas puff valves and two pellet injectors.

Since 2017, LHD has performed the deuterium experiment in which plasma is expected to improve its performance, thanks to the "isotope effect". Achieved plasma parameters to date are summarized in Table 1.

Table 1 Achieved plasma parameters (1998 – 2017).

Parameters	Achieved	Key physics	Target
T_i	10 keV ($n_e = 1.3\times10^{19}$ m^{-3})	Ion ITB Impurity hole	10 keV ($n_e = 2\times10^{19}$m^{-3})
T_e	20 keV (2×10^{18} m^{-3}) 10 keV (1.6×10^{19} m^{-3})	Electron ITB	10 keV (2×10^{19}m^{-3})
Density	1.2×10^{21}m^{-3} ($T_e = 0.25$ keV)	Super dense core	4×10^{20} m^{-3} ($T_e = 1.3$ keV)
β	5.1 % ($B_T = 0.425$ T) 4.1 % (1 T)	MHD in current-free plasmas	5 % ($B_T = 1$ - 2 T)
Steady-state operation	54min. 28sec (0.5MW, 1keV, 4×10^{18}m^{-3}) 47min. 39sec. (1.2MW, 2keV, 1×10^{19}m^{-3})	Dynamic wall retention	1 hour (3 MW)

(T. Morisaki)

High Performance Plasma

Highlight

The isotope effect of ion thermal confinement of high ion temperature plasmas with ion internal transport barrier was investigated, and the study on energetic particles progressed.

A remarkable extension of high-ion-temperature regime was obtained in deuterium (D) plasma experiments in the LHD [1]. The dependence of the ion heat diffusivity on temperature ratio T_e/T_i and the inverse of the normalized scale length of the ion temperature gradient R/L_{Ti} was investigated in the core region [2], where the gyrokinetic simulations using GKV code predict the destabilization of ion temperature gradient (ITG) modes [3]. The T_e/T_i dependence shows ITG-like property, while a significant deviation from the ITG-like property is found in the R/L_{Ti} dependence as shown in Fig. 1. The ion heat diffusivity normalized by gyroBohm factor tended to decrease with increasing R/L_{Ti}. This indicates the suppression of ITG mode in large R/L_{Ti} regime and results in the formation of the ion internal transport barrier (ITB). In the comparison between D and hydrogen (H) plasmas, the lower transport in D plasmas were observed in both ion and electron heat diffusivities, indicating significant isotope effect. It was found with the nonlinear turbulent transport simulation with GKV that the zonal flow enhancement contributes to the ITG suppression in the D plasmas.

Research on energetic particle (EP) confinement has advanced using comprehensive neutron diagnostics prepared for D operation of the LHD plasma [4]. The fusion gain Q_{DD} is evaluated to be 4.0×10^{-4} in the N-NB-heated D plasma, which is comparable with Q_{DD} obtained in large tokamaks with similar heating power. The ratio of Q_{DT}/Q_{DD} is evaluated by means of the FBURN code [5] using the experimental data. We achieved the equivalent Q_{DT} of 0.11.

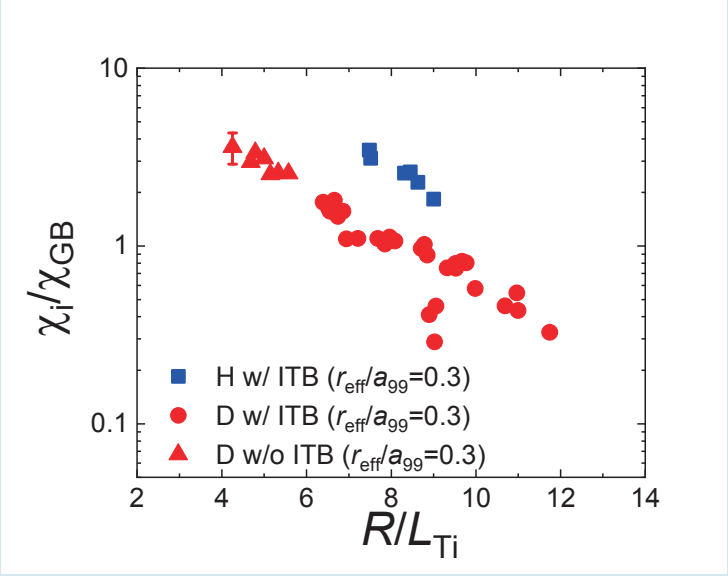

Fig. 1 The ion heat diffusivity normalized by gyroBohm factor as a function of temperature normalized ion temperature gradient at $r_{eff}/a_{99} = 0.3$ [2].

Transport characteristics of D and H plasmas with ion internal transport barrier in the LHD

The D plasma experiments were started in the 19th experimental campaign in 2017. The isotope effects in the core of high-ion-temperature plasma have been investigated in this study. In order to minimize the multi-ion-species effects on ion heat transport, the H and the D plasmas with high-ion-purity were produced and analyzed in this study. The purity of the ion species is over 80% for both plasmas: $n_D/n_e > 0.8$ or $n_H/n_e > 0.8$. The effective charge Z_{eff} was less than 2 in the core region due to the formation of impurity hole. The plasmas were heated with NBIs. The D beams were injected to the D plasmas and the H beams were injected to the H plasmas. The dominant instability in the core region of the high-T_i plasmas is ITG mode [6]. The ITG mode is mainly characterized with R/L_{Ti} and T_e/T_i. The ion heat diffusivity normalized by gyroBohm factor χ_i/χ_{GB} was found to be increased with the temperature ratio. The dependence is consistent with the ITG nature. On the other hand, the χ_i/χ_{GB} decreases with R/L_{Ti} as shown in Fig. 1. This is the opposite tendency to the ITG nature and the transport improves with increase of R/L_{Ti}. The ion ITB formation is attributable to the transport improvement with the breaking of R/L_{Ti} dependence of ITG mode. The difference of transport levels between H and D plasmas can also be seen, although the dependence on R/L_{Ti} was similar between them. This observation suggests that the mechanism of transport improvement is related to some parameters depending on ion mass. The difference in the Larmor radius between H and D might provide an explanation of the experimental observation.

The nonlinear turbulent transport simulations using the GKV code [7] were conducted in order to discuss physical mechanisms of the isotope effect observed in the experiment. The calculation showed the destabilization of the ITG mode in the plasma core both in the H and D plasmas. Figure 2 shows the time evolution of the normalized heat diffusivity at the half minor radius. The turbulent transport was saturated after growth of zonal flow. The saturation level of the turbulent transport in the H plasma is higher than that of the experimental value ($\chi_i/\chi_{GB,H}$ ~10). When the temperature gradient was artificially reduced by 20% in the simulation, the turbulent transport level became almost the experimental value as the dashed line showed in Fig. 2 (a), indicating that the turbulent transport simulation reproduced the ion heat diffusivity within 20% variations from the nominal value of experimentally observed ion temperature gradient. In the estimation of experimental heat diffusivities, the uncertainty is 25% at maximum, which is mainly due to an evaluation of the temperature gradient and the heating power calculations. The simulation also reproduced ion and electron heat

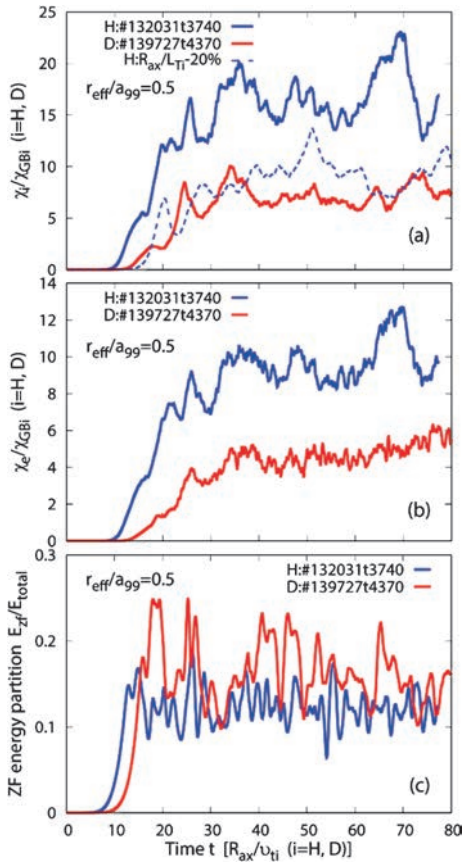

Fig. 2 Gyrokinetic simulation results of (a) normalized χ_i, (b) normalized χ_e, and (c) kinetic energy partition of zonal flow [2].

diffusivities that decreased in the D plasma. The zonal flow energy partition was higher in the D plasma, which indicates the ion mass impact on the zonal flow generation related to the transport suppression [8].

Study of energetic ion confinement by means of comprehensive neutron diagnostics

In the LHD plasma discharge with NB injection, neutrons are mainly created by beam-thermal reactions. Therefore, by using neutron diagnostics, we can obtain information of beam ions confined in the plasma. In order to understand the global confinement of beam ions, total neutron emission rate S_n is measured in plasmas with changing the magnetic axis position [4]. The line-averaged electron density n_{e_avg} dependence of S_n are surveyed in R_{ax} of 3.55 m, 3.60 m, 3.80 m, and 3.90 m (Fig. 3). The peak of S_n is seen at n_{e_avg} of 2×10^{19}-3×10^{19} m^{-3}. In outward shifted configurations, S_n is smaller by almost one order than S_n of the inward shifted configurations in the same density. One of the main reasons of lower S_n in outward shifted configuration is that the electron

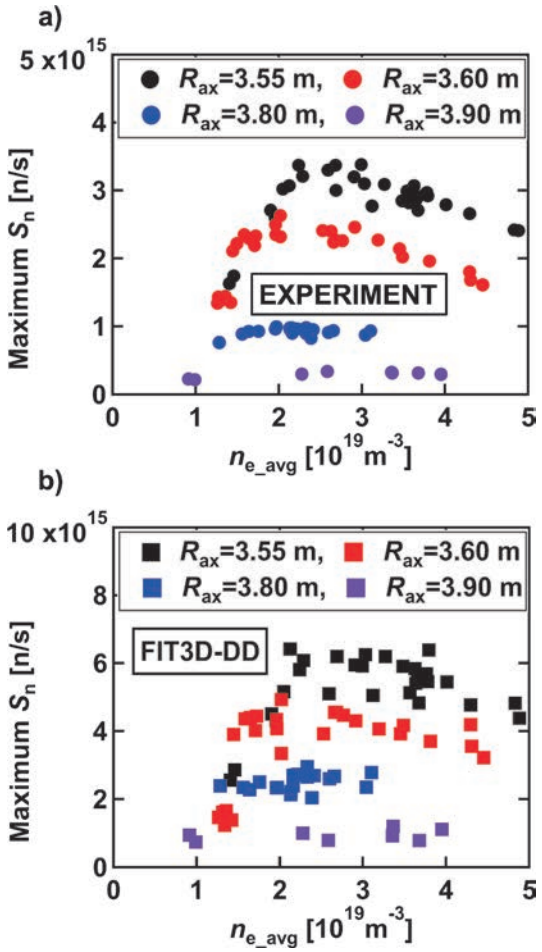

Fig. 3 The plot of the maximum S_n in one discharge as a function of n_{e_avg} in experiment (a), and FIT3D-DD code (b) [4].

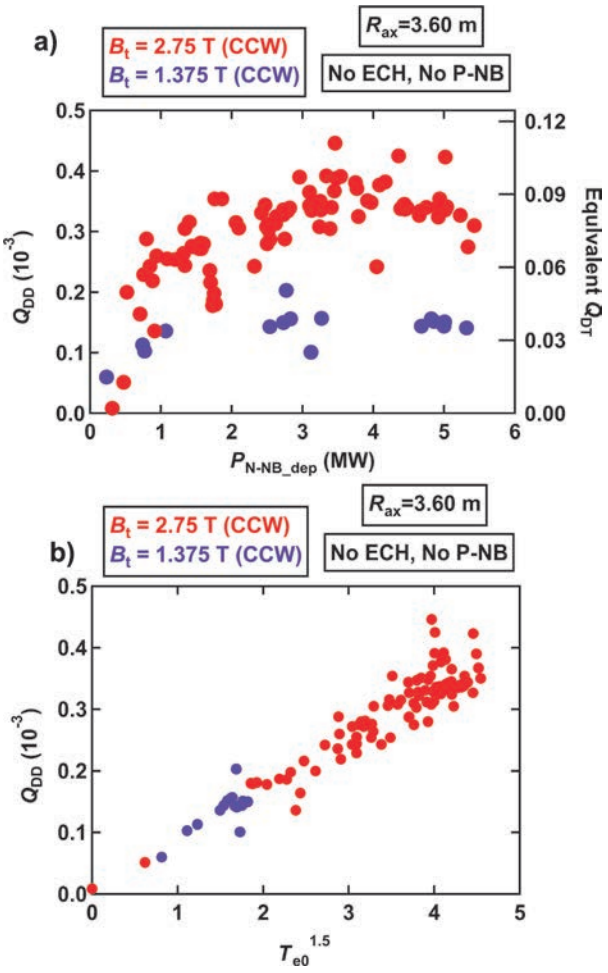

Fig. 4 (a) Q_{DD} as a function of the $P_{N\text{-}NB\_dep}$. Here, the ratio of Q_{DT}/Q_{DD} is based on FBURN calculation. (b) Relation between Q_{DD} and $T_{e0}^{1.5}$ [4].

temperature tends to be lower in the LHD plasmas with outward shift of R_{ax} which induces the shorter beam ion slowing down time. We compare experimentally obtained S_n with S_n calculated by the FIT3D-DD code which is a part of TASK3D code [9]. In FIT3D-DD code, we assumed a pure D plasma and the orbital effect of fast ion in the short time (0.1 ms) is considered. The calculated S_n dependence on n_{e_avg} shows that S_n increases with the electron density in n_{e_avg} less than 2×10^{19} m^{-3}, then has a peak at n_{e_avg} around 2×10^{19} m^{-3} to 3×10^{19} m^{-3}, and then decreases with the electron density in n_{e_avg} greater than 3×10^{19} m^{-3} as obtained in experiments. The absolute value of S_n calculated by FIT3D-DD is almost two times higher than the absolute value of S_n. The main reason of disagreement regarding absolute value may be due to the effect of the effective charge.

The NB deposition power dependence of fusion gain is surveyed in R_{ax} = 3.6 m configuration. Note that the fusion gain Q_{DD} is defined as (fusion output)/(total heating power). Here, in D plasma, the fusion output of each reaction is 7.25 MeV. We evaluate Q_{DD} in D plasma heated only by N-NB (Fig. 4). As expected, Q_{DD} in the normal B_t case is higher than Q_{DD} in the half B_t case. Gradual increase of Q_{DD} with the increase of $P_{N\text{-}NB\_dep}$ is obtained with $P_{N\text{-}NB\_dep}$ of up to 3 MW, and then Q_{DD} is almost saturated. One-dimensional neutron emission calculation code FBURN [5] is used in order to evaluate the equivalent fusion gain in DT plasma Q_{DT}. The ratio of Q_{DT}/Q_{DD} is evaluated to be 249 in triton plasma with D beam injection, which is almost the same value calculated in TFTR [10]. We achieve equivalent Q_{DT} of 0.11 which is almost the same with large tokamaks with 5 MW NB injections [10,11]. A linear increase of Q_{DD} with $T_{e0}{}^{1.5}$ is obtained in those experiments (Fig. 4 (b)). The dependence is found if neutrons are mainly created by beam-plasma reactions. When neutrons are mainly created by a beam-plasma reaction, Q_{DD} is approximately described as $Q_{DD} \sim n_i \times P_{NB} \times \tau_s / P_{NB} \sim T_{e0}{}^{1.5}$.

[1] H. Takahashi *et al*., Nucl. Fusion **58**, 106028 (2018).
[2] K. Nagaoka *et al*., Nucl. Fusion **59**, 106002 (2019).
[3] M. Nakata *et al*., Plasma Phys. Control. Fusion **58**, 074008 (2016).
[4] K. Ogawa *et al*., Nucl. Fusion **59**, 076017 (2019).
[5] K. Ogawa *et al*., Plasma Phys. Control. Fusion **60**, 095010 (2018).
[6] M. Nakata *et al*., Plasma Phys. Control. Fusion **61**, 014016 (2019).
[7] T.-H. Watanabe and H. Sugama, Nucl. Fusion **46**, 24 (2006).
[8] M. Nakata *et al*., Phys. Rev. Lett. **118**, 165002 (2017).
[9] S. Murakami *et al*., Trans. Fusion Technol. **27**, 256 (1995).
[10] D.L. Jassby *et al*., Phys. Fluids B **3**, 2308 (1991).
[11] M. Keilhacker and the JET Team, Phys. Fluids B **2**, 1291 (1990).

(K. Nagaoka, K. Ogawa and H. Takahashi)

Transport and Confinement

Highlight

Isotope effects on turbulence in ECRH plasma of LHD

The turbulence is a key player in the isotope effects of transport. Experiments were performed to compare the difference of turbulence characteristic in H and D plasma in 20th LHD experimental campaign under almost identical condition of ECRH plasma. The turbulence was measured by two dimensional phase contrast imaging [1]. Figure 1 shows the comparison [2]. The comparison of three density regimes (low (1×10^{19} m^{-3}), middle (1.8×10^{19} m^{-3}) and high (3×10^{19} m^{-3}) density regime) are shown. The line averaged density was adjusted as shown Fig. 1 (a-1), (b-1) and (c-1). The heating was 2 MW 154 GHz 2nd harmonic heating. The difference of the deposition power is less than 10%. More than 88% of injection power was absorbed at $\rho < 0.3$. Fig. 1 (a-4), (b-4) and (c-4) shows comparison of central electron and ion temperature. The central electron temperature is comparable in low and middle density regime, while it is clearly higher in high density regime. On the other hand, central ion temperature is almost the same at whole density regime. The scaling study showed that the global energy confinement time was 16% better in D plasma than in H plasma for the same line averaged density and deposition power of ECRH [1]. However, As shown in Fig. 1 (a-4), (b-4) and (c-4), the better confinement improvement is more evident at higher density regime. Figs. 1 (b) shows line integrated fluctuation amplitude from 20~200 kHz components. These are mainly come from core region at $\rho <\sim 0.8$. Figs.1 (c) shows line integrated fluctuation amplitude at 200~500 kHz components. These are mainly come from edge region at $\rho >\sim 0.8$. In low and middle density regime, core fluctuation from 20~200 kHz is higher in D plasma. However, in high density regime, core fluctuation becomes clearly lower in D plasma. The edge fluctuation from 200~500 kHz shows lower fluctuation in D plasma at all density regime, however, the difference is clearer in higher density regime. Observed lower fluctuation amplitude in D plasma possibly play a role in the better confinement in D plasma. Gyrokinetic linear analyses showed that the dominant instability was ion temperature gradient mode (ITG) at $\rho = 0.7$ [3]. The growth rate was lower in D plasma. The hollowed density gradient stabilize ITG [4]. The density profiles are hollower in D plasma [2]. The hollower density profiles in D plasma is one of the possible mechanism for the better confinement in high density regime of ECRH plasma in LHD.

[1] K, Tanaka *et al.*, Rev. Sci. Instrum. **79**, 10E702 (2008).
[2] K, Tanaka *et al.*, to be submitted Nucl. Fusion.
[3] K. Tanaka *et al.*, to be presented at EPS 2019 invited talk.
[4] M. Nakata *et al.*, Plasma Phys. Ctrl. Fusion **61**, 014016 (2019).

(K. Tanaka)

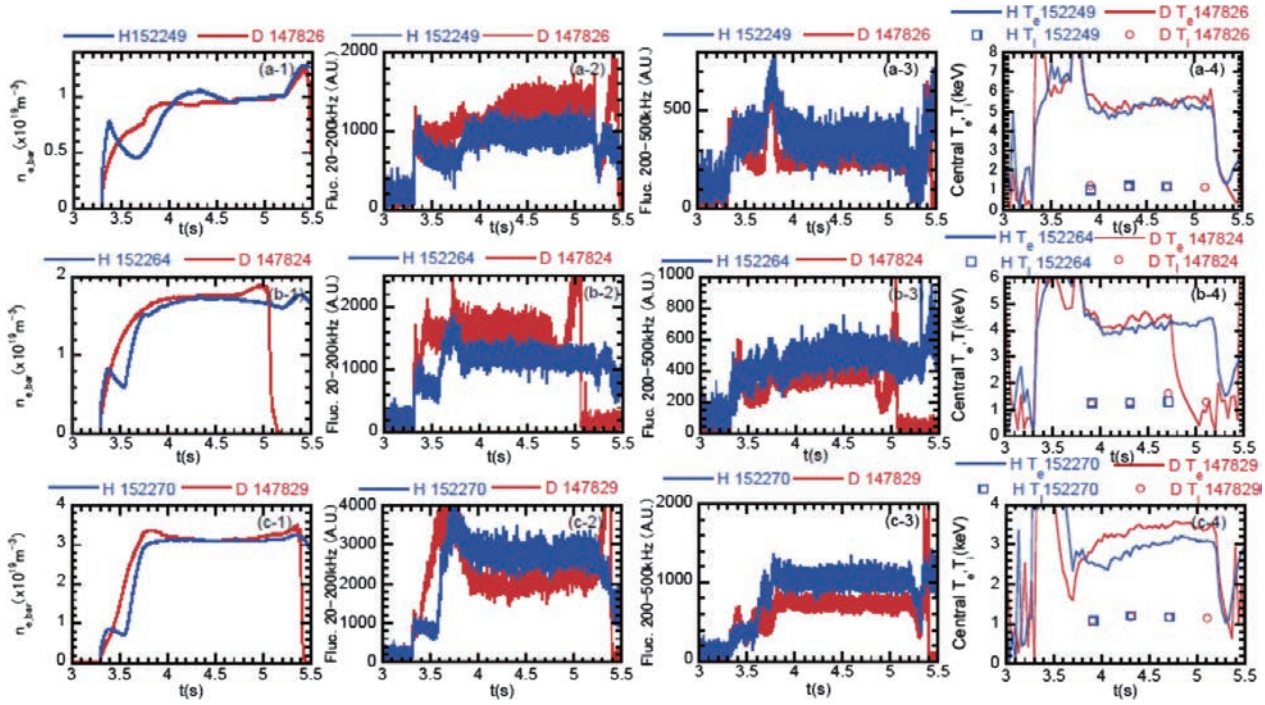

Fig. 1 Comparison of time trace in (a) low, (b) middle and (c) high density.
(a-1),(b-1),(c-1); line averaged density, (a-2),(b-2),(c-2); line integrated fluctuation amplitude for 20–200 kHz by 2D-PCI, (a-3),(b-3),(c-3); line integrated fluctuation amplitude for 200–500 kHz by 2D-PCI, (a-4),(b-4),(c-4); central electron and ion temperature at ρ = 0~0.2 measured by Thomson scattering and CXRS

Real-time injection control of ECH power in LHD

Optimum injection settings of ECH are essential for achieving desired power deposition and reducing the stray radiation level in the vessel. Since the 18th LHD experimental campaign, ray-tracing calculations with the LHDGauss code [1] have been performed on a shot-by-shot basis under the automatic analysis tool AutoAna [2] that have improved heating performance by launcher adjustment during experiments.

In the 20th campaign, we performed real-time deposition location control experiments in order to maintain high absorbed power and on-axis heating during varying electron density. The optimum target settings were calculated in advance using LHDGauss for various electron density profiles. The density profiles are characterized with densities at the magnetic axis, at the last closed flux surface, and at the shoulder for hollow profiles. Then, those parameters were calculated with multi-channel FIR laser interferometer, whose signals were inputted into the newly-developed deposition location control system with real-time FPGA (field programmable gate array) processing [3]. A demonstration was conducted for a density ramp-up case from $1 \times$ to 4×10^{19} m^{-3} as shown in Fig. 1, where the antenna control was started at 3.5 s for comparison with the case without the control. The antenna angles and the resultant target positions successfully followed their command values under the limited

motor rotation speeds. Plasmas were heated and sustained by other ECH. The absorbed power was constant during a relatively low-density case ($< 2.5 \times 10^{19}$ m^{-3}). The high absorbed power was maintained longer in the case with the control than in the case without the control from 5.5 s to 6 s at almost 3×10^{19} m^{-3}. In addition, more center-peaked deposition was maintained longer. On the other hand, no significant difference in the decreased absorbed power between the two cases was observed around 4×10^{19} m^{-3}, which suggests that the multi-pass absorption components are dominant. Pure mode excitation on the refracted wave is needed in order to increase the single-pass absorption. Extension of the high-density operational range and application to long-pulse operations will be future works.

[1] T. Ii Tsujimura *et al.*, Nucl. Fusion **55**, 123019 (2015).
[2] M. Emoto *et al.*, Fusion Eng. Des. **89**, 758 (2014).
[3] T. Ii Tsujimura *et al.*, Fusion Eng. Des. **131**, 130 (2018).

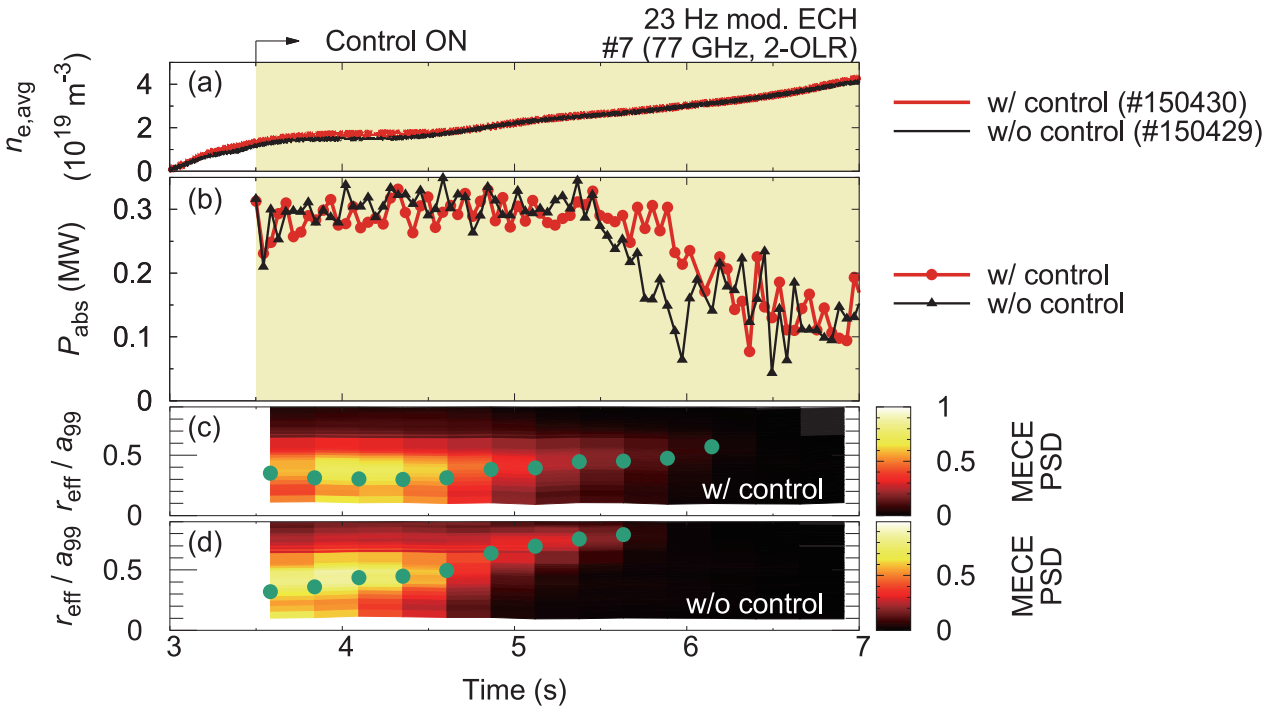

Fig. 1 Time evolution of (a) averaged electron density, (b) absorbed power, and (c)(d) radial profiles of modulation ECE signals on the cases with and without the control.

(T. Ii Tsujimura)

Edge/Device/Atomic and Molecular Processes

Highlight

Divertor tiles made of tungsten coated graphite were installed in an inboard-side divertor

Tungsten (W) is a prime candidate of the plasma facing material in a future fusion reactor. To investigate the effects of divertor tiles made of W on plasma performances, 64 divertor tiles and 30 dome tiles made of W coated graphite were installed in the 9-I closed divertor as shown in Fig. 1. A scanning electron microscopy image of a cross-section of a W coated divertor tile is shown in Fig. 2. On a graphite surface, 10 μm W layer is formed on 2 μm molybdenum (Mo) interlayer which reduce the stress caused by the difference of thermal expansion between W and graphite. Both W and Mo were deposited on graphite tiles by using magnetron-sputtering. During the 20th experimental campaign, clear effects of W released from W coated divertor tiles on the core plasma were not observed clearly by spectroscopic measurements. A filtered CCD camera which observed the 9-I divertor from 9-O port to detect released W atoms also could not observe W clearly. 9-I and other inboard-side divertors were observed by eyes in the LHD vacuum vessel after the end of the 20th campaign. As a result, much smaller amount of flakes which are exfoliated deposition layers are observed at the 9-I divertor than at the other inner divertor. This result is attributed to reduced carbon deposition on the first wall and the dome structure, which are located beside divertor tiles with W coating.

Fig. 1 W coated divertor components

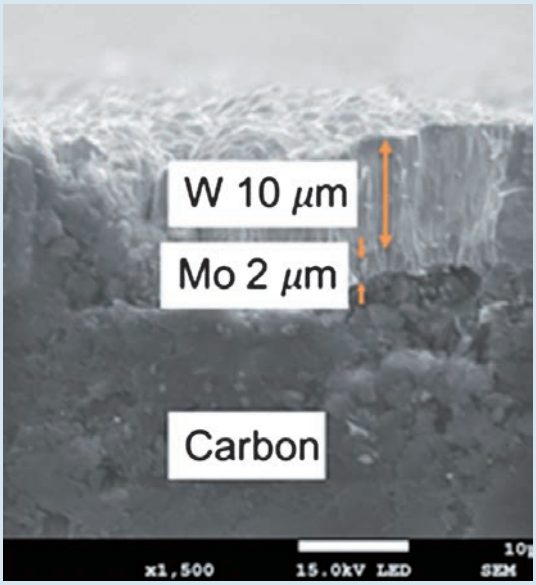

Fig. 2 A cross-section of a W coated divertor tile

(G. Motojima)

New installation of in-vessel Non Evaporable Getter (NEG) pumps for the divertor pump

Non Evaporable Getter (NEG) pumps which use the patented ZAO getter alloy [1] have been installed in the 9-I closed divertor as an in-vessel pump [2] as shown in Fig. 1. Unlike a cryo-pump, the operation temperature of a NEG pump is 100–200°C or higher. The higher operation temperature is an advantage of the NEG pump over a cryo-pump in a vacuum vessel of a fusion experimental device in which plasma facing components have to be tolerant to a plasma radiation and heat loads from heating devices. For the installation in LHD, simulations of the heat load from NEG pumps to the first wall and the conductance of neutral particles towards NEG pumps (Fig. 2) were carried out by using a finite element method based software for multi-physics analysis (ANSYS) and a fully three-dimensional neutral particle transport simulation code EIRENE, respectively. The pumping performance test was conducted in NIFS, and the result shows that the effective pumping speed for hydrogen is 10 m^3/s which is close to the required pumping speed for the in-vessel pump in LHD. In the LHD vacuum vessel, the exposure of the NEG pumps to boronization and glow discharge cleanings have been examined, and no effect of them on the pumping performance have been observed.

[1] F. Sivieroa *et al.*, Fusion Eng. Des., in press.
[2] G. Motojima *et al.*, Fusion Eng. Des. **143**, 226–232 (2019).

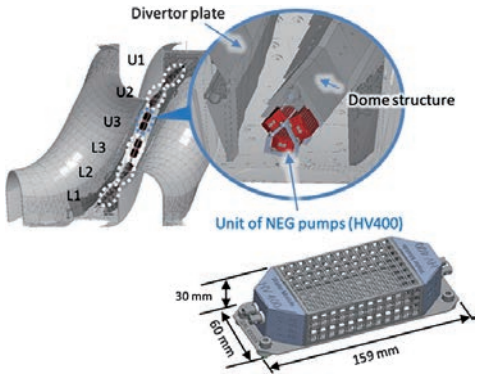

Fig. 1 A NEG pump and the arrangement of NEG pumps in the 9-I closed divertor.

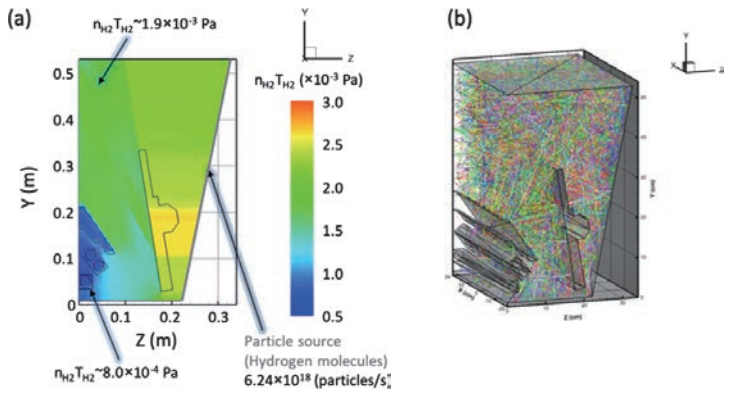

Fig. 2 A result of the simulation using the EIRENE code. (a) A pressure distribution on a cross-section of the closed divertor in which NEG pumps are installed. (b) Trajectories of test particles in the simulation.

(G. Motojima and M. Shoji)

Control of 3D edge radiation structure and compatibility with core plasma performance

The resonant magnetic perturbation (RMP) field has been applied to the LHD plasma, which creates a remnant magnetic island in the edge stochastic layer. The magnetic island is found to affect the edge plasma parameter profiles including impurity radiation. The electron temperature and pressure profiles are flattened at the island. On the other hand, the electron density is slightly peaked at the edge of the island. The impurity radiation profile is estimated assuming non-coronal cooling rate function. The time evolution of the obtained impurity radiation are plotted in Fig.1 (a), together with the magnetic field line connection length (LC) at the edge. It is found that the radiation is enhanced and fixed around the magnetic island during the detached phase, where the discharge is stably sustained with controlled level of radiation [3]. Without RMP (Fig. 1 (b)), the radiation penetrates the confinement region, leading to radiation collapse. In spite of the reduced effective plasma volume caused by the edge magnetic island and by the enhanced radiation there, the central plasma pressure finally exceeds the case without RMP. This is caused by the pressure profile peaking at the central region in the case with RMP, as shown in Fig. 2 [1]. These results indicate clear change of core plasma confinement during the detached phase with RMP.

[1] M. Kobayashi *et al.*, Nuclear Materials and Energy, **17**, 137 (2018).

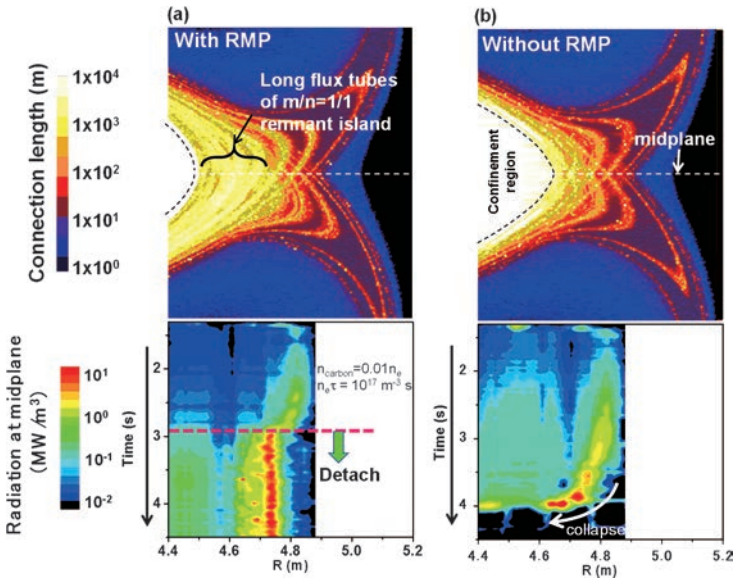

Fig. 1 Upper panels: Connection length (L_C) distributions in the stochastic layer at the outboard side. Lower panels: Temporal evolutions of carbon radiation profiles estimated from T_e and n_e of Thomson measurements, assuming spatially constant carbon concentration of 1% and non-coronal cooling rate ($n_e\tau = 10^{17}$ m^{-3} s). (a) With RMP (#85946), (b) without RMP (#85948). [1]

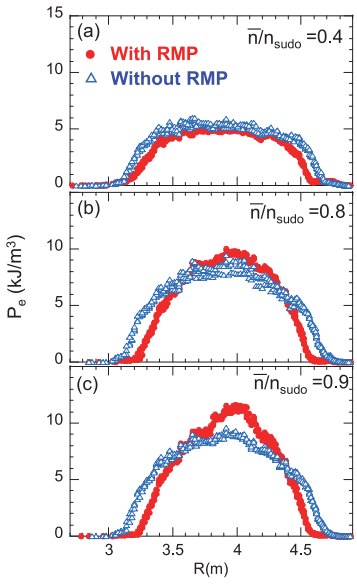

Fig. 2 Radial profiles of electron pressure at $\bar{n}_e/n_{sudo}$ = 0.4, attached, (a), 0.8, detached, (b), and 0.9, detached, (c), respectively. Red: with RMP, blue: without RMP application. [1]

(M. Kobayashi)

High-β/MHD/Energetic Particles

Highlight

Impact of ECH/ECCD on fast-particle-driven MHD instabilities

Fast particle (FP)-driven magnetohydrodynamics (MHD) instabilities enhance anomalous transport and/or induce the loss of fast particle including alpha particles in a fusion reactor. Since redistribution and exhaust of alpha particles lead to reduction of fusion gain Q and damage of first wall, it is required to establish methods of stabilization and/or control of FP-driven MHD instabilities for the fusion reactor, but they have not been established yet. Electron cyclotron heating (ECH)/electron cyclotron current drive (ECCD) are a candidate method to control the FP-driven MHD instabilities because ECH/ECCD may be an ideal tool to control the modes since they can provide highly localized EC waves with a known location and good controllability [1-3]. A linear MHD theory predicts that the changes in electron density and temperature by ECH and in plasma current by ECCD can affect both the growth and damping rates of the FP-driven MHD instabilities.

We have applied ECCD to an NBI plasma on LHD in order to mitigate and eventually suppress the observed FP-driven MHD instabilities. Figure 1 shows clear destabilization and stabilization of GAEs and TAEs with frequency f_{obs} > 100 kHz, and EPMs with f_{obs} < 100 kHz in the LHD plasma with high magnetic shear s when magnetic shear at plasma core is decreased and increased by co- and counter-EC driven plasma current, respectively. The main differences in plasma parameters between both cases are plasma current and magnetic fluctuations. The difference in the amplitude of plasma current can lead to the difference of shear Alfvén continua in whole plasma region. According to reconstructed MHD equilibrium, which qualitatively agrees with the measurement of rotational transform profile by motional stark effect (MSE) diagnostics, co-ECCD and counter-ECCD induced the co and counter plasma current whose profile peaked at plasma core. This increases and decreases the rotational transform, and then magnetic shear will be decreased and increased by co- and counter-ECCD. For co-ECCD, the TAE gap in shear Alfvén continua is aligned from the core toward the edge and many discreate eigenmodes corresponding to TAE and GAE can exist. On the other hand, for counter-ECCD, discrete eigenmodes tend to cross the shear Alfvén continua leading to continuum damping.

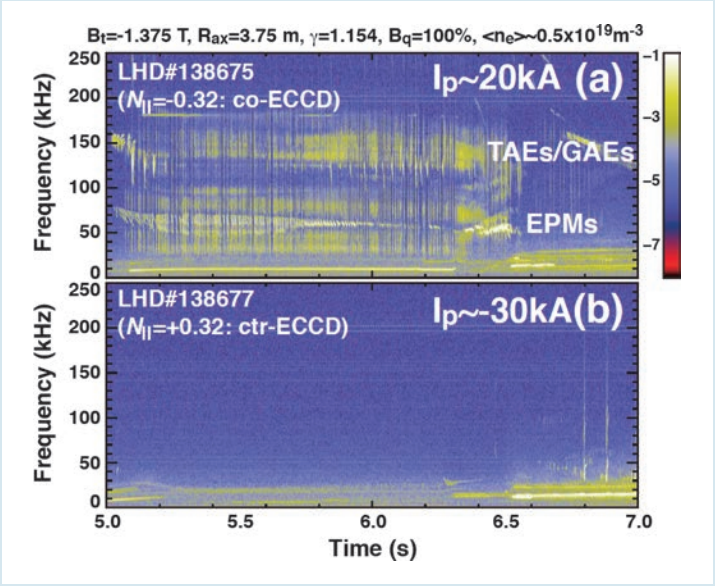

Fig. 1 (a) Destabilization and (b) stabilization of TAEs, GAEs and EPMs due to co- and counter-ECCD in the NBI-heated LHD plasmas. Plasma current is ~20 kA which decreases s in (a) and ~–30 kA which increases s in (b).

[1] K. Nagaoka *et al.*, Nucl. Fusion **53**, 072004 (2013).
[2] K. Nagasaki *et al.*, Nucl. Fusion **53**, 113041 (2013).
[3] S. Yamamoto *et al.*, Nucl. Fusion **57**, 126065 (2017).

(K. Nagaoka)

Suppression of the EIC modes with the m/n = 1/1 RMP

The confinement of energetic particles is essential for the realization of the magnetically confined fusion reactor. Energetic particles are not well confined when the EP driven MHD modes are excited, such as the helically-trapped energetic-particle (EP) driven resistive interchange mode (EIC) [1] observed in LHD. Strategy and the initial results to suppress the EIC mode are presented.

The rotational transform of the LHD device is created by the two helical coils (L=2/M=10). As a consequence, helically twisting region where the magnetic field strength is weak appears. EPs having perpendicular velocity components are trapped in this region and make precession motion helically. The rotation frequency of this precession motion is slow enough to interact with the pressure driven MHD modes.

Two methods to control the EIC have been tested on LHD. One is the ECH application [2]. With the increase of the electron temperature at the mode rational surface, the mode width of the resistive MHD mode becomes narrower. The interaction of the trapped EPs and the MHD mode becomes thereby smaller. This method is quite effective and one of the highest-Ti with high-Te discharge is produced by this method.

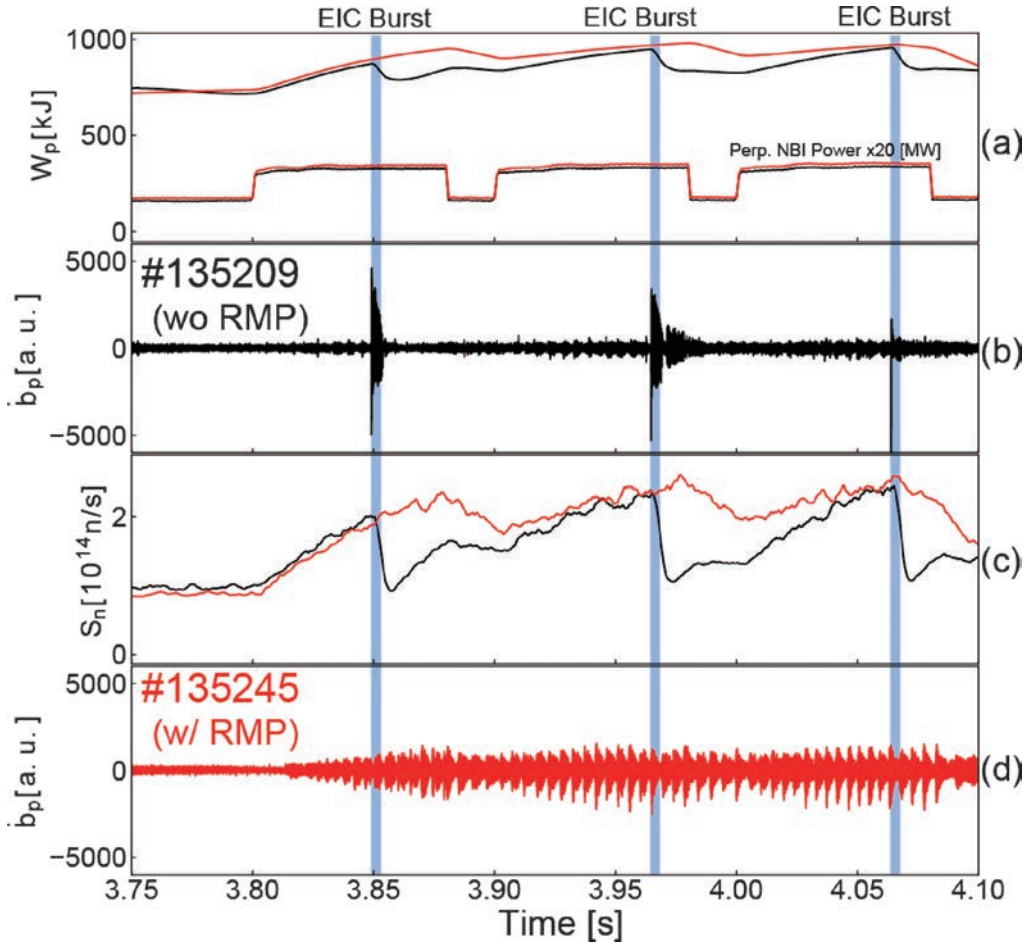

Fig. 2 Comparison of the plasma parameters with (#125245 red lines) and without (#135209 black lines) the RMP field. Heating patterns and the plasma stored energy are shown in (a). The magnetic fluctuations are shown in (b) and (d), and the total neutron emission rate is shown in (c).

Another controlling scheme, resonant magnetic perturbation (RMP) applications is also performed [3]. Bursts of the magnetic fluctuations, which cause the loss of EPs, disappear when the RMP field (m/n = 1/1) is applied as shown in Fig. 2. Small-scaled chirping-up coherent modes remain. However, these magnetic fluctuations do not trigger the bursting EIC modes which cause the EP loss, as shown in the Fig. 2 (c). From the systematic survey of the RMP application in the hydrogen beam experiments, it was found that the EIC bursts completely disappear when the RMP field is sufficiently large. Detailed mechanism of the suppression has not been clarified. However, since the MHD activities having the resonant frequency is reduced with RMP, it is likely EICs are suppressed from the stabilization of the bulk resistive interchange mode by the formation of the magnetic island caused by the RMP.

[1] X. D. Du, *et al.*, Phys. Rev. Lett. **114**, 155003 (2015), Nucl. Fusion **56**, 016002 (2016).
[2] X. D. Du, *et al.*, Phys. Rev. Lett. **118**, 125001 (2017).
[3] S. Ohdachi, *et. al.*, "Excitation mechanism of the energetic particle driven resistive interchange mode and strategy to control the mode in Large Helical Device", in proc. 27th IAEA Fusion Energy Conference, Gandhinagar, India, Oct. 22–27 2019, https://nucleus.iaea.org/sites/fusionportal/Shared%20Documents/FEC%202018/fec2018-preprints/preprint0128.pdf.

(S. Ohdachi)

Study of slowing down mechanism of locked-mode-like instability in helical plasmas

The locked-mode-like instability is one of the MHD instabilities observed in the LHD and it leads to minor collapse after a precursor slows down. In the LHD, there are two types of the locked-mode-like instability categorized by the difference of the radial structure of the precursor. The instability with the odd function type structure is called 'type-I instability' and the instability with even function type structure is called 'type-II instability'. The type-I/II instability is considered to have a large/small magnetic island. The slowing down mechanism of both instabilities, which may be related to the occurrence of minor collapse, has been investigated through the experimental analysis.

Figure 3 (a)–(e) show typical waveforms of a discharge with the type-II instability. In this discharge, the intrinsic error field is almost suppressed. After the precursor with the m/n = 1/1 structure appears at t ~ 3.8 s, the mode frequency f_{mode} and the mode amplitude are almost constant until 4.2 s (constant phase). Then, the f_{mode} gradually decreases and the mode amplitude increases (slowing down phase). Finally, the f_{mode} becomes almost zero at 4.56 s. Comparing the f_{mode} with the $\boldsymbol{E} \times \boldsymbol{B}$ rotation frequency at the resonant surface $f_{\boldsymbol{E} \times \boldsymbol{B}}$, the f_{mode} and the $f_{\boldsymbol{E} \times \boldsymbol{B}}$ are almost the same from the constant phase to the slowing down phase. It suggests that the precursor rotates with the $\boldsymbol{E} \times \boldsymbol{B}$ plasma flow. By investigating the relationship between the $f_{\boldsymbol{E} \times \boldsymbol{B}}$ profile and the resonant surface location, it is found that the slowing down phase consists of the following two stages. Figure 3 (e) shows the time evolution of the radial profile of the $\boldsymbol{E} \times \boldsymbol{B}$ rotation frequency (filled areas) and the resonant surface location (closed circles). Figure 3 (f) shows the radial profile of the $\boldsymbol{E} \times \boldsymbol{B}$ rotation frequency at three timings. In the first stage, such as t = 4.28 and 4.38 s, the resonant surface moves toward the plasma core region (R = 4.16 m

to $R = 4.06$ m), where the $\boldsymbol{E} \times \boldsymbol{B}$ rotation frequency is small. In the second stage (just before $t = 4.58$ s), the $\boldsymbol{E} \times \boldsymbol{B}$ rotation frequency near the resonant surface becomes small. Such a slowing down process is similar to that of the type-I instability [1]. This result suggests that the effect of the magnetic island size on the slowing down of the locked-mode-like instability in the LHD is not significant.

[1] Takemura Y. *et al.*, 2017 Plasma Fusion Res. **12**, 1402028–1402028.

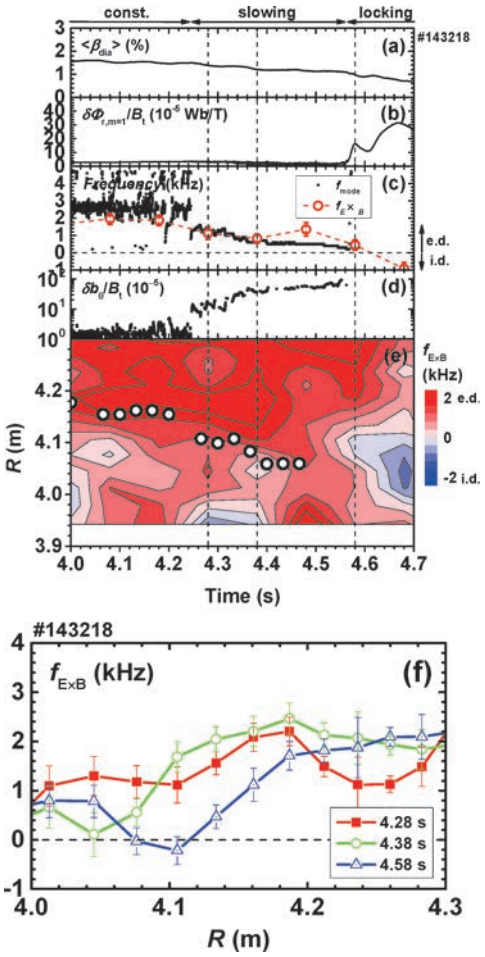

Fig. 3 Time evolution of (a) volume-averaged beta value, (b) radial mode amplitude by saddle loop coils, (c) mode frequency f_{mode} by a magnetic probe (closed circles) and $\boldsymbol{E} \times \boldsymbol{B}$ rotation frequency $f_{E \times B}$ at $\iota/2\pi = 1$ resonant surface (open circles), (d) poloidal mode amplitude by a magnetic probe and (e) radial profile of $\boldsymbol{E} \times \boldsymbol{B}$ rotation frequency and location of $\iota/2\pi = 1$ resonant surface (closed circles). (f) radial profile of $\boldsymbol{E} \times \boldsymbol{B}$ rotation frequency at each time corresponding to vertical lines in Fig. 1 (a)–(e) in the almost-reduced error field discharge. A positive (negative) sign of Fig. 1 (c) and (f) means an electron (ion) diamagnetic direction. The red (blue) area in Fig. 1 (e) corresponds to the electron (ion) diamagnetic direction.

(Y. Takemura and Y. Suzuki)

Research and Development Collaboration Program for LHD-Project

A special collaboration program, which is aimed to support the research and development activities in domestic universities for advanced diagnostics or heating scenarios, is established for future application on the LHD. Two examples of such activities are shown in this section.

a) Hydrogen recycling Model on carbon divertor by molecular dynamics simulation for neutral transport analysis in LHD

When the divertor plates are irradiated by hydrogen ions, some hydrogen atoms and molecules reflect back to the plasma while the other hydrogen atoms are retainedretain in the divertor. These recycled neutral hydrogen atoms and molecules affect the plasma parameter of the core plasma by ionization and charge-exchange reaction caused during their travel to the core plasma via edge plasma. Moreover, in the situation of rising expectations of the detached divertor, recent research revealed that the recombination processes caused by hydrogen molecule, the so called molecular assisted recombination (MAR), plays an important role for the neutral transport in the edge plasma. In particular, the effects of charge exchange recombination and dissociative recombination cannot be ignored for an understanding of the process of the neutral transport at the edge plasma.

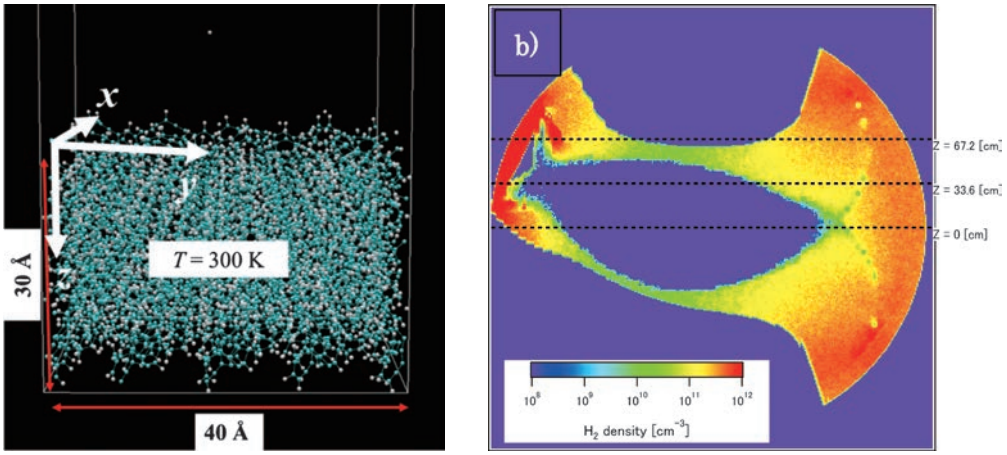

Fig. 1 (a) Molecular dynamics simulation model of carbon and hydrogen atoms. (b) Special distribution of hydrogen molecules density in LHD calculated by new neutral-transport code with developed hydrogen recycling model on carbon divertor.

The transport of the neutral particles can be numerically simulated by neutral-transport code. However, conventional neutral transport codes cannot treat the process of MAR. To avoid this problem, the Shinshu University group is now developing a new neutral-transport code which can treat the process of MAR. In order to provide the information of recycled hydrogen atoms and molecules the neutral-transport code, we have developed [1, 2] a simulation model for hydrogen recycling process on carbon divertor. Our recycling model consists of two regions: MD and HC regions. The inside (MD region) and the outside (HC region) are governed by equations of motion, that is, molecular dynamics (MD) simulation, and heat conduction equation, respectively. In the MD region, as shown in Fig. 1(a), one hydrogen atom is injected into a hydrogen containing amorphous carbon material. Because of the computation time, it is impossible to prepare the MD region large enough to calculate

the process of heat transfer to the bulk which is caused by the kinetic energy entering the target material with the injected hydrogen atom.

The information of emitted hydrogen atoms and molecules are investigated. By multiple trials, the distributions of emission angle, translational energy, vibrational states, and rotational states of emitted hydrogen atoms and molecules are obtained. Code integration of neutral-transport code and our developed hydrogen recycling model is successfully performed as shown in Fig. 1(b).

(S. Saito, Yamagata University)

b) Development for advanced turbulence diagnostics and analyses for magnetically confinement plasmas

The understanding of plasma confinement has made great progress. However, there still are many unsolved problems, such as isotope effects, non-local transport, origins of improved confinement, and background physics for empirical scaling laws. The studies of plasma turbulence are the keys for solving these issues, and the new concepts to understand the plasma turbulence, 'cross-scale couplings' and 'symmetry-breaking' in plasma turbulence, have been proposed to require new and advanced diagnostics for plasma turbulence in order to measure the entire cross-section, at least two dimensions, of plasma. The present collaboration work is undertaking research and development of a tomography system as such a diagnostic in terms of hard- and software.

The turbulence tomography was newly installed on PANTA, a linear cylindrical plasma device in Kyushu University. The diagnostic enables obtaining two-dimensional image of plasmas using 6 directional linear visible imaging systems. Several new analyzing methods were newly developed to quantify the images, such as Fourier-Bessel analysis with optimized choice of the fitting bases [3], and fast algorithm for monitoring images using Tikhonov regularization [3]. The application of the Stokes parameters, known as the indexes to quantify polarization characteristics in optics, has been recently proposed for quantifying the rotation characteristics of azimuthal modes [4]. The method successfully extracts the rotation properties of fluctuation patterns that appear in the turbulent plasmas. It is found, as is shown in Fig. 2, that broad-band fluctuations could show clear polarization characteristics as well as coherent fluctuation patterns in a region of plasma. Further, a Tikhonov method using L1-regularization [5], Time Delay Estimate (TDE) Fourier-Rectangular analysis [6], and others are being developed.

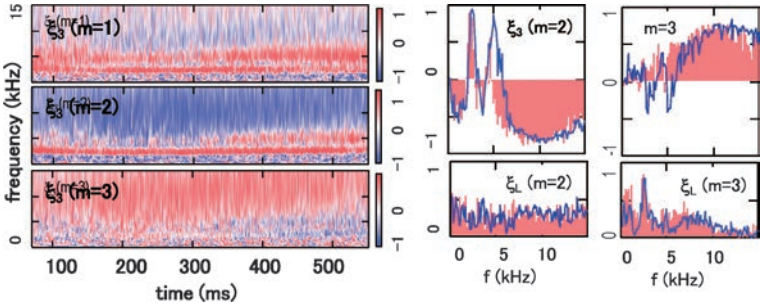

Fig. 2 Examples of Stokes parameter analysis of azimuthal mode dynamics. Here the azimuthal modes of m=1, 2, and 3 are analyzed. Stokes parameters are calculated using the moments of emission distribution.

(A. Fujisawa, Kyushu University)

[1] H. Nakamura *et al.*, 18th ICPP, Taiwan (2016).
[2] S. Saito *et al.*, Proceedings of 37th JSST (2018).
[3] K. Yamasaki *et al.*, Rev. Sci. Instrum. **88**, 93507 (2017).
[4] A. Fujisawa *et al.*, Phys. Plasmas **26**, 012305 (2019).
[5] K. Yamasaki *et al.*, Rev. Sci. Instrum. **88**, 93507 (2017).
[6] K. Yamasaki *et al.*, J. Appl. Phys., being submitted.

2. Fusion Engineering Research Project

The Fusion Engineering Research Project (FERP) started in FY2010 at NIFS. Along with the conceptual design studies for the helical fusion reactor FFHR, the FERP has been developing technologies of key components, such as the superconducting magnet, blanket, and divertor. The research is also focused on materials used for blankets and divertors, the interaction between the plasma and the first wall including atomic processes, handling of tritium, plasma control, heating, and diagnostics. The FERP is composed of 13 tasks and 44 sub-tasks with domestic and international collaborations. (T. Muroga)

Reactor Design Studies

Conceptual design studies of the helical fusion reactor FFHR-c1, which aims at early demonstration of electric power generation with a reasonable construction cost by reducing the reactor size and increasing the magnetic field strength, has been advanced. In FY2017, it was shown that the steady-state operation with a fusion gain of ~15 can be achieved within the physics condition which has been already confirmed in the LHD experiments. Even though this fusion gain is sufficient for the self-sufficiency of electricity, further increase by an improvement of core plasma performance is still desired to increase the operational margin and to explore a more attractive design with a larger net electric output. Optimization of the winding law of the helical coils is one of the promising methods to improve the plasma performance while keeping several merits of the LHD-type configuration; coil winding with a small variation of the curvature, flexible divertor design by utilizing the rigid and robust divertor field structure, and high maintainability of blankets with large port apertures. In FY2018, the effect of changing the pitch modulation parameter, α, has been examined (Fig. 1). It was found that simultaneous improvement in the MHD stability and energy confinement can be achieved by decreasing α from 0.1 (employed in LHD and former FFHR designs) to 0.0 and selecting an adequate magnetic axis position [1]. It was also found that the change in α within the range of $-0.1 \leq \alpha \leq 0.3$ does not significantly affect the stored magnetic energy and electromagnetic stress on the coil supporting structure [2]. Although this tendency was already known in the design phase of LHD, the calculation reliability has been greatly improved and the design with a sufficient blanket thickness is shown for the first time by reflecting the latest ideas including the installation of the supplemental helical coils (NITA coils), which can enlarge the space between the helical coil and plasma without changing the plasma shape.

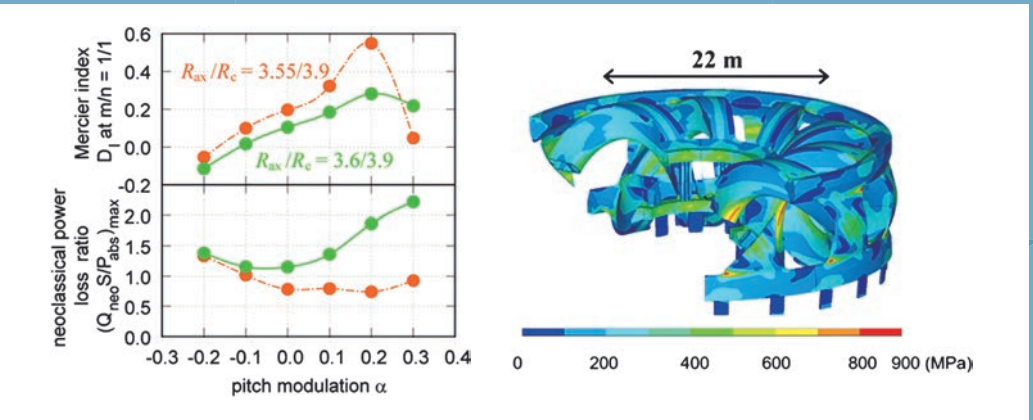

Fig. 1 (left) Dependence of the Mercier index (indicator of MHD instability) and the neoclassical power loss on the pitch modulation parameter α of the helical coil winding with a different magnetic axis position. (right) The stress distribution on the coil supporting structure in the case of $\alpha = -0.1$. The maximum peak stress is within the allowable limit (< 1 GPa).

[1] T. Goto *et al.*, Nucl. Fusion **59**, 076030 (2019).
[2] H. Tamura *et al.*, Fusion Eng. Des. **146**, 586 (2019).

(T. Goto)

Highlight

New ideas on the divertor and blanket

In the latest design of the helical fusion reactor FFHR-c1, a new divertor system using solid tin pebble shower and a new cartridge-type blanket system are adopted. A new tin pebble shower divertor system named REVOLVER-D2 [1] has been proposed. In this system, showers of tin pebble flow are used as the divertor target. The plasma flowing out from the confinement region hits this tin pebble shower before reaching the vacuum vessel wall. Shown in Fig. 1 is the result of an experiment demonstrating that a tin-alloy pebble flow can shut the fire of ~5 MW/m^2 emitted from a gas burner. Related R&D and the design study on the REVOLVER-D2 system are ongoing. A new cartridge-type blanket system named CARDISTRY-B2 [2] has been also proposed (Fig. 2). The main objective is to make construction and maintenance of the complicated helical fusion reactor as easy as possible. Together with the 3D computer-aided design, we are making full use of the recent 3D printing technology to confirm its feasibility (see photos in Fig. 3). Numerical simulations on the structure strength, thermal property, neutron shielding ability and tritium breeding ability of each cartridge, together with discussions on the remote maintenance scenario are now being carried out.

[1] T. Ohgo *et al.*, Plasma Fusion Res. **14**, 3405050 (2019).
[2] J. Miyazawa *et al.*, submitted to Plasma Fusion Res.

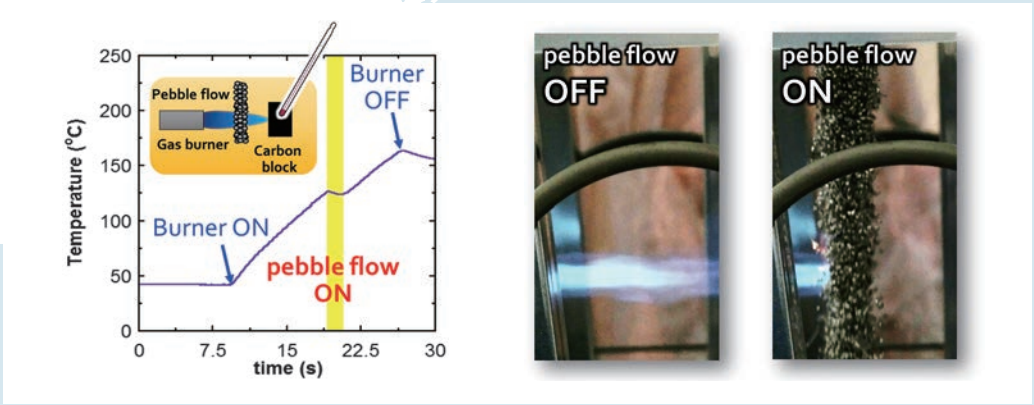

Fig. 1 Experimental results of a gas burner heating experiment on a tin-alloy pebble flow. The temperature of a carbon block, which is set behind the pebble flow and heated by the gas burner, stops increasing when the pebbles are flowing.

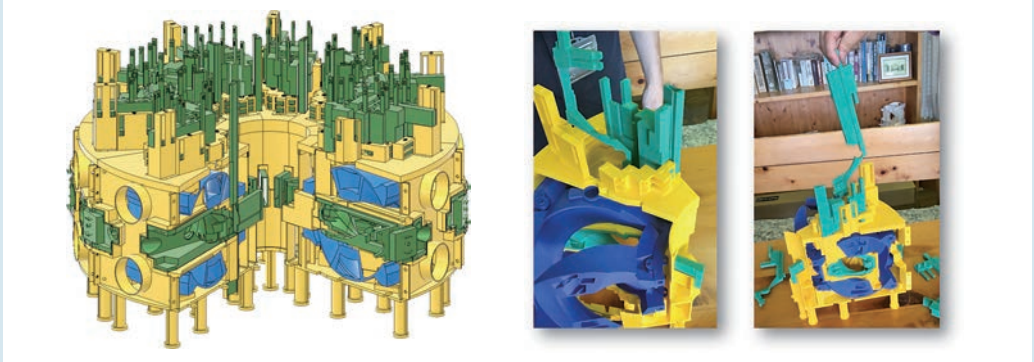

Fig. 2 (left) Bird's eye view of the CARDISTRY-B2 cartridge-type blanket system, and (right) photos of a small model made by 3D printing technology.

(J. Miyazawa)

Research and Development on the Superconducting Magnet

To realize a large-scale superconducting magnet system for the helical fusion reactor, both the Low-Temperature Superconducting (LTS) and High-Temperature Superconducting (HTS) large-current capacity conductors are being developed. For this purpose, the superconductor testing facility, with the maximum magnetic field of 13 T, large bore of 0.7 m diameter, large sample current of 50 kA, and temperature control capability of 4.2–50 K has been operational [1, 2]. Using this facility, an international collaboration experiment was carried out between Massachusetts Institute of Technology (MIT) in the US and NIFS, for the Twisted Stacked-Tape Cable (TSTC) HTS conductor [3, 4]. A one-turn coiled sample, made of a TSTC conductor, was designed and fabricated at MIT, transported to NIFS, and installed into the superconductor testing facility (Fig. 1). The experiment was carried out two times, in September 2018 and in January 2019. Figure 2 shows the cool-down curve of the magnet obtained in the second experiment. The maximum achievable current of the TSTC conductor sample was 19 kA at zero magnetic field. A sample current of 9 kA was measured at the bias magnetic field of 5 T and the inlet temperature of ~5 K.

Apart from this experiment, three kinds of HTS conductors are now being developed to be applied to the next-generation helical experimental device. In addition, as an extension of the ITER technology based on the LTS magnet concept, the development of an internal-matrix-strengthened Nb_3Sn wire is continuing using a ternary Cu-Sn alloy (such as Cu-Sn-Zn) to mitigate the degradation problem of the present Nb_3Sn wires due to mechanical strain [5].

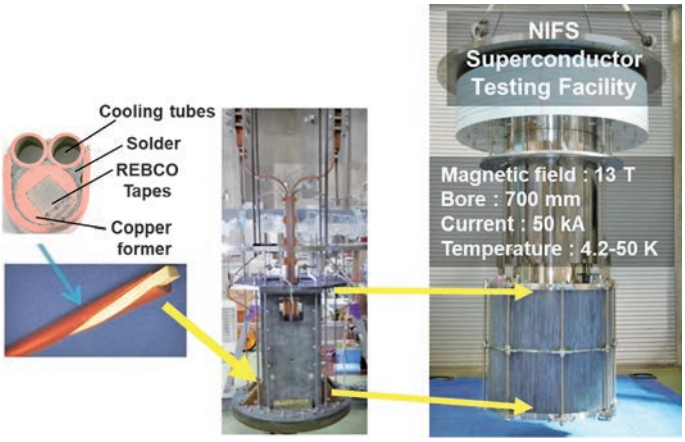

Fig. 1 Experimental setup of a TSTC HTS conductor sample for the international collaboration experiment between MIT and NIFS.

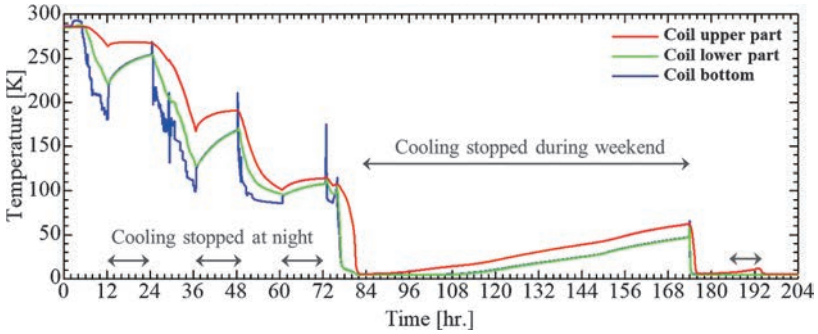

Fig. 2 Cool-down curve of the 13 T magnet from Jan. 8 to Jan. 16, 2019.

[1] S. Imagawa *et al.*, Plasma Fusion Res. **10**, 3405012 (2015).
[2] J. Hamaguchi *et al.*, Plasma Fusion Res. **10**, 3405020 (2015).
[3] M. Takayasu *et al.*, IEEE Trans. Appl. Supercond. **26**, 6400210 (2016).
[4] T. Obana *et al.*, submitted to Cryogenics.
[5] Y. Hishinuma *et al.*, IOP Conf. Series: Materials Science and Engineering **502**, 012175 (2019).

(N. Yanagi)

Research and Development on the Blanket

A FLiNaK/LiPb twin loop system named Oroshhi-2 (Operational Recovery Of Separated Hydrogen and Heat Inquiry-2) is being operated in NIFS as a collaboration platform for integrated experiments on the liquid blanket technologies. In FY2018, thermofluid behaviors of a liquid metal flow were investigated in collaborative experiments with Kyoto University under a strong magnetic field of 3 T provided by the superconducting magnet of the Oroshhi-2 system (Fig. 1). A flow of GaInSn with a free surface was made by an electromagnetic circulation pump in the channel. A magnetic field was applied perpendicularly to the flow. At the bottom of the channel, obstacles are attached as a vortex generator to enhance the heat transfer from the heater set on the free surface to the bottom of the channel. In the experiments, the world's first data of three-dimensional temperature distribution in a liquid metal flow under a strong magnetic field has successfully been acquired using a thermocouple array. The distribution data indicates that the heat transfer from the heater to the bottom becomes nearly parallel to the strong magnetic field, which is perpendicular to the GaInSn flow. The experiments are offering new findings also for the development of liquid divertors.

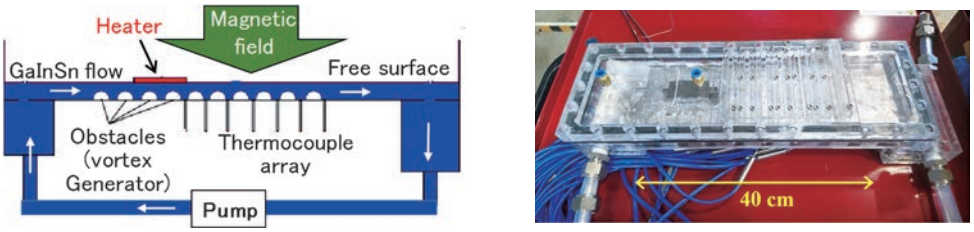

Fig. 1 (left) A schematic drawing and (right) a photo of the experimental device to investigate thermofluid behaviors of a liquid metal flow (GaInSn) under a strong magnetic field of 3 T provided by the superconducting magnet in Oroshhi-2.

Experimental topics to be examined in Oroshhi-2, validities of the experimental methods, schedule adjustment, etc., are regularly discussed in the Oroshhi workshop held at NIFS twice a year. In FY2019, it was decided that the heat removal performance of a molten-salt coolant flow would be examined by a collaborative experiment with Tohoku University through a pebble-bed tube under a 3 T magnetic field. Since the possibility of degradation of the heat removal performance due to suppression of turbulence flow under a strong magnetic field has been pointed out in previous studies, this experiment will be essential for the design of molten-salt-cooled blanket systems. It was also decided that demonstration of continuous and high-efficient hydrogen recovery from circulated LiPb coolant would be performed using the sub-test section of the LiPb loop in FY2019, as the LHD-Project Research Collaboration (see later section).

Other than the research activities using Oroshhi-2, studies on tritium fuel behaviors in high temperature (~500°C) FLiNaK and FLiNaBe tritium breeder/coolants have been performed under a collaboration with Osaka University from FY2017 to FY2018. Low flux neuron irradiation experiments on FLiNaK and FLiNaBe have been performed using an AmBe neutron source at Osaka University, and the world's first tritium release data for both the breeder and coolants has been successfully obtained. Controllability of the chemical forms of released tritium and the tritium release rates by changing the atmospheric condition have also been confirmed [1].

[1] K. Kumagai, Ph.D. thesis, SOKENDAI (2019), in Japanese.

(T. Tanaka)

Highlight

Development of advanced structural materials for fusion reactor blanket

NIFS promotes development of advanced structural materials such as reduced-activation ferritic steels, their oxide-dispersion-strengthened (ODS) alloys, low-activation vanadium alloys, etc., under the collaboration with universities and institutions in the world. ODS steels exhibit excellent high temperature strength and have been considered to extend the maximum operation temperature of blankets to be higher than 600°C, based on hardening by nanometer-size oxide particles dispersed in the alloy matrix. These alloys are made from metal and oxide powders under a high temperature condition, such as 1,150°C, and shaped into plate products. During the hot shaping processes, crystal grains of the alloy matrix are elongated to the preferential crystal orientation. As a result, ODS steels obtain anisotropic mechanical properties, where they lose ductility for tensile deformation if it is vertical to the longitudinal direction of the crystal grains. In order to suppress the anisotropy and improve ductility, recrystallization is required to replace the elongated grains by new ones with less preferential orientation. However, the conventional ODS steels could not complete recrystallization until heating up to 1,400°C, resulting in strength degradation by porosity formation and oxide particle coarsening. Our new fabrication process, two-way cold rolling, effectively introduces crystal defects and their stored energy, and hence induces driving force for recrystallization at even lower temperature, 1,100°C. Figure 1 shows the grain microstructures before and after the two-way rolling, indicating the crystal orientations by colors. The figure proves that the color, the orientation of the crystal, has been completely changed by the new rolling process. At this moment, we have confirmed full recrystallization of the ODS steel after the new rolling process, and we will evaluate high temperature strength and ductility in all directions as a next step. NIFS also leads the development of advanced vanadium alloys which are alternative to the ferritic steels and can raise the operation temperature of blankets up to 700°C. Reduction and optimization of the concentration of the alloying element titanium has been examined to improve their low-activation properties further, therefore, early material recycling is expected after the use in fusion reactors.

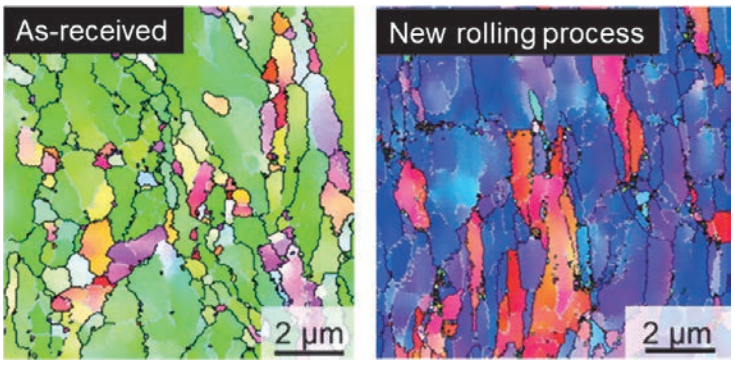

Fig. 1 Images of grain microstructure by electron back scattered diffraction analysis. Black lines indicate the crystal grain boundaries. Red, blue, and green colors are attributed to the crystal orientations of <001>, <111>, and <110> for body centered cubic lattice, respectively.

(T. Nagasaka)

Research and Development on the Divertor

The advanced brazing technique between ODS-Cu (GlidCop®) and tungsten (W) with BNi-6 (Ni-11%P) filler material has been developed for fabricating a divertor heat removal component [1, 2], and optimization of the procedures were greatly progressed in the last fiscal year [3]. By further enhancing the optimized advanced brazing technique, we newly developed a joint of ODS-Cu/ODS-Cu and SUS/ODS-Cu [4]. This newly developed joint has two special features as follows. The first is that these joints have leak tightness against fluids. The second is that the multiple brazing heat treatment can be applicable for fabricating a single divertor component because the prior bonding layer is not affected by the subsequent brazing heat treatment. A small-scale divertor mock-up with a curved cooling flow path channel has been successfully fabricated using the multi-step brazing technique of ODS-Cu/ODS-Cu, SUS/ODS-Cu and W/ODS-Cu, as shown in Fig. 1.

A high heat flux test facility named ACT2 (Active Cooling Test stand 2) has been used for the heat load test of plasma facing components since 2015. ACT2 is capable of performing a reactor relevant heat flux test (> 20 MW/m^2) on a large surface area of >1,000 mm^2. A divertor test component with W-flat tiles brazed on a Cu-alloy heatsink (Fig. 2) was tested in ACT2 at a water-cooled condition (flow speed: 16.8 m/s, pressure: ~0.3 MPa). In this heat load test, a water-cooled copper plate with an aperture called the "beam limiter" was mounted on a test component to maintain the homogeneous heat load and to protect the thermocouples attached to specific points of the test component. The heat load test was successfully carried out without damaging the test component and a good heat removal capability was observed up to 24 MW/m^2. The temperatures measured on the test component with respect to the heat flux are shown in Fig. 2. In this test, the maximum heat flux of 24 MW/m^2 was limited by the capacity of the beam limiter.

New materials of Dispersion Strengthening Copper (DS-Cu) are being developed by means of a combined process of Mechanical Alloying (MA) and Hot Isostatic Pressing (HIP). The DS method can drastically improve the mechanical properties of materials by introducing thermally stable nano-particles (Y_2O_3, for example). Recently, a new process has been developed, in which the dopant materials (CuO) are added to the matrix in the middle of the MA process (Fig. 3). The new process successfully increased the density of the oxide nano-particles. The mechanical properties of the Cu-Y_2O_3 fabricated by the new process will be investigated in future work.

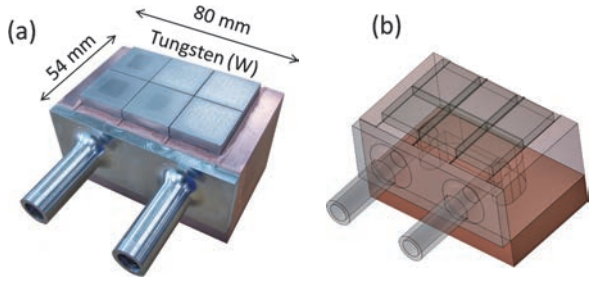

Fig. 1 (a) Photo and (b) a CAD image of a small-scale divertor mock-up with a curved cooling flow path channel fabricated by the multi-step brazing technique.

A superior nano-scale fabrication technique of tungsten by using a focused ion beam – electron beam

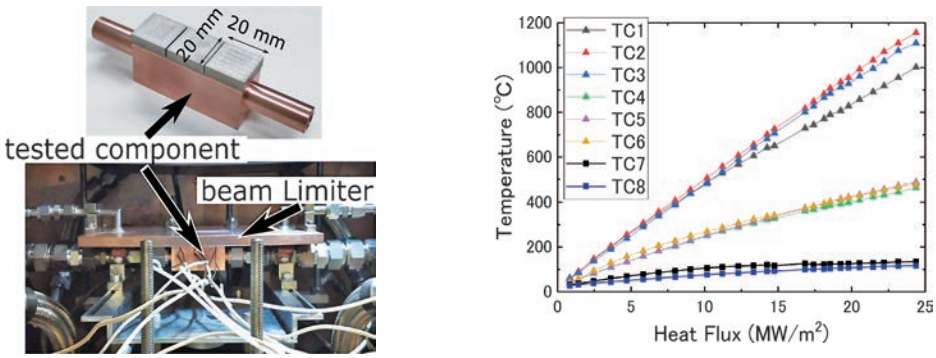

Fig. 2 (left) Photos of a tested component and the experimental setup inside ACT2, and (right) the experimental results of the measured temperature of the tested component with respect to the heat flux.

(FIB-SEM) device has been developed, and is named the "nano-scale sculpture technique" [5]. In order to observe the internal structure of nano-scale materials, the Transmission Electron Microscope (TEM) is commonly used as a powerful tool. In TEM, accelerated electrons are transmitted through target materials. To observe a cross-sectional view of the very close region to the top surface of a tungsten sample by TEM, a small piece of cross-sectional sample is extracted from the surface at first. Then, the extracted small piece is modified to an ultra-thin film sample with a thickness of <~ 100 nm. The FIB-SEM device enables a nano-scale material fabrication by using a focused Ga ion beam. Adjustment of the Ga beam intensity is not an easy procedure, because tungsten is a quite hard material. The very close region to the top surface of the tungsten sample could be lost undesirably, even with a beam intensity slightly stronger than the appropriate value. To solve this problem, we tried to make a special Ga beam operation to maintain the top surface in the ~100 nm level thin film fabrication. Consequently, we succeeded in fabricating an ultra-thin film with a thickness of ~100 nm, or less, while maintaining the top surface of the tungsten sample. Figure 4 shows the details of this "nano-scale sculpture technique." By observing the ultra-thin film using TEM, it becomes possible to clearly identify the atomic level damages formed in the very close region to the top surface of the tungsten sample with high-resolution, as shown in Fig. 5 [6].

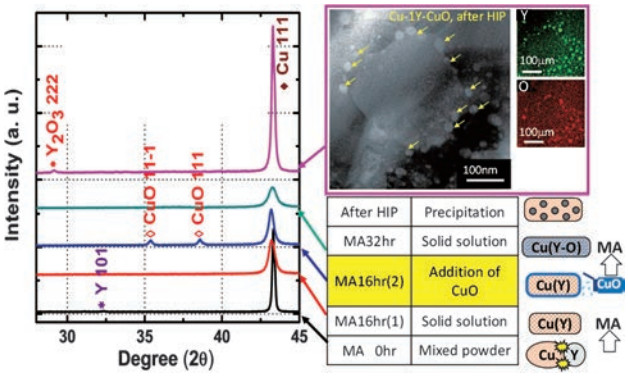

Fig. 3 In-situ fabrication of Cu-Y_2O_3 alloy.

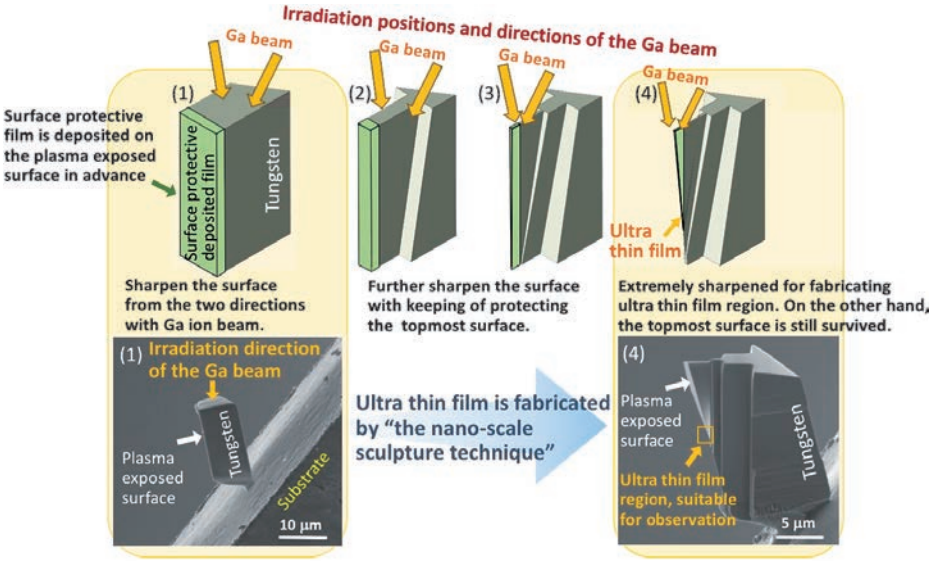

Fig. 4 The "nano-scale sculpture technique" by using a focused ion beam – electron beam (FIB-SEM) device. The upper series shows a schematic view of the fabrication process using a Ga ion beam. The images of (1) and (4) in the bottom series are the corresponding scanning electron microscope (SEM) images to those of (1) and (4) in the upper series.

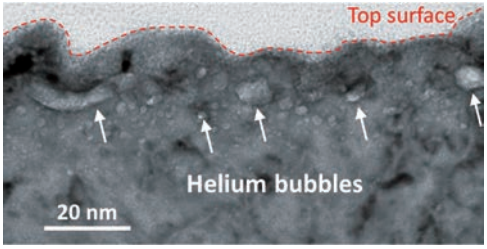

Fig. 5 A cross-sectional TEM image of a tungsten sample exposed to the helium divertor plasma in LHD. The ultra-thin film TEM sample was fabricated by "the nano-scale sculpture technique." This very high-resolution image could not be obtained without the ultra-thin film fabricated by the nano-scale sculpture technique. The bright spherical shape images are helium bubbles. The top surface of the tungsten sample is retained even in an ultra-thin film with a thickness of ~100 nm or less [11].

In-vessel material transport on the plasma-facing walls in LHD has been investigated using the Rutherford backscattering spectrometry (RBS) with 2.8 MeV ^{4}He ions generated by a tandem accelerator (NEC Pelletron accelerator, Fig. 6). Ten Si plates had been placed on the outer side of the first-wall surface for every 36° toroidal sections in LHD, during one experimental campaign. A characteristic RBS spectrum of the mixed-material layers deposited on one of the Si plates is shown in Fig. 6 [7]. The RBS spectrum shows that Cr, Fe, Ni, Ti, Mo, and W are included in the mixed-material layer deposited on the Si plate. Various RBS spectra have been observed for each of the ten Si plates. A detailed data analysis on those spectra is now being carried out. The RBS analysis is a powerful tool for elucidating the material transport (impurity transport) inside the LHD vacuum vessel from the viewpoint of material science.

Spectroscopic measurement of the light emitted from highly charged tungsten ions has been conducted using an electron beam ion trap (CoBIT), and the data is used to identify the emission lines observed in the LHD plasma experiment (Fig. 7). This time, for the first time in the world, we succeeded in observing a strong forbidden transition called the "Electrical octupole transition (E3)" by using CoBIT. This is a phenomenon that occurs with a probability of about 10 billionth of the normally allowed transition (E1 transition), and we succeeded in elucidating its physics mechanism.

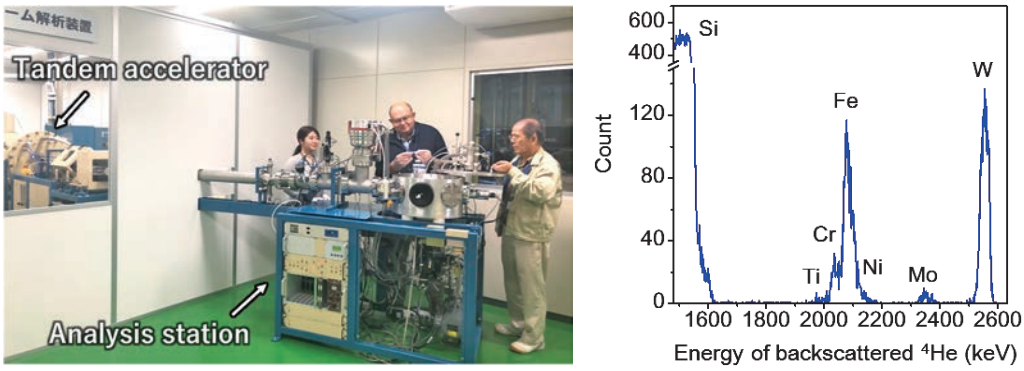

Fig. 6 (left) The ion beam analysis device consisting of an ion beam injector, a tandem accelerator, and an analysis station, and (right) an example of the Rutherford backscattering spectrometry (RBS) spectrum of the mixed-material layers deposited on a Si plate placed inside the LHD vacuum vessel during one experimental campaign.

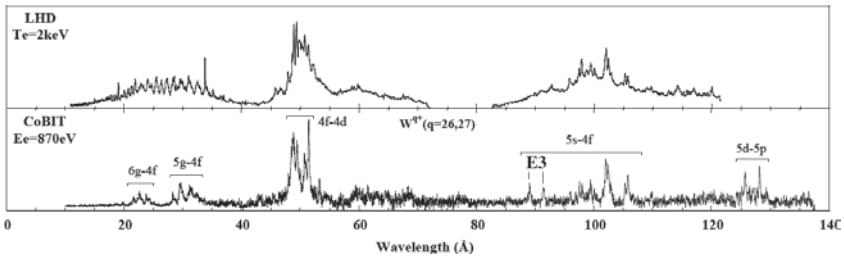

Fig. 7 Comparison of the spectrum observed in LHD with the spectrum observed in CoBIT.

[1] M. Tokitani *et al.*, Plasma Fusion Res. **10**, 340503 (2015).
[2] M. Tokitani *et al.*, Nucl. Fusion **57**, 076009 (2017).
[3] M. Tokitani *et al.*, Fusion Eng. Des. (2019), in press.
[4] M. Tokitani *et al.*, Fusion Eng. Des. (2019), to be published.
[5] D. Nagata *et al.*, Materia, in Japanese. https://doi.org/10.2320/materia.57.604
[6] M. Tokitani *et al.*, Nucl. Mater. Energy **12**, 1358 (2017).
[7] V.Kh. Alimov *et al.*, Fusion Eng. Des. **147**, 111228 (2019).

(M. Tokitani, Y. Hamaji, H. Noto, M. Yajima and H. Sakaue)

LHD-Project Research Collaboration

The LHD Project Research Collaboration program has been contributing to enhancing both the scientific and the technological foundations for the research related with the LHD project as well as the future helical fusion reactors. The characteristics of this collaboration program are that the researches are performed at universities and/or institutions outside NIFS. In the research area of fusion engineering, the following ten subjects were approved and conducted in FY2018:

1. Knowledge and technology transfer from IFMIF-EVEDA accomplishment to systemization of liquid blanket research
2. Development of irradiation-resistant NDS-Cu alloys for helical reactor divertor
3. Development of effective heat removal method from liquid metal free-surface with local heating under strong magnetic field and its demonstration by Oroshhi-2
4. Engineering study on lithium isotope enrichment by ion exchange
5. Tritium behavior in a secondary cooling system in a fusion DEMO reactor
6. Establishment of high susceptible detection assay for biomolecule response and estimation of the biological effects of low-level tritium radiation by utilizing its assay
7. Development of highly-ductile tungsten composite systems
8. Fundamental engineering of tritium recovery process for liquid blanket of helical reactor
9. Development of new rapid-heating and quench processed Nb_3Al large-scaled cables for the helical winding due to the react-and-wind method
10. Field estimation for improvement of environmental tritium behavior model

From the above ten research items, two of them (7 and 8) are briefly described below:

7. Development of highly ductile tungsten composite systems

Tungsten is promising as a plasma facing armor material, because of its high melting point, low plasma erosion rate and low permeation loss of the fuel hydrogens. However, the tungsten armor exhibits disadvantageous ductility loss under the harsh fusion environment. Conventional tungsten reveals the ductility loss at 1,100°C and above due to recrystallization (crystal co arsening), and below 600°C due to their intrinsic brittleness. On the other hand, a potassium (K)-doped advanced tungsten is resistant to the recrystallization and shows no ductility loss up to 1,250°C. In order for compatible low-temperature ductility with the excellent high-temperature ductility, the present project developed layered novel composite systems of the K-doped tungsten and ductile other metals. As shown in Fig. 1, the K-doped tungsten and pure vanadium layer composite successfully maintain ductility at room temperature, even after an exposure to heat loading at 1,250°C.

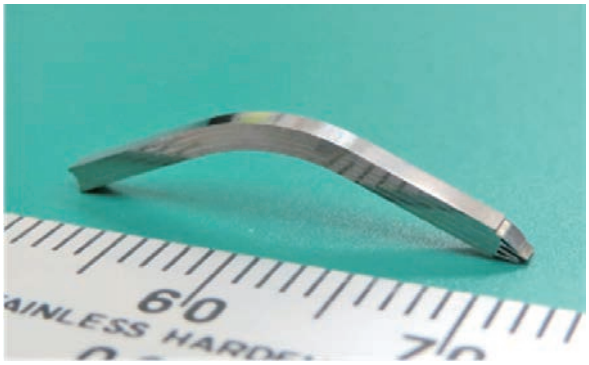

Fig. 1 K-doped tungsten and pure vanadium layers composite after a bend test at room temperature. The visible bending and no fracture prove large ductility.

8. Fundamental engineering of tritium recovery process for liquid blanket of helical reactor

High-efficient hydrogen fuel recovery from high temperature liquid fuel breeder is one of the key technologies required for fusion blanket systems. An innovative idea to recover hydrogen from circulated liquid LiPb breeder has been proposed in Kyoto University and experimental validation is being conducted. In the proposed vacuum sieve tray (VST) system, droplets of liquid LiPb at ~350°C are made with a sieve tray in a vacuum chamber and hydrogen in the droplets is efficiently extracted to vacuum before reaching the bottom (Fig. 2). Stand-alone tests of the function and performance have successfully been accomplished in Kyoto University and the system has been installed to the Oroshhi-2 heat and mass transfer loop at NIFS (Fig. 3). The first demonstration of continuous hydrogen recovery from circulated high temperature LiPb by the VST system will be performed in the summer of 2019.

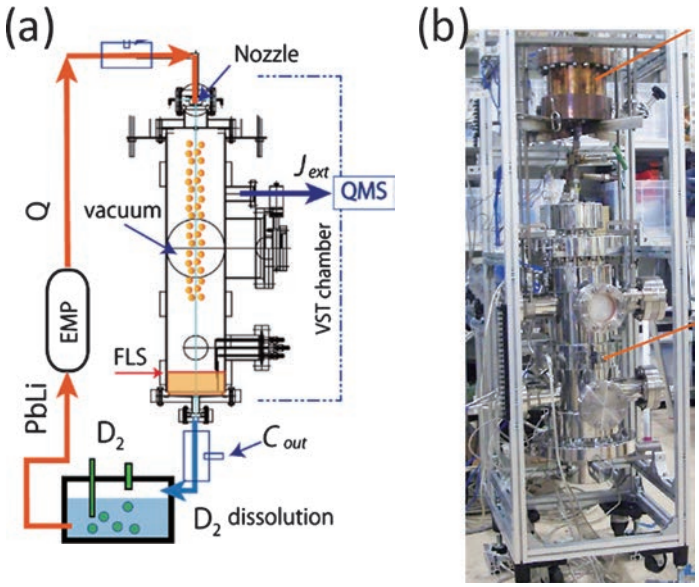

Fig. 2 (a) Schematic drawing of the vacuum sieve tray (VST) chamber for hydrogen recovery. (b) Photo of the VST chamber tested in Kyoto University.

Fig. 3 Expansion of an experimental stage on Oroshhi-2 for the validation experiment of continuous hydrogen recovery from circulated LiPb by the VST technique.

(J. Miyazawa, T. Nagasaka and T. Tanaka)

3. Numerical Simulation Reactor Research Project

Fusion plasmas are complex systems which involve a variety of physical processes interacting with each other across wide ranges of spatiotemporal scales. In the National Institute for Fusion Science (NIFS), we are utilizing the full capability of the supercomputer, Plasma Simulator (Fig.1), and propelling domestic and international collaborations in order to conduct the Numerical Simulation Reactor Research Project (NSRP). Missions of the NSRP are i) to systematize understandings of physical mechanisms in fusion plasmas for making fusion science a well-established discipline and ii) to construct the Numerical Helical Test Reactor, which is an integrated system of simulation codes to predict behaviors of fusion plasmas over the whole machine range.

Presented below in Figs. 2 and 3 are examples of successful results from collaborative simulation researches in 2018–2019 on kinetic ballooning mode (KBM) turbulence and on generation of helical structures in a reversed field pinch (RFP) plasma. Also, highlighted in the following pages are achievements of the NSRP on plasma fluid equilibrium stability, energetic-particle physics, neoclassical and turbulent transport simulation, integrated transport simulation, and plasma-wall interaction.

(H. Sugama)

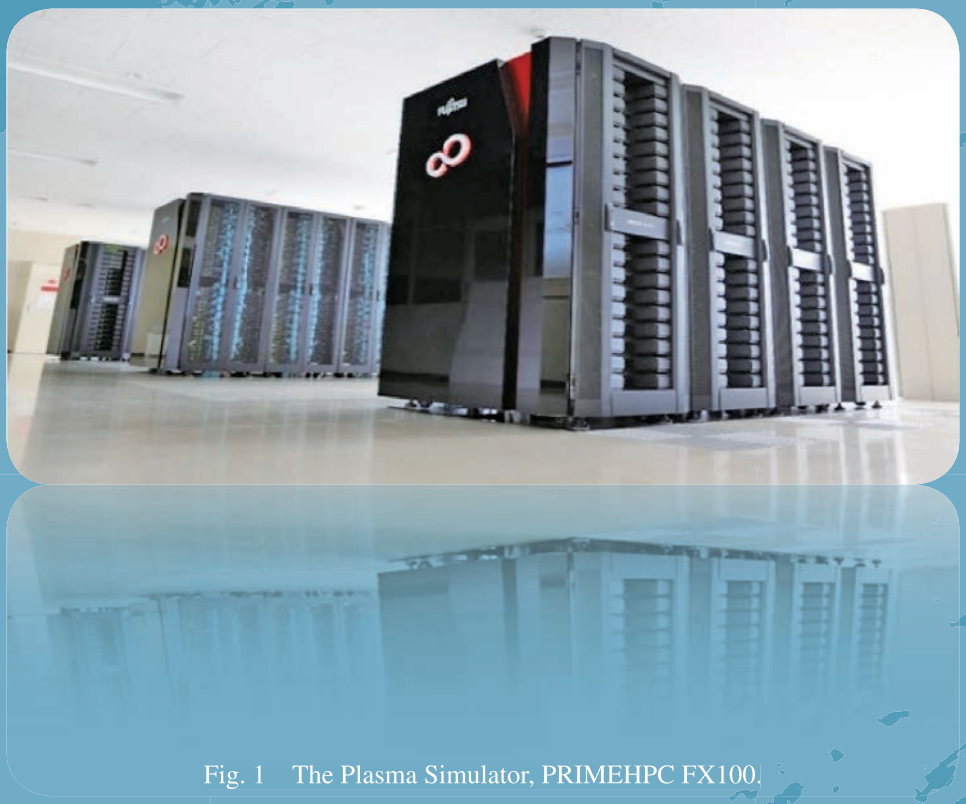

Fig. 1 The Plasma Simulator, PRIMEHPC FX100.

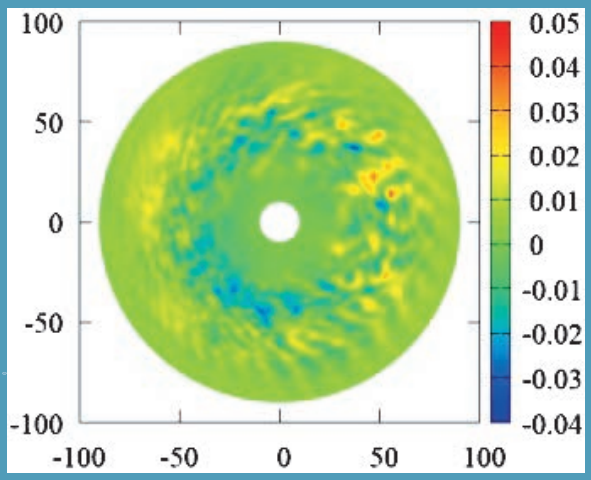

Fig. 2 Electrostatic potential fluctuations obtained by global gyrokinetic simulation of kinetic ballooning mode (KBM) turbulence in a tokamak plasma [presented by A. Ishizawa (Kyoto University)].

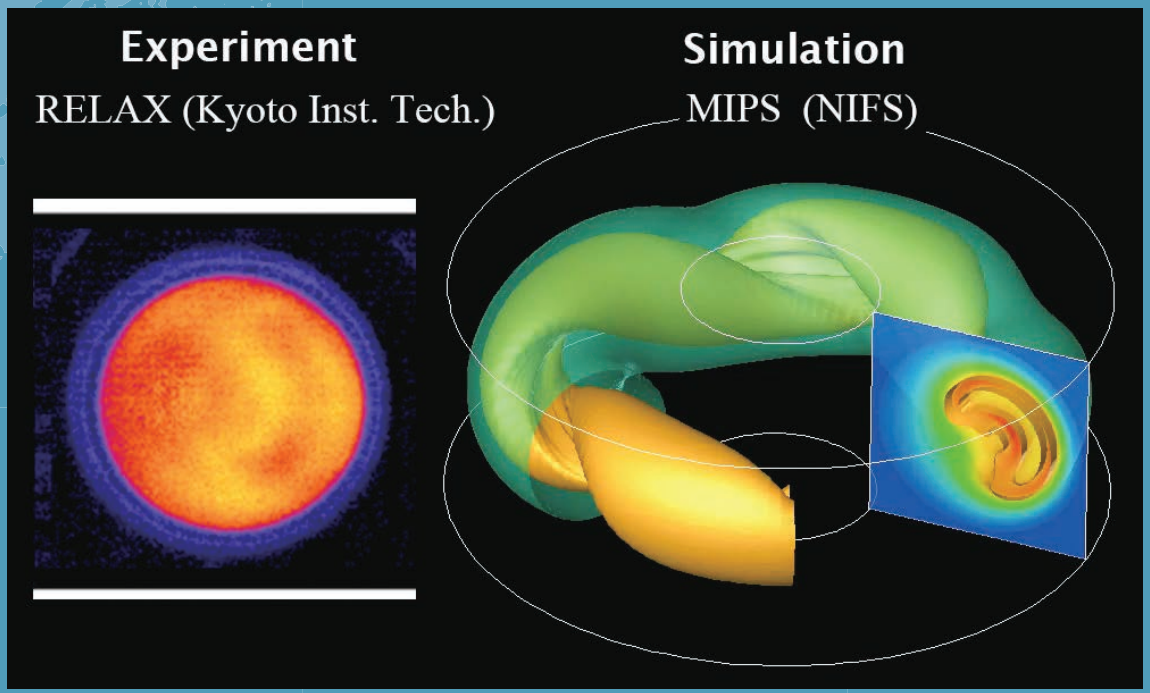

Fig. 3 Pressure of a reversed field pinch (RFP) plasma obtained by nonlinear MHD simulation [presented by collaboration of N. Mizuguchi (NIFS) and Kyoto Institute of Technology]. Generation of helical structures in the RFP plasma is clarified.

Numerical and theoretical MHD studies for Heliotron plasmas

Highlight

Numerical analysis of MHD instabilities based on kinetic MHD model with kinetic effects of thermal ions

For the inward shifted LHD configurations, where the magnetic axis is shifted inward relative to the center of helical coils, the MHD stability was considered to be unfavorable since there is always a magnetic hill. However, high beta plasmas with β~5% have been experimentally established in the inward shifted LHD configurations where β is the volume averaged beta value. It is a crucial issue to clarify the mechanism how such high beta plasmas are obtained. In this study, we have extended the numerical model such that the kinetic effects of thermal ions are taken into account, i.e., kinetic MHD model, and the kinetic effects of the thermal ions on resistive ballooning modes in high beta LHD plasmas have been investigated. From the numerical analysis based on the kinetic MHD model, it is found that the kinetic effects reduce the linear growth rate of pressure driven MHD instabilities. Figure 1 shows the trajectory of a deeply trapped ion and the image map of the perturbed electron pressure due to the resistive ballooning mode on a magnetic surface where the red and the blue correspond to the positive amplitude and the negative amplitude, respectively. The trapped ion has the precession motion in both poloidal and toroidal directions. When the precession drift frequency of the trapped ions with respect to the mode phase is close to or larger than the linear growth rate of the instability, the response of the trapped ions is weakened. This results in the suppression of the ion perpendicular pressure perturbation to the magnetic field leading to the reduction of the linear growth rate.

[1] M. Sato and Y. Todo, Proc. IAEA FEC 2018 (Ahmedabad, India), TH/P5-25.

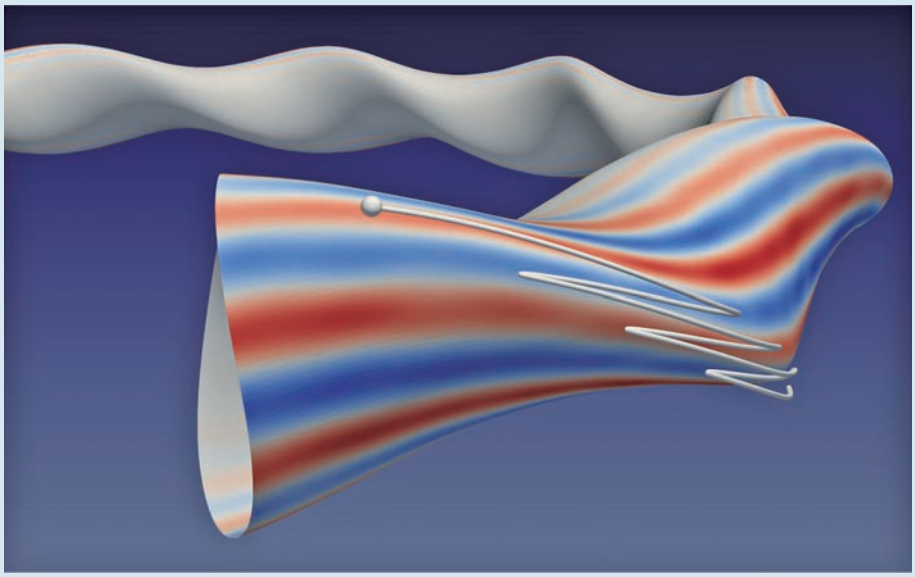

Fig. 1 The trajectory of a deeply trapped ion and the image map of the perturbed electron pressure due to the resistive ballooning modes on a magnetic surface. Here the red and the blue correspond to the positive and the negative amplitude, respectively.

(M. Sato)

Toroidal MHD equilibrium calculation via simulated annealing

We have demonstrated that simulated annealing (SA), a new method to calculate equilibria of ideal fluids, successfully achieves toroidal equilibria of tokamak and toroidally-averaged heliotron plasmas. The SA is a kind of relaxation theory that utilizes the Hamiltonian nature of the ideal fluids, including MHD. By solving an initial-value problem of an artificial dynamics derived on the basis of the Hamiltonian and the Poisson bracket. If the system is described by noncanonical variables, the Poisson bracket has null spaces called Casimir invariants. The artificial dynamics of the SA is constructed so that the energy of the system changes monotonically while the Casimir invariants are preserved. The system asymptotically approaches an energy extremum that is an equilibrium. In this study, we have extended the previous studies using low-beta reduced MHD model for cylindrical plasmas, and have succeeded to calculate large-aspect-ratio and circular cross-section equilibria of tokamak and toroidally-averaged heliotron plasmas by using high-beta reduced MHD model. For the toroidally-averaged heliotron plasmas, we have compared our numerical results for Heliotron E by the STEP-EQ code. In Fig. 2, the magnetic axis shift against the central beta value (Left) and flux surfaces on a poloidal cross-section (Right) are shown. Complete agreement is difficult to obtain mainly because the net-current-free condition cannot be imposed in the SA at present. However, we have obtained reasonable agreement with the previous results.

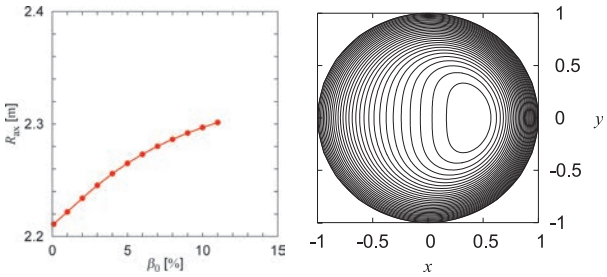

Fig. 2 Left: Magnetic axis shift increases as the central beta value is increased. Right: Flux surfaces are plotted for an equilibrium with central beta value 11%.

[1] M. Furukawa *et al.*, Phys. Plasmas **25**, 082506 (2018).

(M. Furukawa, Tottori University)

Numerical simulation of interaction between global flow and interchange modes in heliotron plasmas

In some special discharges in the Large Helical Device (LHD) experiments, partial collapses of the electron temperature profile due to the interchange mode are observed. In the collapses, the onset of the mode growth and the mode rotation stop are synchronized [1]. This phenomenon suggests the stabilizing contribution of the background flow on the interchange mode. Thus, we analyze the nonlinear evolution of the interchange mode with keeping the flow by means of three-dimensional (3D) simulations. For this purpose, we have developed the numerical scheme to calculate the 3D profile of the flow consistent with experimental data at first [2], which is observed in a one-dimensional direction in LHD [3]. A static equilibrium calculated with the HINT code [4] is utilized as the initial state in the nonlinear dynamics simulation with the MIPS code [5]. The 3D flow results are incorporated in the initial perturbation. We apply this procedure to a strongly unstable static equilibrium. As shown in Fig. 3, the pressure profile is deformed due to the interchanged mode in the no flow case. When we increase the flow up to the 10 times larger amount of that in the experiment, such deformation is reduced. However, when we apply 30 times larger flow, the Kelvin-Helmholtz instability appears and enhances the deformation again. Thus, the background flow can provide the stabilizing window between the interchange and the Kelvin-Helmholtz instabilities.

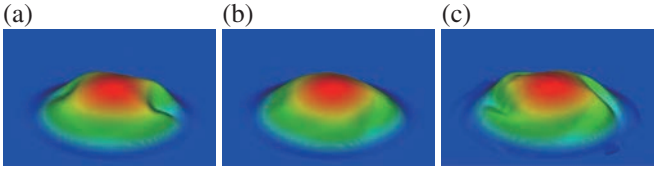

Fig. 3 Total pressure profile at early nonlinear saturation phase for the cases with (a) no flow, (b) flow with 10 times larger amount of the experiment, and (c) flow with 30 times larger amount of the experiment.

[1] S. Sakakibara *et al.*, 2015 Nuclear Fusion **55**, 083020.
[2] K. Ichiguchi *et al.*, Proc. IAEA FEC 2016 Kyoto, TH/P1-4.
[3] M. Yoshinuma *et al.*, Fusion Science Tech. **58**, 375 (2010).
[4] Y. Suzuki *et al.*, 2006 Nucl. Fusion **46**, L19.
[5] Y. Todo *et al.*, 2010 Plasma and Fusion Res. **5**, S2062.

(K. Ichiguchi)

Energetic Particle Physics

Highlight

Ion heating by plasma oscillations is demonstrated by the state-of-the-art simulation

In the future fusion reactors, energetic alpha particles born from the deuterium-tritium fusion reaction are expected to heat the bulk plasma through collisions to sustain the high temperature needed for the fusion reaction. However, the bulk ion heating by the energetic alpha particles through collisions is weak, while the electron heating is dominant. If the ion heating efficiency is enhanced, this leads to the improvement of the performance of fusion reactor. A mechanism called "alpha channeling" where alpha particle energy is transferred to bulk ions through the interaction with plasma oscillations was proposed a long time ago but has not been demonstrated.

Energetic particle driven geodesic acoustic modes (EGAMs) are electrostatic plasma oscillations in toroidal plasmas. EGAMs in the Large Helical Device (LHD) plasmas were studied with hybrid simulations for energetic particles interacting with a magnetohydrodynamic (MHD) fluid [1,2]. Recently, the program was extended to simulate bulk ions as particles in addition to energetic particles [3]. This extension enables us to investigate the energy channeling from energetic particles to bulk ions. The extended simulation was applied to EGAMS in the LHD plasmas. The plasma pressure fluctuations of an EGAM in the simulation are shown in Fig. 1. It was demonstrated for the first time that the energetic particle energy is transferred to the bulk ions through the interaction with the EGAM [4]. This result is expected to accelerate the studies of alpha channeling in experiment, theory, and simulation.

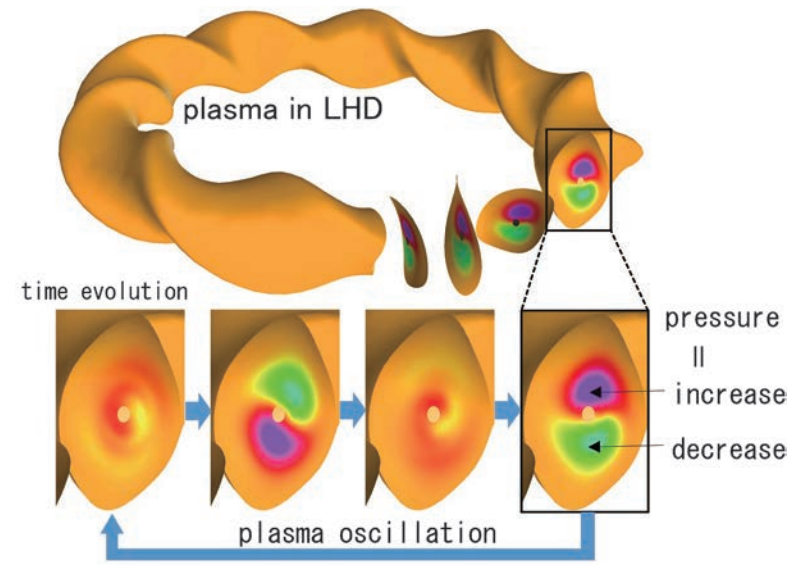

Fig. 1 Plasma oscillation excited by energetic particles in LHD. Plasma pressure fluctuations on the cross-sections of the doughnut-shaped plasma are shown in the figure. The red and green colors represent increase and decrease, respectively. The blue arrows indicate the time evolution.

[1] H. Wang *et al.*, Phys. Plasmas **22**, 092507 (2015).
[2] H. Wang *et al.*, Phys. Rev. Lett. **120**, 175001 (2018).
[3] Y. Todo *et al.*, "A new magnetohydrodynamic hybrid simulation model with thermal and energetic ions", in ITC-26 and APFA-11 (Dec. 5-8, 2017, Toki, Japan).
[4] H. Wang *et al.*, Nucl. Fusion **59**, 096041 (2019).

(Y. Todo and H. Wang)

Critical energetic particle distribution in phase space for the Alfvén eigenmode burst with global resonance overlap

Comprehensive computer simulations of the Alfvén eigenmode burst, which is the synchronized sudden growth of multiple Alfvén eigenmodes interacting with energetic particles, were conducted with continuous neutral beam injection, collisions, and particle losses [5]. Figure 2 shows the amplitude evolution of multiple Alfvén eigenmodes and the evolution of energetic particle transport flux profile. It is found in the simulation result that the energetic-particle distribution in phase space reaches a "critical distribution" with a stairway structure where a resonance overlap triggers the Alfvén eigenmode burst. Before the burst, the gradual growth of the Alfvén eigenmodes associated with the beam injection broadens the resonant regions in phase space forming the distribution into a stairway shape. When the distribution reaches the "critical distribution", a resonance overlap triggers multiple resonance overlaps leading to the synchronized growth of Alfvén eigenmodes and the collapse of the distribution. For another run with the beam deposition power reduced to one-half, the fast ion distribution function just before the Alfvén eigenmode burst is close to that for the original beam power. This result indicates that the critical distribution for the Alfvén eigenmode burst is present.

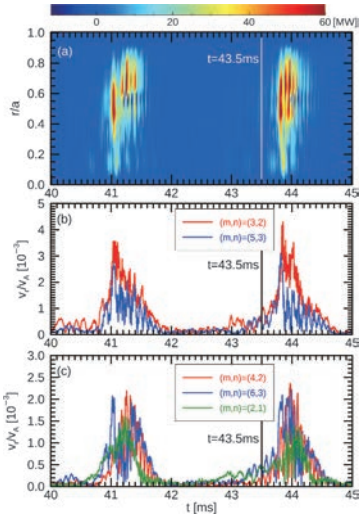

Fig. 2 (a) Radial profile evolution of fast ion energy transport flux in the radially outward direction, and amplitude evolution of radial MHD velocity fluctuation for (b) the dominant n=2 (red) and n=3 (blue) Alfvén eigenmodes and (c) the other Alfvén eigenmodes with n=1–3. The unit of color bar is MW [5].

[5] Y. Todo, Nucl. Fusion **59**, 096048 (2019).

(Y. Todo)

Energetic Ion Driven Instabilities near the Lower Hybrid Resonance Frequency

Using a one-dimensional electromagnetic particle code which simulates self-consistently the full ion and electron dynamics, we studied instabilities driven by energetic ions injected continuously in a plasma where the density and the lower-hybrid resonance frequency ω_{LH} increase with time [6]. We show in Fig. 3 the amplitudes of all the waves in the frequency range $0.5 < \omega/\Omega_i < 8$, where Ω_i is the ion cyclotron frequency, the color indicates the amplitudes of the magnetic fluctuations, and the yellow line represents the frequency ω_{LH}. We see in Fig. 3 that the ion cyclotron harmonic wave with $\omega \approx l\Omega_i$, where l is an integer, is excited when ω_{LH} becomes close to $l\Omega_i$. When ω_{LH} is greater than $l\Omega_i$, this wave couples with the ion Bernstein mode that has the dispersion curve connecting to ω_{LH}. We also see in Fig. 3 that as a result of the instabilities and the wave-wave coupling, the stair-like frequency chirping with the riser Ω_i appears in the magnetic fluctuations in the frequency range of ω_{LH}. The frequency chirping has characteristics similar to the frequency chirping observed in the radio frequency radiations at the plasma start-up phase of the LHD experiments.

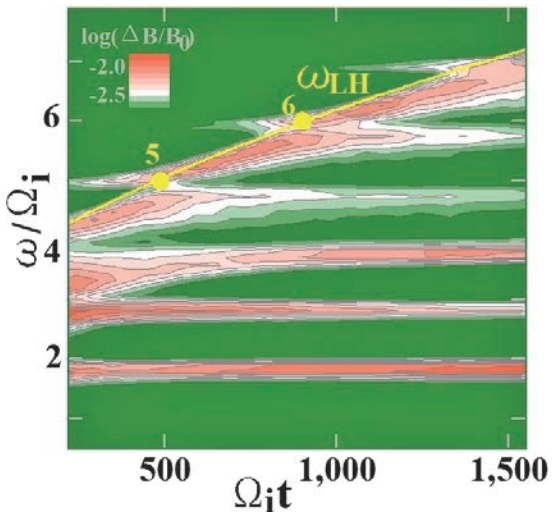

Fig. 3 Time variations of magnetic fluctuations in the frequency range of $0.5 < \omega/\Omega_i < 8$. The stair-like frequency chirping appears near the line $\omega = \omega_{LH}$ [6].

[6] M. Toida *et al.*, Plasma Fusion. Res. **14**, 3401112 (2019).

(M. Toida)

Study on the impurity transport phenomenon in LHD plasmas

Highlight

Global neoclassical transport simulation including the effect of small potential variation on the flux surfaces tackles with the unresolved problem of "impurity hole"

To realize steady-state operation of fusion reactor, accumulation of heavy impurity ions which come out from plasma-facing walls to the core plasma should be mitigated because they lead to radiation energy loss and decrease the performance of the plasma. From the conventional neoclassical transport theory, it is expected that the ambipolar radial electric field in $T_i \simeq T_e$ helical plasma is negative, which drags the impurity particle flux inward. Therefore, impurity accumulation is concerned in the future helical reactor. In LHD experiments, however, it was observed that impurity ions were sometimes expelled from the core region, although the neoclassical calculation predicted the negative electric field. Many theories and simulation studies have been trying to explain this "impurity hole phenomenon". One of possible extensions to the neoclassical transport simulation is to include the effect of electrostatic potential variation on the flux surface, which is caused by density anisotropy of bulk hydrogen ions. The potential variation, called "ϕ_1 potential", is usually as weak as $e\phi_1/T_e \sim 10^{-3}$, and its effect is negligible for bulk hydrogens and electrons. However, some preceding simulation studies have shown that the ϕ_1 potential substantially changes the impurity flux if the condition is set similar to the impurity hole plasma. Although the importance of ϕ_1 potential is recognized, no simulation studies so far have reproduced the outward impurity neoclassical flux to explain the impurity hole. However, the neoclassical transport simulation model can be further improved. FORTEC-3D code [1], which has been developed in NIFS, solves the global 5D drift-kinetic equation to evaluate the neoclassical transport. Since all the preceding ϕ_1-effect studies are based on the radially-local approximation, extension of FORTEC-3D to include the ϕ_1-effect is the world first challenge to study this problem using a global code. We have evaluated the ϕ_1 potential in an LHD plasma which is similar to the condition of impurity hole plasma and compared with local approximation simulations [2]. As shown in fig. 1, it is found that not only the amplitude but also the phase of the ϕ_1 potential is different between the radially-local and global simulation models. It is thought that the tangential magnetic drift, which is neglected in the radially-local model, is actually comparable to the E × B drift by the radial electric field in impurity hole plasma, and it affects the hydrogen density and the ϕ_1 potential variation. This finding suggests that the local approximation model is insufficient to predict the impurity neoclassical flux including the ϕ_1-effect. FORTEC-3D now is being upgraded for multi-species plasma, and the impurity flux in the global code will be calculated in the near future.

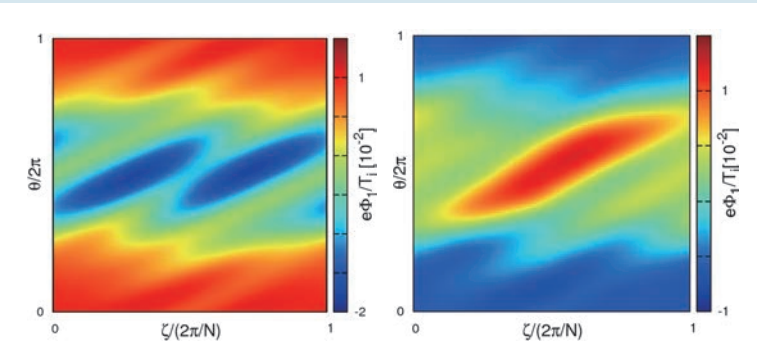

Fig. 1 Potential variation on a flux surface (r=0.6a) in an LHD plasma, calculated from a radially-local approximation (left) and global FORTEC-3D code (right). Here, (θ, ζ) represents the poloidal and toroidal angle [2].

[1] S. Satake, Y. Idomura, H. Sugama *et al.*, Computer Phys. **181**, 1069 (2010).
[2] K. Fujita, S. Satake *et al.*, Plasma Fusion Res. **14**, 3403102 (2019).

(S. Satake)

Reduced models for particle and heat transport by gyro-kinetic analysis with kinetic electron response

The particle and heat transport driven by the ion temperature gradient instability in helical plasmas is investigated by the gyrokinetic analysis taking into account the kinetic electron response [3]. Two types of transport models with a lower computational cost to reproduce the nonlinear gyrokinetic simulation results within allowable errors are presented for application in quick transport analyses. The turbulent electron and ion heat diffusivity models are given in terms of the linear growth rate and the characteristic quantity for the linear response of zonal flows, while the model of the effective particle diffusivity is not obtained for the flattened density profile observed in the LHD. The quasilinear flux model is also shown for the heat transport. The quasilinear flux models for the energy fluxes are found to reproduce the nonlinear simulation results at the accuracy similar to that of the heat diffusivity models. In addition, the quasilinear particle flux model, which is applicable to the transport analysis for LHD plasmas, is constructed and reproduces the nonlinear simulation results in the left of Fig.2. These turbulent reduced models enable coupling to the other simulation in the integrated codes for the LHD.

(S. Toda)

Temperature profile stiffness in turbulent transport of helical plasmas for flux-matching method

The plasma temperature profile sensitivities of the turbulent transport fluxes in helical plasmas are evaluated by the gyrokinetic simulations. Especially, in the simulations for the ion temperature gradient (ITG) turbulence in the LHD, it is found that the ion temperature gradients around the experimental observations are near the threshold of the instability, and the ion heat transport coefficients are quite sensitive to the temperature gradient. Using the statistical technique of Akaike's Information Criterion (AIC), a novel technique to determine the ranges of the temperature gradients possible given the experimentally obtained temperature data with errorbars is proposed. And the flux-matching method to predict the ion temperature gradient against the ranges of the temperature gradients is demonstrated for high ion temperature LHD plasma [4]. See the right of Fig.2. The results in the case of the simulations with adiabatic electron responses assumptions can predict the ion temperature gradient which agrees with the allowable temperature gradient ranges obtained from the AIC technique. On the other hand, in the simulations with kinetic electrons, the results are less than the adiabatic electron cases, because the simulations performed here are restricted under the assumptions that there are unintroduced effects such as ExB shearing effects, which may improve the predictions for ion heat transport, we should improve the simulation model.

[3] S. Toda *et al.*, Phys. Plasmas **26**, 012510 (2019).
[4] M. Nunami *et al.*, Phys. Plasmas **25**, 082504 (2018).

(M. Nunami)

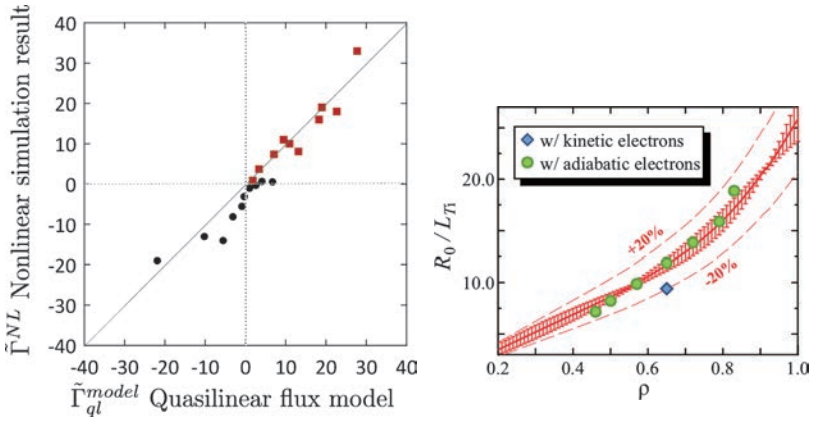

Fig. 2 Left: The comparison of the nonlinear simulation results for the particle flux with the quasi-linear flux model. Right: The allowable ranges of the temperature gradients evaluated by AIC technique (red curves) and the applications of the flux-matching method to expect the ion temperature gradients based on the simulations with kinetic electrons (blue diamond) and with adiabatic electrons (green circles).

TASK3D-a

TASK3D-a, Integrated Transport Analysis Suite, Has Been Facilitating LHD Deuterium Experiment Analyses

Further extension has been made in TASK3D-a [1], in particular, for facilitating analyses of LHD deuterium plasmas, such as on NBI (neutral beam injection)-heating and neoclassical transport in the presence of multiple ions (including hydrogen and deuterium as main species), neutron emission rate, and behaviour of energetic particles. The applications of this extended TASK3D-a (as shown in Fig. 1) have provided systematic analyses datasets and experimental validations for important research topics of LHD deuterium experiment. Issue-resolutions related to its applications have been made by TASK3D-a developer(s), which has been also critical for TASK3D-a to be routinely applied to experiment analyses.

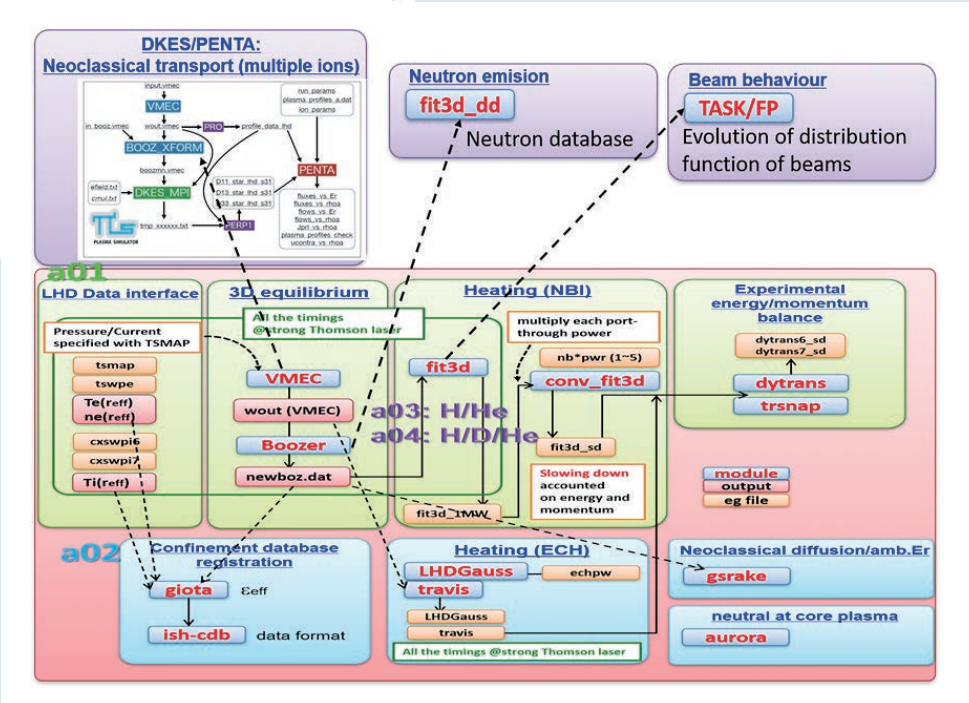

Fig. 1 Overview of extension of TASK3D-a series. Based on the first version, TASK3D-a01 released in 2012, several modules have been implemented (a02) and NBI module was upgraded (a03 and a04). Purple parts are related to analyses on the neoclassical transport in the presence of multiple ion species, neutron emission rate and energetic particles behaviour.

The integrated transport analysis suite, TASK3D-a [1], has been further extended mainly pursuing the increase of analyses capabilities of LHD deuterium experiments and of plasmas consisting of multiple ion species. The current overview of TASK3D-a suite is shown in Fig. 1. This extension includes extension of NBI heating analysis module in order to be applicable to the plasmas with hydrogen, deuterium and helium [2], and subsequent release of extended versions of TASK3D-a, such as TASK3D-a03 and -a04 as indicated in Fig. 1 (NBI module). This extension has been critical to provide systematic transport analyses database to investigate isotope effects in LHD deuterium experiments [3, 4].

Programmatic actions have also been made for analyses of the neutron emission rate and the energetic particles behaviour. The database, created by employing the TASK3D-a framework for the neutron emission rate in a wide range of temperature and density [5], has been routinely utilized to machine time allocations. TASK/FP [6], which is the module of TASK [7] for solving the Fokker-Planck equation, has been implemented in TASK3D-a framework. It has greatly facilitated the energetic particles behaviour of LHD deuterium plasmas, such as analyses on distribution functions of beam energy in NBI-blip experiment [8], and validation calculations on nonlinear collision effects during the process of slowing down [6].

In this way, TASK3D-a has been extended by implementing new modules and upgrading the previously included modules, to be more relevant to experimental conditions. It has been routinely utilized as the integrated analyses framework for a variety of research topics.

An example of accumulated transport analyses database is shown in Fig. 3 [9] (this is only a tiny part of overall TASK3D-a analyses results), which has opened a linkage to so-called data-driven science. Some trials for modelling ion heat diffusivity [10,11] have been made based on statistical approach exploiting “largeness” of TASK3D-a analyses database. This is another aspect of the significance of TASK3D-a.

[1] M. Yokoyama *et al.*, Nucl. Fusion **57**, 126016 (2017).
[2] P. Vincenzi *et al.*, Plasma Phys. Control. Fusion **58**, 125008 (2016).
[3] H. Yamada *et al.*, 27th IAEA Fusion Energy Conference (FEC), EX/P3-5 (Ahmedabad, Oct. 2018).
[4] K. Tanaka *et al.*, 27th IAEA FEC, EX/P3-6 (Ahmedabad, Oct. 2018), submitted to Nucl. Fusion (2019).
[5] R. Seki *et al.*, accepted for publication in Plasma Fus. Res. (2019).
[6] H. Nuga *et al.*, Nucl. Fusion, **59**, 016007 (2019).
[7] A. Fukuyama, http://bpsi.nucleng.kyoto-u.ac.jp/task
[8] H. Nuga *et al.*, European Physics Society Conference 2017, P1.146 (Belfast, Jun. 2017).
[9] M. Yokoyama, Plasma Fus. Res. **9**, 1302137 (2014).
[10] M. Yokoyama and H. Yamaguchi, Plasma Fus. Res. **14**, 1303095 (2019).
[11] M. Yokoyama, submitted to Nucl. Fusion (2019).

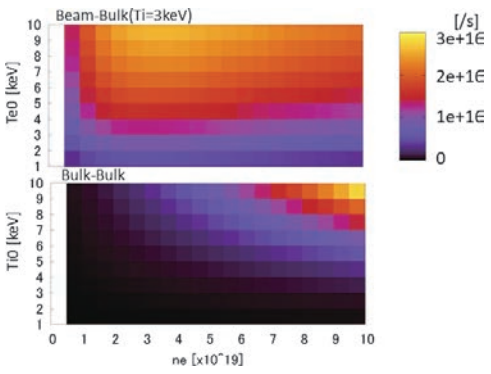

Fig. 2 Sample of database of neutron emission rate for (upper) beam-bulk and (lower) bulk-bulk components. The color represents the neutron emission rate. This figure is a reproduction from Ref. [5].

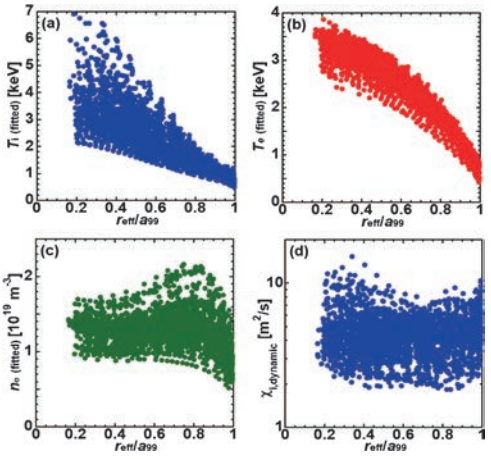

Fig. 3 An example of transport analyses database created by TASK3D-a applications, (a) ion temperature, (b) electron temperature, (c) electron density, and then (d) ion heat diffusivity. These plots are reproduced from Ref. [9].

(M. Yokoyama)

Numerical Simulations on Plasma-wall Interaction

FDTD simulation on absorption of electromagnetic waves in tungsten fuzz structure

Tungsten fuzz structure was found in the plasma-wall interaction study in fusion science by the Takamura group at Nagoya University [1]. We, the PWI simulation group at NIFS, have been succeeding in creating the initial fuzz structure "in silico" by BCA-MD-KMC hybrid simulation [2]. The fuzz structure is regarded as a nuisance to confine the plasma in the nuclear fusion device, but as a by-product it has possibility to behave as a photonic crystal, because the optical absorptivity of the fuzz structure becomes almost 100% from visible to near infrared wavelength range. Thus it was known that the fuzz structurization increases the aborptance of electromagnetic (EM) wave in tungsten.

We revealed the mechanism of the high absorptivity of the tungsten fuzz structure by finite-difference time-domain (FDTD) simulation of simplified tungsten structures, i.e., the convex, the concave and the porous models [3]. Using FDTD simulation, we found that the nano-structures cause the enhancement of the EM-wave around them and then enhanced EM-wave generates the induced current in the surface of the tungsten. Thereby, the energy of the incident EM-field is transferred to the Joule heat derived by the induced current around the tungsten surface.

We, moreover, simulated "real fuzz structure" which was measured with transmission electron microscopy (TEM. Tecnai Spirit G2, 120 kV, ×15 k, spot size 6) at the Yasunaga laboratory of Kyushu Institute of Technology. The three dimensional structure (Fig. 1) of the fuzz was reconstructed from tilt series (2 degrees from –64 to +64) by electron tomography (ECT using our developed Eos image processing package and eTomo provided by Dr. Mastronarde et al. at the University of Colorado). From the simulation (Fig. 2), it is found that optical reflectance reduction is caused by confinement of the electromagnetic field in the tungsten fuzz structure as well as in the simplified tungsten structures.

Fig. 1 Tungsten fuzz structure by transmission electron microscopy (TEM. Tecnai Spirit G2, 120 kV, ×15 k, spot size 6) at the Yasunaga laboratory of Kyushu Institute of Technology. The structure size is 202 nm × 202 nm × 530 nm.

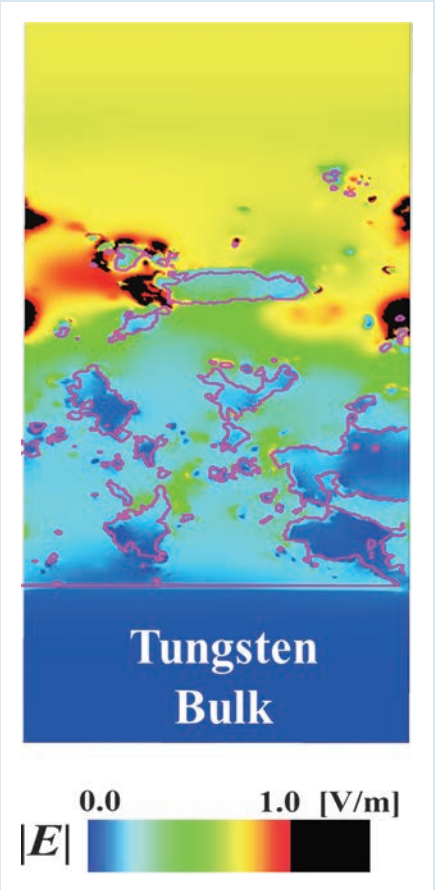

Fig. 2 Spatial-distribution of the time averaged electric field $|\boldsymbol{E}|$. The regions surrounded by the closed pink curve indicates tungsten fuzz structures. The electric field is enhanced by the tungsten fuzz structure in the black region.

[1] S. Takamura *et al.*, Plasma Fusion Res. **1**, 051 (2006).
[2] A. M. Ito *et al.*, Plasma and Fusion Res. **13**, 3403061 (2018).
[3] H. Nakamura *et al.*, International Conference on Plasma Surface Interactions in Controlled Fusion Devices (PSI-23), Princeton University, NJ, USA, 17–22 June 2018.

(H. Nakamura)

Neutron irradiation effects on bubble formed tungsten material

As a result of the nuclear fusion between deuterium and tritium, neutrons are generated with an energy of 14.1 MeV. By the neutron irradiation, nuclear transmutation and defects are induced in the divertor. These damages cause the change of property as plasma facing materials (ex., tungsten). Helium bubbles are generated in the surface of the tungsten, which is irradiated by helium plasma. We, therefore, investigate the neutron irradiation effects on bubble formed tungsten by Monte Carlo simulation code PHITS (Particle and Heavy Ion Transport code System)[4].

Tungsten is set in the region where z>0. A circle with the radius of 5 cm is prepared as a neutron beam. The neutron emission points are set uniformly on the circular surface. Helium bubbles spread near the surface of the tungsten. The number and the positions of helium bubbles are determined by binary collision approximation based simulation [5]. From the simulation results (Fig. 3), we found that the helium bubbles affect trajectories of the neutrons and the electron generation at the surface of the helium bubbles [6].

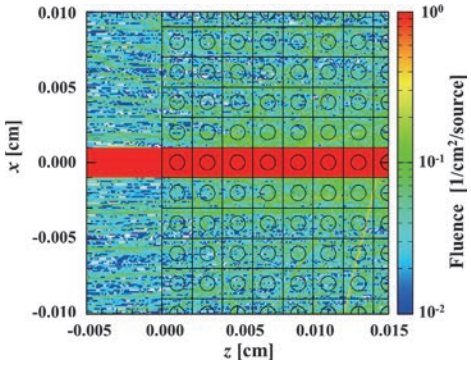

Fig. 3 Trajectories of Neutron. The incident kinetic energy of the neutron beam is fixed to 14.0 MeV. The radius of the neutron beam is 0.001 cm. The color of the trajectories denotes the flux of the neutrons. Helium bubble in tungsten target is set in the region ($z > 0$).

[4] T. Sato *et al.*, J. Nucl. Sci. Technol. **55**, 684 (2018).
[5] S. Saito *et al.*, Jpn. J. Appl. Phys. **55**, 01AH07 (2016).
[6] S. Saito *et al.*, 11th International Symposium on Advanced Plasma Science and its Applications for Nitrides and Nanomaterials, 12th International Conference on Plasma-Nano Technology and Science (ISPlasma2019/IC-PLANTS 2019), March 17–21, 2018 Nagoya Institute of Technology, Nagoya Japan.

(T. Sato, Yamagata University)

Molecular Dynamics Study on DNA Transformation by Tritium Disintegration

Towards better physical understanding of DNA transformation by tritium, we have examined double strand breaks of giant DNA molecules using a single molecule observation (SMO) technique at Toyama University [7]. However, separation of effects of ray irradiation (direct and indirect actions) from those of bond cleavage by tritium decay to inert helium-3 is difficult even if we use SMO method. Therefore, we have decided to adopt molecular dynamics (MD) simulation to elucidate the mechanism how beta-decays of substituted tritium give the effect to DNA [8].

We adopted a human telomeric DNA structure, where we replaced some hydrogen atoms in guanines to helium atoms. This replacement denotes the beta-decay of tritium into helium-3.The temperature of the system composed of DNA and water molecules is fixed to 310K with Langevin thermostat algorithm. Using NAnoscale Molecular Dynamics (NAMD) code[9]. Using these telomere structures where N hydrogen atoms are replaced with helium atoms in the guanine, we perform the MD simulation. To clarify the fragility of the DNA, we calculated the root mean square deviation (RMSD) for each N. In the case of N=0 (the original DNA), the DNA structure is saturated around 2 Å (Fig. 4). As N is increased, the RMSD becomes larger. From this result, we found that, as the number of the replaced helium increases, the double helix structure of the telomere becomes more fragile [10, 11].

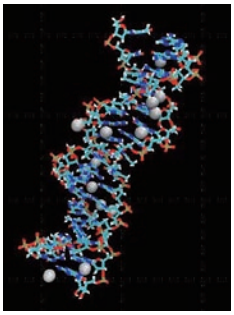

[7] Y. Hatano *et al.*, Fusion Eng. Des. **146**, 100 (2019).
[8] S. Fujiwara *et al.*, J. Adv. Simulat. Sci. Eng. **6**(1), 94 (2019).
[9] http://www.ks.uiuc.edu/Research/namd/
[10] H. Nakamura *et al.*, 11th international Symposium on Advanced Plasma Science and its Applications for Nitrides and Nanomaterials, 12th International Conference on Plasma-Nano Technology and Science (ISPlasma2019/IC-PLANTS 2019), March 17–21, 2018 Nagoya Institute of Technology, Nagoya Japan.
[11] H. Nakamura *et al.*, Jpn. J. Appl. Phys. (accepted), https://doi.org/10.7567/1347-4065/ab460d.

Fig. 4 The telomeric DNA structure. The length between DNA chains becomes larger as time passes. Wide gaps between chains are found clearly at the ends of DNA.

(H. Nakamura)

4. Basic, Applied, and Innovative Research

As an inter-university research institute, NIFS activates collaborations with researchers in universities as well as conducting world-wide top level researches. The collaboration programs in basic, applied, and innovative research support research projects motivated by collaboration researchers in universities. It is also important to establish the academic research base for various scientific fields related to fusion science and to maintain a powerful scientific community to support the research. Programmatic and financial support to researchers in universities who work for small projects are important. As an inter-university research institute in fusion science, NIFS performs such an important role and the programs in basic, applied, and innovative research are prepared for this purpose.

For basic plasma science, NIFS operates several experimental devices and offers opportunities to utilize them in the collaboration program for university researchers. A middle-size plasma experimental device HYPER-I is prepared for basic plasma research. The compact electron beam ion trap (CoBIT) for spectroscopic study of highly charged ions, atmospheric-pressure plasma jet devices for basic study on plasma applications, and other equipment are operated for collaborations.

(I. Murakami)

Development of thermal conductivity in warm dense matter using pulsed-power discharge

A warm dense matter (WDM) is the intermediate state of matter, which is neither solid nor plasma. To understand the relation between solid state and plasma physics, a theoretical description of WDM is one challenge. Since the WDM has high pressure and dense matter state, we should develop how to observe the properties of WDM with well-defined state. To observe the thermal conductivity of a WDM sample, we developed a laser-induced fluorescence method to observe the thermal conductivity of tungsten WDM confined within a ruby capillary. We determined the density and temperature of the plasma generated by an isochoric heating device using a pulsed-power discharge. The density and the temperature were determined by the initial diameter of the tungsten wire, and were obtained by spectroscopic measurements, respectively. The temperature of the ruby capillary was obtained from its fluorescence intensity, which depends on the temperature of the outer wall. The experimentally obtained thermal conductivity is approximately 30 W/K m. We succeed that the thermal conductivity of WDM states is directly evaluated using the proposed method [1].

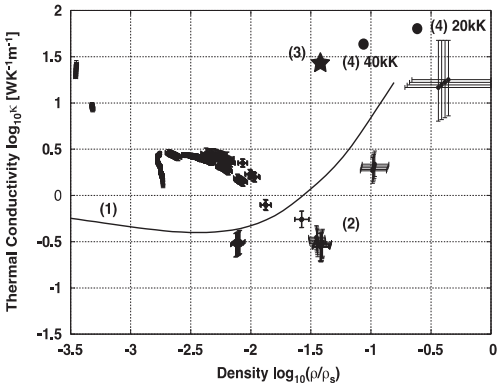

Fig. 1 Thermal conductivity of tungsten plasma as function of density at 10,000 K. (1) The solid line indicates the thermal conductivity given by the Kuhlbrodt-Holst-Redmer model from COMPTRA04. (2) The data points with error bars show semi-empirical estimates obtained using the Wiedemann-Franz law. (3) The star point plots the results obtained in the present study. (4) The circle point plots semi-empirical estimates obtained using the Wiedermann-Franz law with Rakhuk's results. Cited from [1].

(K. Takahashi and T. Sasaki, Nagaoka Univ. Tech.)

Development of a polarization-modulation spectroscopy system for helium atom emission lines

The deviation of the electron velocity distribution (EVD) from isotropic Maxwellian is seen in various interesting plasma phenomena. For a better understanding of these phenomena and detailed comparisons between experiments and kinetic simulations, it is necessary to develop a method that can measure the three-dimensional EVD. As a possible method, we focus on the polarization of atomic emission lines. When the EVD shape becomes anisotropic, the emission lines are slightly polarized. The intensity and polarization degree for a given EVD vary with the type of transition, thus, the EVD shape can be deduced by measuring these quantities of multiple emission lines. We have developed a polarization-modulation spectroscopy system to measure full Stokes parameters of visible emission lines and applied the system to a helium ECR plasma (Fig. 2) [2].

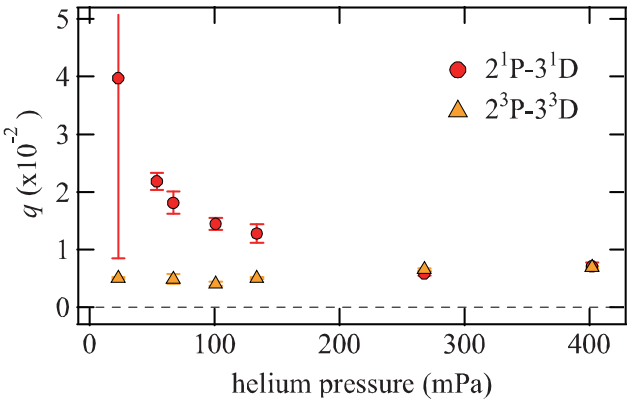

Fig. 2 Helium pressure dependence of a normalized Stokes parameter q (corresponding to the linear polarization degree in the direction perpendicular to the magnetic field) for two types of helium atom emission line.

(T. Shikama, Kyoto Univ.)

Improving biocompatibility of titanium alloy by atmospheric-pressure plasma nitriding

Several studies reported that the biocompatibility of titanium alloys can be improved by doping nitrogen atoms into the titanium surface. Our research group has developed the simplest technology of nitrogen doping with atmospheric-pressure plasmas, where no vacuum equipment is necessary although conventional plasma technology requires it. We recently achieved nitrogen doping to titanium surface by using our original atmospheric-pressure plasma nitriding with the pulsed-arc plasma jet [3]. In this article, we report the newest results on biocompatibility of titanium alloy into which nitrogen atoms have been doped by the plasma-jet nitriding. As shown in Fig. 3, the nitrided (left, golden color due to TiN surface) and the untreated samples (right, original gray color) are immersed into the simulated body fluid at 37°C for 10 days. Here, both of the samples have lost metallic luster owing to the formation of calcium phosphate layer. As a result of thickness comparison of the formed layer, we have demonstrated that the formation ability of the calcium phosphate on the nitrided sample outperforms that on the untreated sample [4]. This indicates that nitrogen doping by our method can upgrade hard-tissue compatibility of titanium alloy.

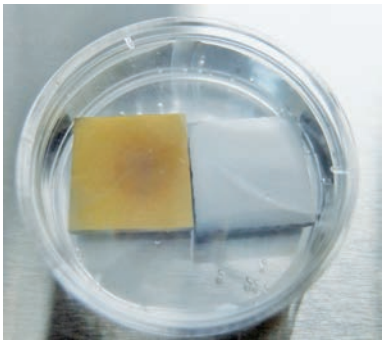

Fig. 3 Plasma-nitrided (left) and untreated (right) titanium immersed in simulated body fluid.

(R. Ichiki, Oita University)

[1] S. Sugimoto *et al.*, Phys. Plasma **24**, 072703 (2017).
[2] T. Teramoto *et al.*, Appl. Phys. Lett. **112**, 214101 (2018).
[3] Y. Yoshimitsu *et al.*, Jpn. J. Appl. Phys. **54**, 030302 (2015).
[4] R. Sannomiya *et al.*, Plasma Fusion Res. **13**, 1306120 (2018).

5. Fusion Science Archives (FSA)

The Fusion Science Archives was established in 2005 to learn lessons from the past fusion science archives preserved and to maintain collections of historical documents and materials that are related to fusion research in Japan. These activities are important from the viewpoint of the historical evaluation of fusion research, its social accountability and making references for seeking future directions.

Since then, historical materials on fusion research and/or organizations related to fusion research have been collected and preserved at FSA. They are stored in acid-free folders and boxes. The total number of registered items is now approximately 25,400. Most of those catalogues are available to the public through the internet in a hierarchical structure and can be accessed by the use of an electronic retrieval system.

The following collaborative works are performed this fiscal year along this line:

- **Establishment and Evolution of the Inter-University Research Institute Corporation System (NIFS16KVXV010)** K. Matsuoka (NIFS, FSA) *et al.*
  Fusion research at inter-university research institute should be basic and academic taking the realization of fusion energy into consideration as Hideki Yukawa pointed out in the 1950s. Research at IPP Nagoya University was not based on this guideline because of the following reasons. 1) Basic plasma experiments in 1960s at IPP Nagoya University were excellent, but not useful for fusion energy. 2) JIPP T-II of stellarator/tokamak hybrid type, the principal machine of the second term program, was the strongest machine having magnetic field of 3 Tesla. To cope with the tilting force of TF coil, it was equipped with shear panels that severely hindered diagnostics essential for academic research without serious discussion on what was the academic purpose of JIPP T-II.
- **Archives of the Historical Material related to the Plasma Spectroscopy (NIFS17KVXV0011)**
  N. Yamaguchi (Comprehensive Research Organization for Science and Society (CROSS)) *et al.*
  Workshops called "Plasma Elementary Process workshop" or "Spectroscopy workshop" have been held as a collaboration research of Institute of Plasma Physics, Nagoya University (IPP) and NIFS from 1969 to the present. The editing work of the history of the these workshops is continued from last fiscal year. The agenda and reports of each workshop are piled up as an annex of the history.
- **Studies on History of Activities of Researchers at the dawn stage of Fusion Research in Japan (NIFS17KVXV012)** T. Amemiya (CST, Nihon Univ.) *et al.*
  The History of Science Group of CST, Nihon University investigated the history of fusion research in Japan from the 1950s to the 1960s. In this collaborative work, the focus is placed on the individual researchers or the organizations that have led research in the dawn of fusion in Japan utilizing the historical documents in the NIFS FSA and the KEK archives office. The subjects specifically investigated in this fiscal year are as follows: (i) On the drafting and postponing of the B-plan by the Special Panel on Nuclear Fusion Research (Kakuyugo Senmonbukai), (ii) On the background about drafting of Institute of Plasma Physics based on letters between Kodi Husimi and Eiichi Kawasaki, and (iii) On the efforts to address the Atomic Energy by Japanese Physicists at the dawn of the nuclear age in Japan.
- **Development of a Cooperating System of Archives Finding Aids and Technical Terms Databases as a Supporting Tool (NIFS16KVXV013)** Y. Takaiwa (KEK, Archives Office) *et al.*
  The aim of this work was to prepare dictionaries of technical terms, proper nouns of important persons or a project's name and to relate them to the the catalog database of archived materials. This fiscal year, identifying the technical terms, proper nouns to be picked up, and searching the mechanism to relate them are tried. Regarding the collection of the technical terms, the glossary which collected the columns appeared in the *Journal of Plasma and Fusion Research* is identified to be an adequate starting point. The collection of proper nouns is covered by other collaborative works (NIFS17KVXV014). Furthermore, it is identified that establishment of the mechanism to relate them to the present catalog database requires too much work under the present collaboration framework.
- **Making name authority data about persons, groups, and organizations appearing in FSAD, related to fusion science in Japan (NIFS17KVXV014)** H. Gotoh (The Kyoto University Museum) *et al.*
  FSA accepts various materials related to the fusion science history. It picks up essential information from materials, organizes it, and stores it in the database. The archives catalog created in such a way is provided to the users of interest. Researchers or research groups on fusion science and their mutual relations are not clear for the user only from the catalog. The purpose of this research is to clarify the method of accumulating and sorting the directories of those who have committed to fusion science. Issues found during last year and progress for resolving these issues during this year were the following: (1) Realized the standard electrical database of the researchers on fusion science from its early stage to the present is missing. In total 1,300 researchers are registered from the directory of "KAKUYUGO (HANNOH) KONDANKAI" *etc.* and compared with other databases to confirm the validity. (2) Identified the existence of important elements that are not included in the standard authorized

database. Tried to find the relations or interactions between other researchers and research groups, but found it requires a more efficient method and much more effort. (3) Need to find the method to modify the existing databases of authority records in library world. The method of the authority control will be examined.

- **Archival Studies on Collaborations in Heliotron Studies at Kyoto University (NIFS17KVXV015)**
  T. Mizuuchi (Kyoto Univ.) *et al.*
  The activity of the archives of this fiscal year focused on the materials related to the development of the plasma experimental devices in contrast to the FSA activity in NIFS mainly on the fusion researchers and research organization. In this regard, the archives activity are promoted on the development of the series of Heliotron devices originated from Kyoto University. The range of objects of the archives is extended to the researchers, research group, and their activity which led the Heliotron development.
- **Investigation and Analysis of Historical Materials on Startup and Development Phase of Fusion Technology Research in Japan (NIFS17KVXV016)** H. Yoshida (Nippon Advanced Technology) *et al.*
  The startup and development phase of the fusion technology research in Japan was investigated from the view point of Japan Atomic Energy Research Institute (JAERI) and the Institute of Plasma Physics, Nagoya University (IPPJ) under the collaboration with FSA. Following the interview with Shigeru MORI last year about the origin and the background of the fusion reactor technology research in JAERI, he suggested that there had not been close relationship between those in JAERI and in IPPJ and universities. In this year the cooperation with Shiori ISHINO (Prof. Emeritus, Univ. Tokyo) has began about the investigation of the origin and the background of the material research development in universities. With this three year collaboration project, we have fixed the concept to investigate the startup and development phase of the fusion reactor engineering research in Japan. This collaboration will be succeeded as a new theme in the next year.
- **History of the early days of Nuclear Fusion Research Group in Japan (NIFS17KVXV017)**
  C. Namba (NIFS FSA) *et al.*
  The organization "Nuclear Fusion Research Group of Japan" (KAKUYUGO KONDANKAI) was established in 1958. Dr. H. Yukawa was the first president of this organization. This KAKUYUGO KONDANKAI continued to perform an important role in the research and development in fusion science in Japan as a voluntary organization for researchers until it became "The Japan Society of Plasma Science and Nuclear Fusion Research" in 1983. The theme of this work is to clarify the establishment process of the KAKUYUGO KONDANKAI and how organized researchers and how planned to promote the fusion development research. KAKUYUGO KONDANKAI was formed as a researcher's voluntary organization to promote plasma physics which is the base of fusion science independent but derived from "Assembly for Nuclear Fusion Reactions" (KAKUYUGO HANNOH KONDANKAI) established under Science Technology Agency.
- **Collaborative Activities at NIFS Fusion Science Archives (NIFS FSA) (NIFS17KVXV018)**
  S. Kubo (NIFS, FSA) *et al.*
  The purpose of this collaboration is to arrange and promote the general archival activities under the NIFS collaboration framework. More than 50 researchers from universities and research institutions have joined this collaboration research. Ten collaboration programs were approved and performed as a NIFS general collaboration (NIFSKVXV010-019). One workshop type collaboration (NIFS18KKGV003) is approved and performed as a second Archives in Natural Science Workshop in January 2019 at NIFS.
- **Construction of Digital Library of Husimi Kodi Archives (NIFS18KVXV019)** H. Iguchi (NIFS, FSA) *et al.*
  Historical documents left by Kodi Husimi, the first director of Institute of Plasma Physics, Nagoya University, are the most important property of the NIFS Archives. Many documents are more than 50 years old, and their paper quality is seriously degraded. We are promoting digitalization of these documents. It is necessary not only for permanent preservation of the historically useful documents but also for opening the documents for public use. About 600 documents among a total of more than 5,000 Husimi documents are now preserved as PDF files. The job is just getting started and continuous work is necessary.
- **Studies of archival activities in research institutes from various points of view (NIFS18KKGV003)**
  E. Kikutani (KEK, Archives Office) *et al.*
  Archives activities in the Inter-University Research Institute Corporation of mainly in the natural sciences have been studied for more than ten years. During this process, the importance of the theoretical and technical methods of collection, preservation, registration, cataloging, and archiving are re-realized. The information exchange among the organizations for archives is also important. Workshops for discussing the archives in the field of natural sciences have been held twice a year for these few years. The workshop held under the support of NIFS collaboration in this fiscal year focussed on the "Official Document Management Law".

(S. Kubo)

6. SNET Collaborative Research

SNET has been operating dedicated to the fusion research collaborations, *i.e.*, the Fusion Virtual Laboratory (FVL) in Japan. SNET consists of a cluster of layer-2 and layer-3 virtual private network (L2/L3-VPN) circuits which inter-connect the collaborative universities and institutes via the national academic network backbone SINET5 operated by National Institute of Informatics (NII). Since 2017, SNET has given the priority to the bilateral collaborations on remote data acquisition and archiving because other remote accesses are already served by SSL–VPN. In 2018 fiscal year (FY), the fusion experiments of three Japanese universities, QUEST in Kyushu University, GAMMA10/PDX in University of Tsukuba, and TST-2 in University of Tokyo, are connected via SNET to share the LHD data storage.

The TST-2 experiment remotely acquires the MIR data synchronously with its operational sequence, whose amount was 86.6 GB on 960 plasma discharges in 2018 FY. Figure 1 shows a typical result of the MIR data analysis on the TST-2 ohmic plasma. Two-dimensional fluctuations of equal density surface just before, in the middle, and just after the internal magnetic reconnections happened were observed by using 6 × 6 array.

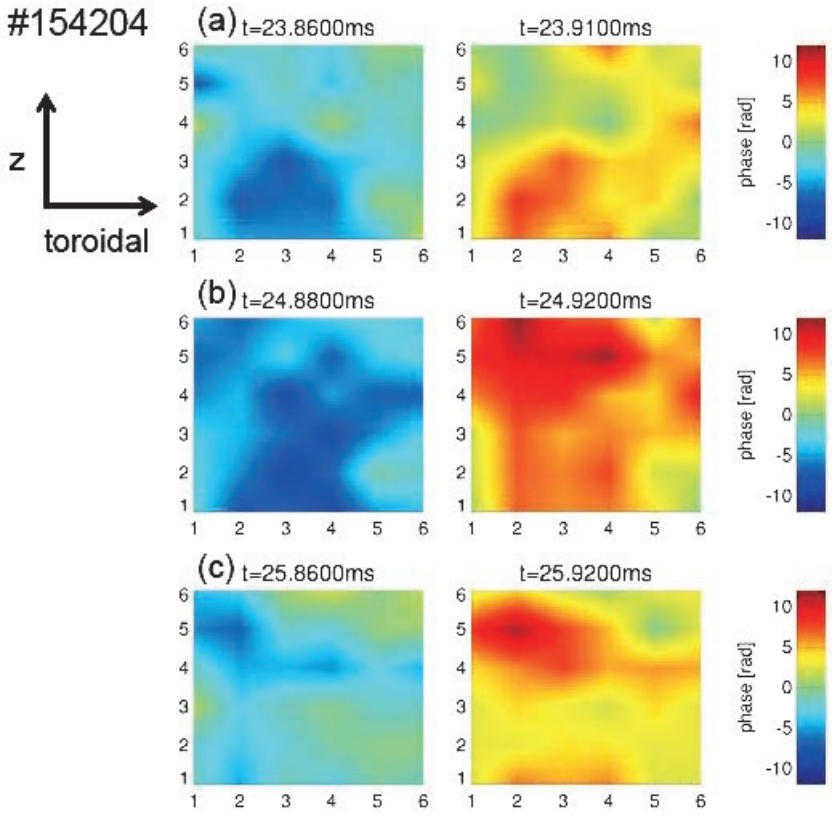

Fig. 1 Two-dimensional phase images where (a) t_{sp} ~ –1.08 ms, (b) t_{sp} ~ –0.08 ms, and (c) t_{sp} ~ +0.92 ms, respectively. X and Y axes show the channel nos. whose intervals are approximately 27 mm. Left and right images show the phases in the fluctuation's bottom and top time, respectively.

Research highlights

One of the important objectives of the SNET collaboration is to execute the feasibility study on the real-time replication between multiple data repository sites by using 10 Gbps and higher bandwidth long-distance network, such as SINET. For the multi-point date replication, two possible approaches can be considered, daisy-chain and parallel transfers. The most effective solution would probably be the combination use of these two methods. National Institute of Informatics (NII), National Institutes for Quantum and Radiological Science and Technology (QST), and NIFS have been collaborating to conduct some performance comparison tests across those three sites by using the real LHD data of the 20th campaign.

The uplink bandwidth of each site is 20 Gbps (NIFS), 40 Gbps (NII), and 10 Gbps (QST), respectively. Thus, the transfer tests were made under the traffic limitations of 16 Gbps between NIFS and NII, and 8 Gbps to QST. Figure 2 shows the traffic results made by the daisy-chain and parallel transfer tests. The whole LHD data of the day were always able to be replicated to the other two sites within 40 minutes. By changing the applied transfer method, we have successfully compared the characteristic differences and also the overall throughputs between these two methods. Through the verification tests, the daisy-chain transfer can been found to be faster in total replication time than the parallel one with the following conditions:

i. The network bandwidth at the source site is insufficient for performing parallel transfers to all the destination sites at once
ii. A destination site has a higher bandwidth than the source site
iii. The empty time after completing the transfer to the relay site could be used effectively.

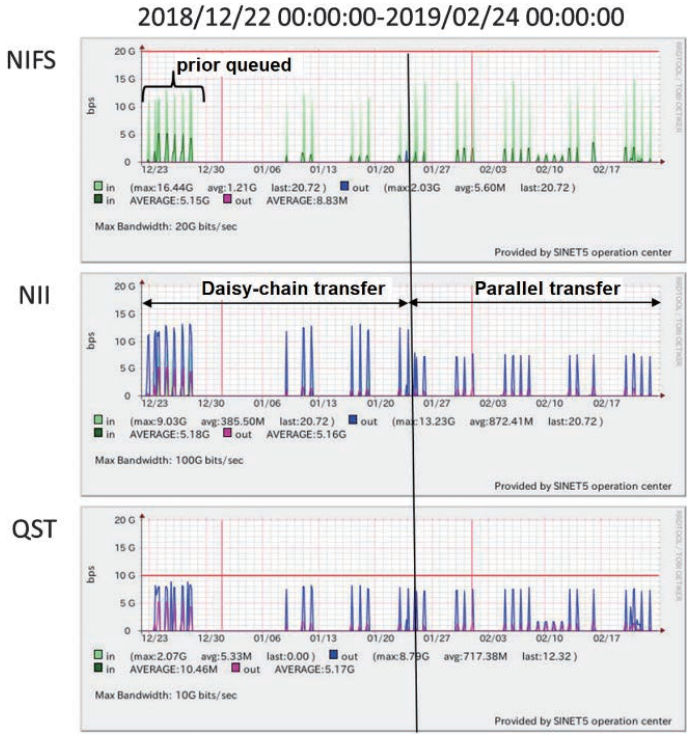

Fig. 2 Observed traffic at sender (NIFS), relaying (NII), and receiver nodes (QST), in both daisy-chain and parallel transfer tests.

(H. Nakanishi)

7. Network-Type Collaboration Research

The NIFS General Collaboration has been basically based on a one-to-one (especially, NIFS-to-University) collaborative system. Some collaborations, however, require the use of more than one experimental facility in different universities and institutes to achieve their objectives. In the network-type collaboration, this type of collaboration becomes practicable by admitting travel expenses for moving between universities, which have not been admitted as a rule in the general collaboration projects.

Since FY 2011, NIFS has employed this network-type collaboration. Three projects of the different fields were accepted in FY 2011 for the first time. Challenges in these collaborations spread over various fields. Before starting the collaborations, a collaboration plan for the year should be submitted. The plans include the items how the collaborations between research institutes are planned, that is, who goes when and where by what purpose.

In this fiscal year, eight proposals were submitted and six were accepted. The titles of the research items are listed below.

(1) "Effect of the resonant magnetic perturbation on MHD phenomena of toroidally magnetized plasmas" M. Okamoto (National Institute of Technology, Ishikawa College)
(2) "Hydrogen isotope retention of plasma facing materials damaged by neutron irradiation" N. Ohno (Nagoya University).
(3) "Interdisciplinary study of plasma heating at O-point and X-point using laboratory experiments, numerical simulations and solar observations" M. Ono (The University of Tokyo).
(4) "Comprehensive Understanding of Plasma Flow by Creation of a Basic Plasma Network" T. Kaneko (Tohoku University)
(5) "Tritium, radon and radium concentrations in environmental water samples in Japan" M. Hosoda (Hirosaki University)
(6) "Construction of gyrokinetic simulation research network" T. Watanabe (Nagoya University)

The items (1) to (3) are continuing items and others are new items in FY2018. The items (1), (3) and (4) are related to the intercommunication of researchers and students, and are the comparative researches of the results obtained in the different devices in universities, institutes, and NIFS.

The item (2) is related to the inspection of neutron-irradiated materials by utilizing the compact divertor plasma simulator (CDPS) installed at the Oarai Center of Tohoku Univ. The item (5) requires the movement of researchers and students over wide areas to collect samples in different places. The item (6) is related to construct a simulation research network to enhance the simulation research activities using gyrokinetic codes in Japan.

And all proposals take advantage of the merit of the network-type collaboration.

(S. Masuzaki)

8. Bilateral Collaboration Research Program

The purpose of the Bilateral Collaboration Research Program (BCRP) is to enforce the activities of nuclear fusion research in the universities by using their middle-size experimental facilities of the specific university research centers as the joint-use facilities for all university researchers in Japan. The current program involves 5 university research centers, as follows:

- Plasma Research Center, University of Tsukuba
- Laboratory of Complex Energy Process, Institute of Advanced Energy, Kyoto University
- Institute of Laser Engineering, Osaka University
- Advanced Fusion Research Center, Research Institute for Applied Mechanics, Kyushu University
- Hydrogen Isotope Research Center, University of Toyama

In BCRP, each research center can have its own collaboration programs using its main facility. Researchers at other universities can visit the research center and carry out their own collaboration research there, as if the facility belongs to NIFS. That is, all these activities are supported financially by NIFS as the research subjects in BCRP. The BCRP subjects are subscribed from all over Japan every year as one of the three frameworks of the NIFS collaboration program. The collaboration research committee, which is organized under the administrative board of NIFS, examines and selects the subjects.

(T. Morisaki)

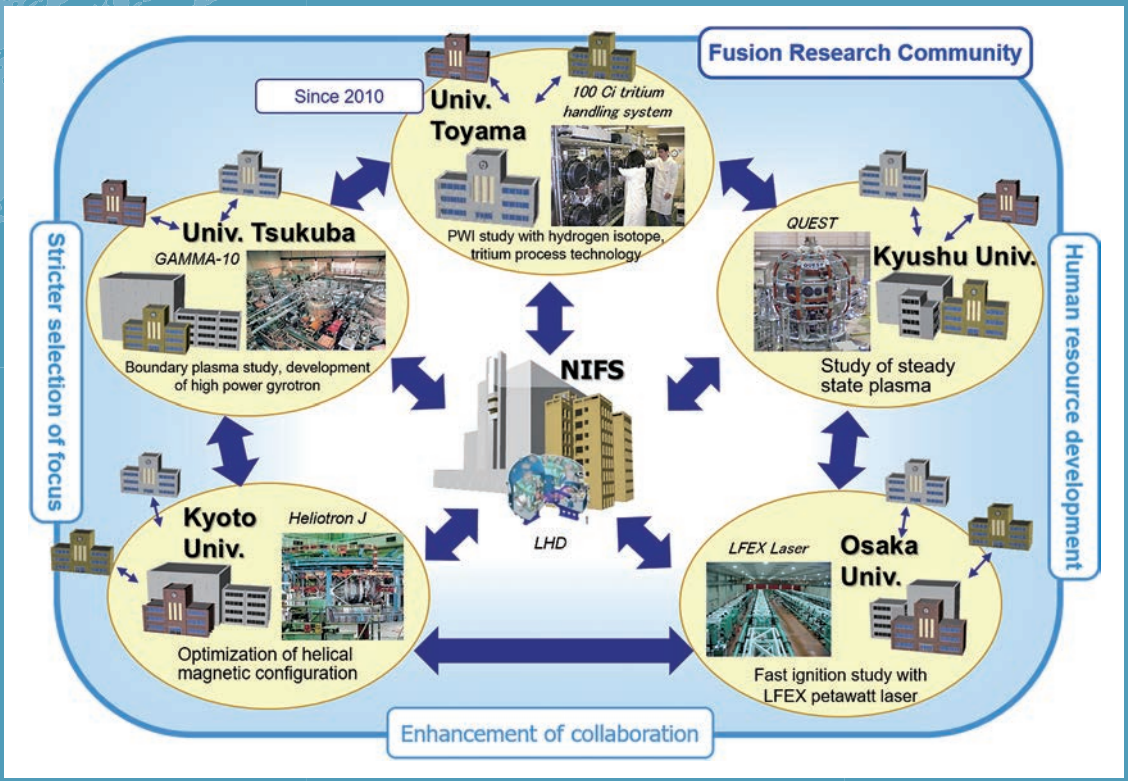

University of Tsukuba

Study of boundary plasmas by making use of open magnetic field configuration and development in high power gyrotrons towards the DEMO project

In the Plasma Research Center, University of Tsukuba, studies of boundary plasma and development of high-power gyrotrons have been performed under the bilateral collaboration research program. GAMMA 10/PDX is the world's largest tandem mirror device and has many plasma production/heating devices with the same scale of present-day fusion devices. In FY2018, 24 subjects including the base subject were accepted and were productive of a number of excellent results.

Numeraous divertor simulation experiments at the end region have been carried out with strong ICRF and ECH systems. Figure 1 shows a schematic view of GAMMA 10/PDX and a divertor simulation experimental module (D-module) that is installed at the west end region. The D-module consists of a rectangular box (0.5 m square and 0.7 m in length) with an inlet aperture at the front panel and a V-shaped target system inside the box. Plasma facing material of the V-shaped target is tungsten. The target size is 0.3 m in width and 0.35 m in length. The end loss plasma is exposed to the target. Additional hydrogen gas and several kinds of radiator gasses (N_2, Ne, Ar, Kr, and Xe) can be supplied into the D-module.

When the neutral pressure in the D-module was increased higher than 12 Pa by the additional hydrogen gas supply, Balmer line emissions from highly excited hydrogen atoms ($n \geq 5$) significantly increased. In addition, a population inversion with n_H (n=5) larger than n_H (n=4) was observed although T_{vib} became rather low (~2,000 K). Detailed analysis revealed the production of the highly excited hydrogen atoms, and the population inversion are attributed to the reaction of mutual neutralization between molecular ions and negative ions. The negative ions are considered to be produced by the resonant ionization process between H(2s).

In the radiator gas injection experiments for detached plasma formation, additional heating pulses of ECH were applied in the upstream region and the effect of plasma heating on the detached plasma was investigated.

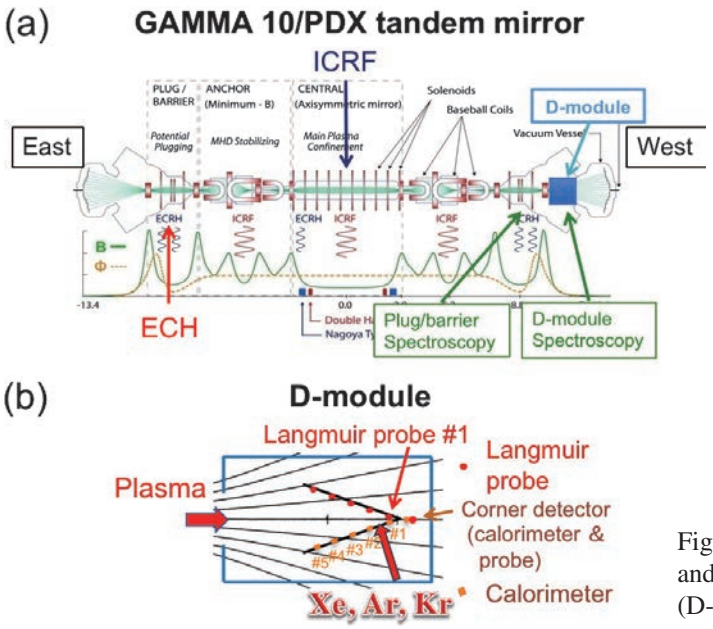

Fig. 1 Schematic view of GAMMA 10/PDX and divertor simulation experimental module (D-module).

Figure 2 shows dependence of heat flux at the corner of the V-shaped target on the Xe plenum pressure P_{Xe} in the cases of with and without the additional ECH. When the Xe gas was not supplied (i.e., $P_{Xe} = 0$), the heat flux was increased by about twice due to ECH. On the other hand, the heat flux was increased by more than 10 times due to ECH when the Xe gas was supplied, and the heat flux decreased with increase in the Xe plenum pressure. It is found that ion flux and heat flux are abruptly increased during ECH and the detached to attached transition occurs. Moreover, combination of hydrogen gas and a small amount of nitrogen gas causes significant decrease in plasma density and ion flux to the target, indicating importance of a recombination process (N-MAR) related to nitrogen gas.

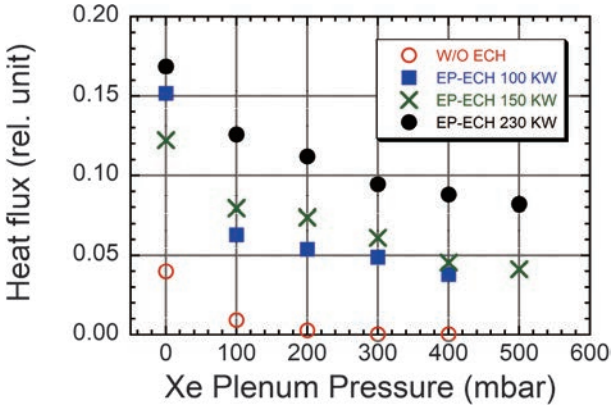

Fig. 2 Dependence of heat flux at the corner of the V-shaped target on the Xe plenum pressure P_{Xe} in the cases of with and without the additional ECH.

Figure 3 shows a schematic view of the Thomson scattering system at the west end region. The electron density and temperature at the D-module could be measured for the first time due to reduction of stray light. Further, the multi-pass Thomson scattering system was improved to double the number of passes through installation of a laser amplification system.

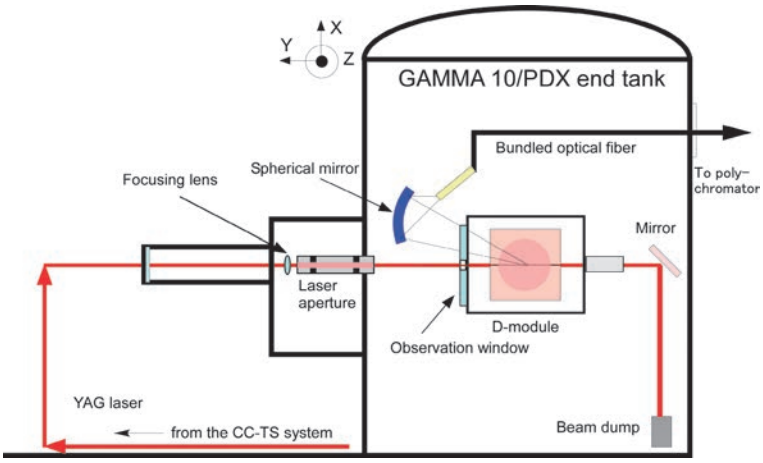

Fig. 3 Schematic view of the Thomson scattering system at the west end region.

In ICRF heating studies, the following subjects were studied: the effect of end-loss ion flux on increase in plasma density and potential at the central cell due to ICRF heating, and spatial structures of AIC (Alfvén-ion-cyclotron) waves and difference frequency waves at the central cell and energy distribution of high energy ions which flowed out to the end region by interaction with the above mentioned waves.

In the 2018 experimental test of a new 28/35 GHz dual-frequency gyrotron (2 MW for 3 s and 0.4 MW CW) for QUEST, NSTX-U, Heliotron J, and GAMMA 10/PDX, maximum powers of 1.65 MW at 28.04 GHz and 1.21 MW at 34.83 GHz were achieved by improving the power supply. A detailed design for a 14 GHz 1 MW gyrotron is advancing toward its fabrication. For a 14 GHz radio frequency (RF) beam with high divergence, a calculated transmission efficiency of 94% to the corrugated waveguide coupling position was obtained by introducing the design concept (direct RF beam coupling by built-in waveguide) to minimize the RF transmission path. Installing a double-disk sapphire window will make it possible to develop a 1 MW gyrotron with a continuous wave (CW) at 14 GHz.

(M. Sakamoto)

Kyoto University

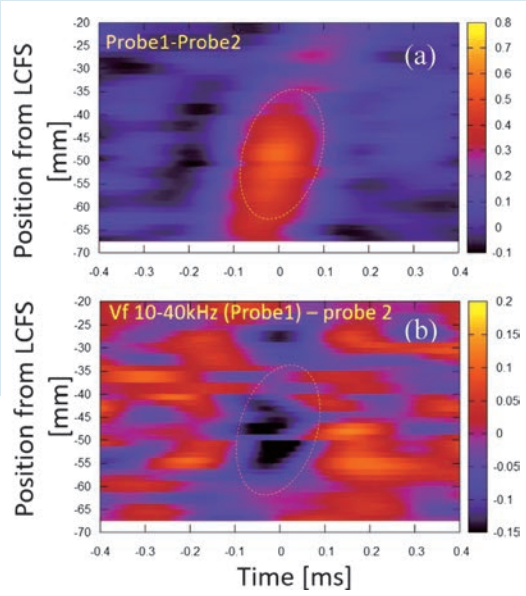

Fig. 1 Zonal flow (ZF) measurement: (a) spatio-temporal structure of ZF obtained with correlation analysis between different probe signals, and (b) correlation between ZF and turbulence amplitude in the frequency range of 10–40 kHz [1].

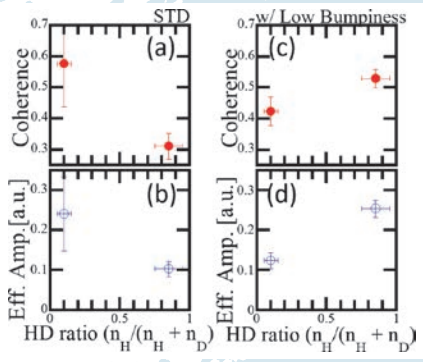

Fig. 2 Isotope dependence of coherence ((a)&(c)) and effective amplitude ((b)&(d)) in the frequency component (<4 kHz) corresponding to zonal flow in standard and low-bumpiness configurations.

Highlight

The configuration dependence of isotope effects on turbulence system in Heliotron J

The hydrogen/deuterium (H/D) isotope effect on fluctuations and its configuration dependence are studied in Heliotron J. The isotope dependence of a toroidally symmetric fluctuation in a low frequency range of < ~ 4 kHz, which is considered as a zonal flow, is observed in low-density ECH plasmas. A zonal flow is considered relating to transport physics in plasmas, such as steady-state transport, L-H transition, limit cycle oscillation, avalanche and isotope effects on confinement properties. Main diagnostics in this experiment are multiple Langmuir probes installed at different toroidal/poloidal sections, which are separated by 67.5° in toroidal angle. In order to extract a structure of zonal flow, an effective zonal flow amplitude was evaluated, based on the technique using the total amplitude and coherence in the zonal flow frequency range. Figure 1 shows that the turbulence suppression is observed only at ~ 50 mm where the zonal flow amplitude has a maximum. Figure 2 shows the dependence of the coherence less than 4 kHz and the effective amplitude on H/D ratio by fuel gas change. The fraction of D is more than ~ 80% in the D discharges, and less than ~ 15% in the H discharge. Two columns of figures show the comparison between the standard (medium-bumpiness) configuration and low-bumpiness configuration in Heliotron J. The results exhibit that both coherence and effective amplitude of ZF decrease in D plasmas, differently from the standard configuration and Tokamaks, but similarly to the observation in a helical machine, TJ-II. The fact simply suggests that the isotope effects on turbulence system should be dependent on the magnetic configurations. The fluctuation with long-range toroidal correlation becomes stronger and the correlation is enhanced in D dominant plasmas in standard configuration of Heliotron J, which shows that the confinement of turbulence transport should be improved in D plasmas. Interestingly, however, the opposite dependence on isotope ratio is observed in the magnetic configuration tagged here “low-bumpiness”.

[1] S. Ohshima *et al.*, “The Configuration Dependence of Isotope Effects on Turbulence System in Heliotron J”, 27th IAEA Fusion Energy Conference (FEC2018), 22–27 Oct. 2018, Gandhinagar, India, EX/P3-3.

Research Topics from Bilateral Collaboration Program in Heliotron J

The common objectives of the researches in Heliotron J under this Bilateral Collaboration Program are to investigate experimentally/theoretically the transport and stability of fusion plasma in advanced helical-field, and to improve the plasma performance through advanced helical-field control. Picked up in FY2018 are the following seven key topics; (1) studies of plasma transport and related plasma self-organization through advanced helical magnetic field control, (2) study of electron cyclotron heating (ECH)/current drive (ECCD) heating mechanism and its improvement, (3) production of high density NBI plasmas and confinement study of high-beta plasmas, (4) boundary plasma study in an advanced helical device, (5) study of instability control, (6) experimental study of plasma current by field configuration control in an advanced helical device, and (7) empirical research of new experimental methods and analysis methods. Two key topics are described below.

Effect of magnetic field structure on electron internal transport barrier (eITB) and its role for the transport barrier formation: The internal transport barrier has been observed widely in helical devices such as CHS, LHD, TJ-II, W7-AS, and Heliotron J. During eITB, effective heat transport in the plasma core region is reduced in low density ECH plasmas in Heliotron J. The effect of the ripple on the eITB formation was investigated by changing bumpiness of the magnetic configuration. The central electron temperature of the ECH plasma as a function of the injected power divided by the line averaged density in low density region ($\bar{n}_e < 1 \times 10^{19}$ m^{-3}) depends on the bumpiness. The power thresholds to form the eITB in the low and the high bumpiness configurations are larger (550×10^{-19} kWm^3) than that of the medium bumpiness (250×10^{-19} kWm^3). Consequently, the smaller ε_{eff} configuration has the lower power threshold in Heliotron J, and this result does not agree with the CHS results. It is possible that the rational surface or the magnetic island affects the eITB formation in Heliotron J result. For the investigation of rational surface effect, current ramp-up experiment is performed near the threshold heating power of the formation of eITB. The bootstrap current gradually increases during the discharge, the central value of T_e increases at the plasma current of near 0.9 kA. At this timing, the central temperature increased and the eITB expands outwardly with a fast time scale compared to the energy confinement time. The 4/7 low-order rational surface is expected to be created by the current ramp up. This eITB is caused by the rational surface formation inside plasma.

Control of fast-particle-driven MHD instability by using ECH/ECCD: Fast-particle (FP)-driven magnetohydrodynamics (MHD) instabilities enhance anomalous transport and/or induce the loss of fast particle including alpha particles in a D-T fusion reactor. Since redistribution and exhaust of alpha particles lead to reduction of fusion gain Q and damage of first wall, to establish methods of stabilization and/or control of FP-driven MHD instabilities is required for the D-T fusion reactor, but they have not been established yet. ECH/ECCD are a candidate method to control the FP driven MHD instabilities because ECH/ECCD may be an ideal tool to control the modes since they can provide highly localized EC waves with a known location and good controllability of heating position and parallel refractive index $N_{\parallel}$. Both negative and positive magnetic shear, which is induced by co- and counter-EC-driven plasma current, suppress the observed energetic particle modes (EPMs) with $m/n = 2/1$. EPM amplitude has a maximum around plasma current of $I_p = 0.2$ kA and decreases with the increase of the plasma current regardless of sign of plasma current. The absolute value of rotational transform is considered to contribute to this mode suppression. The global Alfvén eigenmodes (GAEs) with $m/n = 4/2$ has the same tendency. Such suppression effect of FP-driven MHD instabilities is also observed in other helical devices, LHD and TJ-II. ECCD stabilization seems to be a common effect for helical devices.

(K. Nagasaki, H. Okada, S. Ohshima, T. Minami, S. Yamamoto, S. Kado and S. Kobayashi)

Osaka University

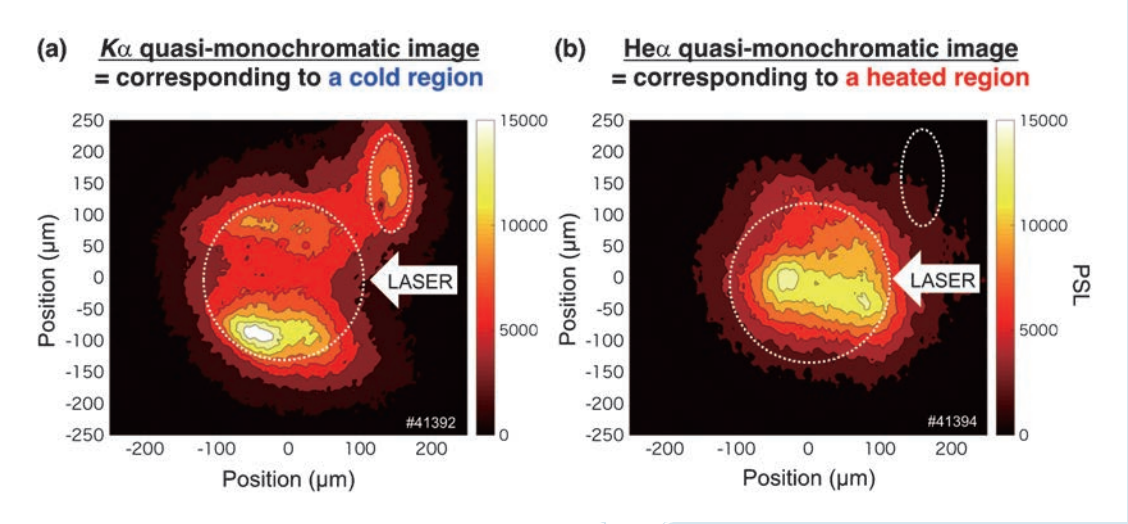

Fig. 1 X-ray emission images of (a) K-alpha lines and (b) He-like lines from doped Ti ions.

Highlight

Heating performance of Fast Ignition target by intense short-pulse irradiation

We have developed a Fresnel zone plate imager spectrally tuned to specific x-ray line emissions from the dopant element (Ti) in the compressed plasma which enables us to obtain monochromatic images to visualize the plasma states with a high spatial resolution. Figure 1 (a) shows an image of K-alpha x-ray emissions from the imploded plasma, which corresponds to the relatively cold region of the plasma in which the dopant (Ti) was not highly ionized and can emit K-alpha lines via collisions of hot electrons. On the contrary, Fig. 1 (b) shows an image of He-alpha lines of Ti, which means the Ti ions were heated and ionized to He-like state there. These images clearly indicate that the heating was performed at around the central axis of the imploded plasma by fast heating, and the regions surrounding the axis were kept relatively cold.

Fast Ignition of Super High-Dense Plasmas

Laser-driven inertial confinement fusion by the Fast Ignition (FI) scheme has been intensively studied as the FIREX-1 project at the Institute of Laser Engineering, Osaka University. The researches consist of target fabrication, laser development, fundamental and integrated implosion experiments, simulation technology and reactor target design, and reactor technology development. In FY2018, the following progress was made through the Bilateral Collaboration Research Program with NIFS and other collaborators from universities and institutes (NIFS12KUGK057 as the base project and 17 individual programs).

Theory and Simulation, Target Design

It has been demonstrated so far that the imploded plasma was heated up to 1.7 keV with a heating efficiency up to 8%. In FY2018, we have investigated the physical mechanisms there by using a PIC simulation code named "PICLS" which includes atomic processes such as collisions, ionizations, and so forth. It was found that the thermal diffusion from the directly laser-heated region to the neighboring areas in the imploded plasma is performing an important role in the total plasma heating as shown in Figure 2. Also found is that a kilo-Tesla class magnetic field was generated by resistive current and was guiding the fast electron flow together with the externally applied magnetic field. We studied the heating efficiency taking into account such physical mechanisms to establish a scaling law of the heating.

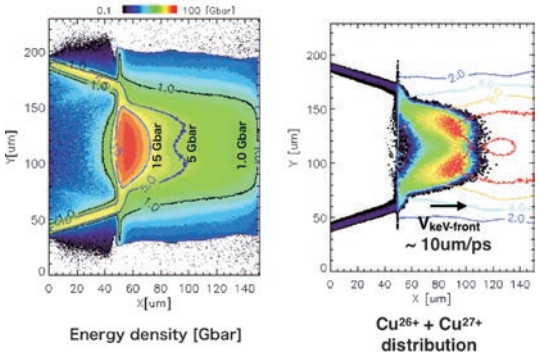

Fig. 2 Simulation results of magnetically assisted fast ignition. (a) Electron pressure distribution after the heating by LFEX laser. (b) Spatial distribution of 26th and 27th ionized Cu dopants which correspond to the heated region.

By taking into account those findings, heating of the fuel plasma with a density of 100 g/cc by a 10 kJ/10 ps class laser was evaluated in order to design 5 keV heating.

Target Fabrication and Reactor Technology

Refractive index of liquid/solid DT mixture is of great importance in inertial fusion research since the fuel pellet is expected to be inspected by using optical diagnostics. We performed an experiment to create solid-state D_2 and T_2 mixture, and successfully measured its refractive index, which was found to be close to the expected value inferred from the similarity with D_2 and H_2. It also was found that the spatial distributions of D_2 and T_2 are slightly different with each other, which is attributed to the heat generation due to beta-decay of T.

Operation and improvement of GEKKO-XII/LFEX Laser system

Isentropic implosion is essential for controlling the shock wave velocity from each part of the fuel layer. Advanced pulse shape control technology was developed for GEKKO-XII laser oscillator system. A simulation code was developed taking into account amplifier performance as well as frequency conversion parameters in KDP crystals. Figure 3 (a) shows typical results of 4-ns flat-top pulse shape for three beams, all in a sufficiently good agreement. Three-step pulse shape is one of the candidates for high-density implosion. Blue line in Fig. 3 (b) is the designed shape, and black line is a typical result. Although the 1st and the 2nd steps (flat-top) were well controlled, the peak power of the 3rd pulse was still lower than expected. Further improvement will be continued in FY 2019.

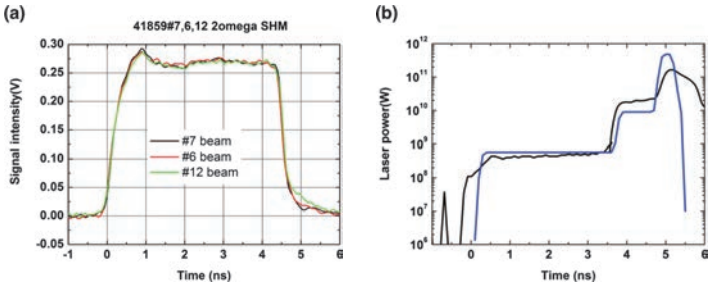

Fig. 3 (a) Flat-top pulse shapes of three beams. (b) A three-step pulse, designed (blue line) and achieved (black).

Individual Collaborations

In parallel with the main project described above, 17 other collaborations by individual researchers including two from abroad have been performed. Those projects were on electron-driven fast ignition (8 collaborations), ion-driven fast ignition (2), alternative scheme of laser-driven inertial fusion (2), diagnostics of high-temperature and high-density plasmas (4), and reactor technology (2). 9 were projects continued from the previous year(s) and 8 were newly accepted in FY2018.

(R. Kodama, H. Shiraga, S. Fujioka, Y. Sentoku, K. Yamanoi and Y. Arikawa)

Kyushu University

Research activities on QUEST in FY2018

We will summarize the activities on advanced fusion research center, research institute for applied mechanics in Kyushu University during April 2017 – March 2018. The QUEST experiments were executed during 12th May – 5th Aug. (2017 Spring/Summer; shotno 34700–35819) and 30th Nov. – 9th Mar. (2017 Autumn/Winter; shotno 35820-36662). Main topics of the QUEST experiments in FY2018 are listed below.

1) The highest plasma current discharge of 93kA in non-inductive current drive adding a bit of ohmic heating was obtained by 28 GHz microwave injection which developed with Tsukuba University (Gyrotron) and NIFS (polarizer) (shotno 35682). The control of refractive index parallel to the magnetic field, N// could give us the controllability of branching in electron energy selectivity during plasma start-up without fundamental ECH.
2) The neutral compression behind the lower divertor plates with downward ion toroidal drift and up-down asymmetry of the hot wall temperature during more than an 1h discharge. (The lower hot wall temperature was higher than upper one.) The compression was observed after approximately 2000 sec from the plasma initiation, and then a bright area measured with a visible video-camera came up around the center stack beside the lower divertor plate. This suggests that fuel neutral got collected at the lower natural divertor area, although the reason is still unclear.
3) The densities measured by the Thomson scattering system were calibrated using a newly fabricated microwave interferometer with the probing frequency of 50 GHz. We obtained the density and temperature profiles of the plasmas sustained by 8.2 GHz ECH. For the case of inboard poloidal field null configuration, the maximum electron temperature was about 300 eV (at the inboard side) and the density was about 2×10^{17} m^{-3}.
4) Recovery of the previous permeation probes that were installed in QUEST several years ago was conducted for the measurement of hydrogen atomic flux at the wall. Functionality of the devices has been confirmed successfully as detection of signal from a quadrupole mass analyzer, for 4 probes out of 5 installed.
5) The plasma shape reconstruction by the Cauchy condition surface method with the Mirnov type magnetic sensors, which have very large coupling area and were made for JT-60SA, and ex-vessel hall sensors is being prepared for QUEST.
6) In order to improve the high plasma current divertor operation, to help the transition from CHI discharge to Ohmic discharge, and to provide the vertically unstable negative triangular plasma, the feedback control system for the plasma vertical movement is required in the present QUEST. To design this control system, the plasma circuit equations with the vacuum chamber currents with 30 loops, the horizontal field coil and the plasma vertical movement should be solved numerically. In 2018, the basic research has been started how to tackle this problem and the research target has been clarified to go forward.
7) Considering the toroidal rotation, the equilibrium is fitted within nested magnetic surfaces by SU-EFIT. Sweeping the ratio of the current density due to the toroidal rotation and the one due to the pressure gradient, the relation between the peak toroidal rotation speed squared and the poloidal beta value is linear. Namely, sum of contributions from toroidal rotation and pressure gradient to plasma current density is constant.
8) The W sample was placed on the plasma facing wall in QUEST and exposed to hydrogen plasma during 2017 SS, 2017 AW or 2018 SS campaign. Additional D2 + implantation and then TDS experiments were performed. It was found that a lot of damages were introduced ifor the short-discharge 2017 sample, and D was also retained by these damages. But, for 2018SS, D retention was clearly reduced and only lower D desorption at low temperature was found, suggesting that the irradiation damages do not depend on the discharge time but the plasma current.
9) A comparative measurement of the ion toroidal velocity was conducted at the midplane in 28 GHz and 8.2 GHz IL and IPN discharges using optical emission spectroscopy. A particularly large velocity of up to 4 km/s (Mach number ~1) was found in the outer SOL of IPN discharge.
10) Thermal desorption of hydrogen from atmospheric plasma spray tungsten (APS-W) layers, plasma-facing material of QUEST, was examined after exposure to QUEST plasma. The release of hydrogen from APS-W started at around 100°C and peaked at around 400°C. This observation suggests significant reemission of hydrogen from APS-W at wall temperature of QUEST.
11) A multi-aperture grid of the low energy ion source (10 kev) was designed to produce high current ion beams for the QUEST NBI. 14.9 A ion beams are extracted from a 30 cm diameter area with 1180 numbers of

apertures and cooling channels at 100 mA/cm2 ion current density. It enables 101 kW injection power. Focusing of beams to the injection port were analyzed with 3D beam trajectory simulation. 0.42 mm displacement of the extraction grid aperture axis deflects the ion beam by 36 mrad for focusing.

12) Overall control system of QUEST has been modified continuously according to the progress of recent technology. As an example, an administration system for entry experimental hall has been developed, which is composed of pocket-size PC with Wi-Fi and touch panel display. This system is contributory to the secure operation of QUEST with shutting down the sequence safely when someone stays in experimental hall.
13) A new drift tube, inside of which is a CT guiding tube made of OFC-Cu for conservation of CT magnetic flux, has been installed on the CT injector. The replacement of the drift tube leads to improve CT fueling efficiency. The injector has been detached from QUEST and set up for wall-conditioning and test operation.
14) Hybrid probe, which consist of the magnetic probes and Langmuir probes, was installed in QUEST to get the electro-magnetic signal associated with peripheral plasma fluctuation. This time it is confirmed the probe function by using 28 GHz ECH injection experiment.
15) Temperature dependence of tritium retention in tungsten under irradiation of tritium ions has been examined using β-ray induced X-ray spectrometry. Retention of tritium in surface layers decreased with temperature rise, while it contrarily increased above 523 K, and it was suggested that change in the tritium retention strongly depends on solubility of tritium in surface layers in comparison with effect of diffusion into the bulk of tungsten.
16) Electron cyclotron non-inductive plasma start-up of an 90 kA level has been achieved with an obliquely injection of a polarized 28 GHz focusing-beam. The incident-wave polarization was carefully controlled to obtain significant single pass absorption. Bulk-electron heating was attained in a perpendicular injection. Relatively high electron temperature of 200 eV was attained in a plasma with density of 5×10^{18} m^{-3} and current of 25 kA.
17) The paper "Initial results from solenoid-free plasma start-up using Transient CHI on QUEST," by K. Kuroda *et al.*, was published in Plasma Physics and Controlled Fusion 60 (2018) 115001. The paper describes the generation of 45 kA of toroidal current from the operation of a new reactor-relevant transient CHI electrode configuration that should be easier for implementation in reactor configurations. In a supporting paper, "TSC Simulation of Transient CHI in New Electrode Configuration on QUEST", by K. Kuroda *et al.*, published in the journal Plasma and Fusion Research, 13, (2018) 3402058, the numerical simulation results aimed at improving the CHI experimental performance on QUEST is described.
18) A new series of Chubu-Kyushu Univ. joint experiments have been conducted to investigate the effect of forced convection on the heat transport in liquid metals, using a modified TDS setup brought from NIFS in the last fiscal year. Results indicate that the heat transport is significantly enhanced by liquid convection induced by the J×B-electromagnetic force.
19) In tokamak plasmas produced by 28 GHz ECH launching, divertor biasing experiment was carried out, aimed at two purposes: (1) to drive SOL current for generating resonant magnetic perturbations (RMP), and (2) to broaden divertor heat load. The experimental data show a potentiality of the divertor biasing.
20) Electron Bernstein wave (EBW) heating/current drive is one of the key issues to attain steady state tokamak configuration in the QUEST. The collective scattering system utilizing the 400 GHz gyrotron and quasi-optical transmission/antenna/reflector gratings are designed to detect EBW in the core of the QUEST. The 400 GHz gyrotron developed in the Univ. of Fukui, and the quasi-optical system will be installed on the QUEST from mid FY2019.

Kazuaki Hanada (Kyushu University) 1), 2)
Akira Ejiri (University of Tokyo) 3)
Masahiro Kobayashi (NIFS) 4)
Manabu Takechi (QST) 5)
Osamu Mitarai (Institute for Advanced Fusion and Physics Education) 6)
Kazuo Nakamura (Kyushu University) 7)
Yasuhisa Oya (Shizuoka University) 8)
Taiichi Shikama (Kyoto University) 9)
Yuji Hatano (University of Toyama) 10)
Masanobu Tanaka (Pulsed Power Japan Laboratory Ltd.) 11)
Makoto Hasegawa (Kyushu University) 12)
Naoyuki Fukumoto (University of Hyogo) 13)
Nobuhiro Nishino (Hiroshima University) 14)
Masao Matsuyama (University of Toyama) 15)
Hiroshi Idei (Kyushu University) 16)
Roger Raman (University of Washington) 17)
Yoshihiko Hirooka (Chubu University) 18)
Kazuo Toi (NIFS) 19)
Shin Kubo (NIFS) 20)

(K.Hanada)

University of Toyama

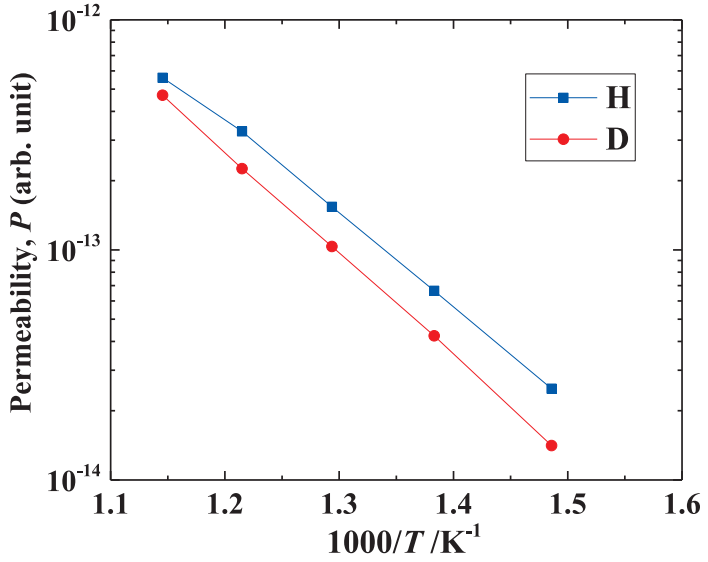

Arrhenius plot of permeation rates of H_2 and D_2 through Cu-0.5 mass% Al_2O_3 oxide dispersion strengthened alloy under exposure to H_2 or D_2 mixture gas.

Highlight

Research Activities in Hydrogen Isotope Research Center, Organization for Promotion of Research, University of Toyama

Permeability, diffusivity and solubility of hydrogen and deuterium in Cu-0.5 mass% Al_2O_3 oxide dispersed strengthened alloy were examined in 2018 by permeation tests using H_2, D_2 and H_2-D_2 mixture gases. Clear isotope effects were observed on permeability and diffusivity; the values obtained for hydrogen were larger than those for deuterium by a factor of $\sqrt{2}$. Namely, the difference between H and D corresponded to ratio of square root of mass.

The titles and principal investigators of research projects performed in University of Toyama in 2018 are listed below.

(1) Isotope effects on trapping and release of hydrogen isotopes in fusion reactor materials (Y. Hatano, U. Toyama)
(2) Hydrogen isotope transport through plasma modified fusion reactor materials (H. T. Lee, Osaka U.)
(3) Hydrogen isotope behavior for W with controlled damage profile (Y. Oya, Shizuoka U.)
(4) Tritium removal from tungsten by baking under deuterium gas atmosphere (Y. Nobuta, Hokkaido U.)
(5) Tritium removal on deposited layers by glow discharge cleanings (N. Ashikawa, NIFS)
(6) Measurment of depth disitribution of hydogen isotopes in plasma facing wall of QUEST by using GD-OES (N. Yoshida, Kyushu U.)
(7) Tritium retention on facing materials modified by plasma wall interactions (K. Tokunaga, Kyushu U.)
(8) Influence of impurity on the hydrogen isotope recovery performance in the plasma exhaust system (M. Kobayashi, NIFS)
(9) The development of tritium water for inertial confinement fusion (Y. Arikawa, Osaka U.)
(10) Gamma-ray irradiation effect on hydrogen isotopes at fusion material surfaces (T. Chikada, Shizuoka U.)
(11) Effects of double strand break to radiation tolerance in the tardigrades (T. Miyazawa, Shizuoka U.)
(12) Double-strand breaks in a genome-sized DNA caused by beta-ray using fluorescence microscopy (T. Kenmotsu, Doshisha U.)

The effect of microstructure on tritium transport in tungsten (W) was examined. The following results suggest tritium transport is enhanced due to the presence of grain boundaries: (1) Tritium penetration in single crystal samples was shallower in comparison to poly-crystal samples, and (2) Tritium penetration was deeper for poly-crystal samples with grains oriented perpendicular to the surface in comparison to parallel orientation.

Hydrogen isotopes retention in W with various defect distributions was evaluated. The total deuterium retention decreased with increasing damage level near the surface introduced by 3.4 MeV Fe^{+} ion implantation. This observation indicates that the irradiation damages near the surface trap most of the deuterium and reduce the deuterium diffusion toward the bulk.

Isotope exchange in W during bake out was examined. The deuterium exposure following tritium exposure resulted in removal of ~96% of tritium. This removal extent was larger than that observed after heating in vacuum and indicates isotope exchange could enhance tritium removal.

Removal efficiencies of surface tritium on plasma facing materials by glow discharge cleaning (GDC) were investigated. Due to low sputtering yield of W by deuterium and helium, a difference between the amounts of remained tritium after GDC and initial tritium is too small. In future, operational parameters will be optimized using stainless steel samples, and then tritium removal from W will be attempted using those optimized conditions.

Behaviors of injected deuterium in several kinds of W materials were investigated by using glow-discharge optical emission spectroscopy and thermal desorption spectroscopy. In the case of hot rolled W plates, some part of the injected deuterium penetrates deeply and are strongly trapped by residual defects such as cavities.

Tritium gas exposure experiments have been carried out on high energy electron irradiated W and long term installed samples on first wall in spherical tokamak QUEST. The amount of tritium retained in surface layers of the samples has been evaluated by β-ray-induced X-ray spectrometry and imaging plate measurements. Tritium retention in defects/redeposition layer formed by the high energy electron irradiation/plasma-wall interactions has been discussed.

Tritium processing in the exhaust detritiation system and cryogenic isotope separation system was modeled using a simulation code. Diffusion based tritium migration in a solid with interactions to irradiation defects is applied. Gas/liquid equilibrium is a model for the isotope separation. These simulation codes will be used for the safety analysis in fusion reactor design.

Tritium doped D_2O is under development for inertial confinement fusion target. In this project, T_2 gas is oxidized to synthesize T_2O, and then it is filled (doped) into a small pellet containing D_2O. In 2018, “cold run” of the system was performed by synthesizing H_2O from H_2 and dope to D_2O filled target. These results were presented as an invited talk in International Conference on Tritium Science and Technology 2019.

Deuterium depth profiles of unirradiated zirconium oxide coating samples showed a gradual decrease with depth. After gamma-ray irradiation, the deuterium concentration decreased by up to 0.1 at% with gamma-ray dose, indicating that gamma-ray irradiation reduced deuterium retention in the coatings.

Aquatic tardigrades show high radiation tolerance. The mechanisms of this tolerance are not well understood. This motivates us to investigate the effects of indirect action by gamma-rays in tardigrades (Milnesium tardigradum). 100 tardigrades were installed into a sample tube with a spin trap agent DMPO, and gamma-rays were irradiated up to 6000 Gy. Thereafter, electron spin resonance was applied to evaluate the quantities of radicals.

An application to measure a length of DNA before and after receiving double-strand breaks due to irradiation of beta-rays from tritium is under development by adopting analytical method of the Hough transform in image analysis of DNA taken from fluorescence microscopy observation, which is able to calculate a length of DNA more efficiently and accurately in comparison with the conventional method.

(Y. Hatano)

9. Activities of Rokkasho Research Center

At Rokkasho village in Aomori Prefecture, the International Fusion Energy Research Centre (IFERC) project and the International Fusion Materials Irradiation Facility/Engineering Validation and Engineering Design Activities (IFMIF/EVEDA) project have been conducted under the Broader Approach (BA) agreement between the EU and Japan from June 2007. The roles of the NIFS Rokkasho Research Center (RCE) established on in 2007 are to assist NIFS and universities to cooperate with those activities, and to prepare the environment for promoting various collaborative research including technology between activities at Rokkasho and at universities. As cooperation activities, the head of the NIFS RCE is undertaking tasks as the IFERC Project Leader (PL) from September 2009, and the NIFS RCE has been set inside the Rokkasho Fusion Institute of QST, where the IFERC and the IFMIF/EVEDA projects are located. Also, the head of the NIFS RCE is working as the leader of the general coordination group of the Joint Special Team for a Demonstration Fusion Reactor (DEMO) design, which is the organization set in May 2015 for establishing technological bases required for the development of DEMO as an all-Japan collaboration. In addition, the NIFS RCE performs communication work with the organizations related to ITER-BA, the Aomori prefectural office, and the Rokkasho village office, and also publicity work so to have local residents understand nuclear fusion research.

In order to complement ITER and to contribute to an early realization of the DEMO reactor, the IFERC project implements the three sub-projects under the coordination by IFERC PL: DEMO Design and R&D Coordination Centre composed of the DEMO Design Activities (DDA) and the DMEO R&D activities, the Computational Simulation Centre (CSC), and the ITER Remote Experimentation Centre (REC). The IFERC project itself was and is implemented on schedule as originally planned. However, the update of the IFERC project plan with the extension until the end of March 2020 was approved in order to ensure the smooth transition to the BA phase II planned from April 2020 to March 2025.

In 2018, the DEMO Design Activity (DDA) continues to investigate key issues, which will impact the selection of main machine parameters and technical specifications for pre-conceptual designs of DEMO. In addition, new joint activities started in several topics in order to share and improve physics results and engineering designs were developed previously by either side or under different conditions.

The compilation of Material Properties Handbook is ongoing in the framework of the DDA, and the analysis of JET tile and dust continues in accordance with Work Programme 2018 for new specimens such as bulk Be limiter tiles and a new set of sample materials. Three shipments of samples occurred in July and September, 2018: (1) Be first wall and limiter tiles (ILW-1), (2) W-Lamella divertor tiles (ILW-1), (3) divertor tiles of W-coated CFC (JET-ILW 3rd campaign: ILW-3), and (4) dust (collected after ILW-3). The aims of research carried out in 2018 were threefold: 1) to conclude studies of the divertor and dust specimens from the 2011–2012 operation in ILW-1; 2) to begin studies of divertor cores and dust from ILW-3 in order to gather data for detailed comparisons of the two campaigns ILW-1 and ILW-3; and 3) to develop methodology and define a programme for analyses of beryllium limiters and to prepare for analyses of bulk tungsten tiles.

After successful completion of CSC activity, “IFERC HPC follow-up working group” was established in 2017. The main results of the “IFERC HPC follow-up working group” activities in 2018 are 1) to have shared experience and best practices in the design and operations of HPC centres for fusion users and in the usage of such centres by fusion users in Europe and in Japan, 2) to have finalized a new PA for providing the computer time for “Joint EU-JA HPC simulation projects” to EU and JA users from April 2019 to March 2020 (the PA was finalized in December 2018 and signed in January 2019), and to have set up the joint allocation committee

in parallel, and 3) to have confirmed a possible timeframe for the introduction of a joint supercomputer in the context of BA Phase II based on the expected lifetime of the current systems in EU and in JA.

As for REC, after completing preparation of the remote facility, the development of remote participation tools, and various verification tests in 2017, massive data transmission tests with LHD in NIFS via L2VPN, and data transmission tests with JET via L3 Layer were executed. After those, the demonstration of remote participation in the WEST experiment was successfully implemented on 28 November 2018 from 18:00 in Japan (10:00 in France) after much preparation work. The demonstration started by the pulse preparation in REC, where the remote session leader edited pulses remotely accessing the pulse editor, XEdit, on the Altair server prepared in WEST. The shot schedule was edited smoothly, and the sequence of plasma discharge started after the validation and approval by the authorized operator in WEST. The large video wall in the REC room displayed the real time countdown of the plasma discharge, a video of plasma generated in WEST tokamak, and the live data of the time trace of the main parameters of the plasma, such as the current and the plasma density, in addition to the view of the video conference system, as shown in the figure.

The head of NIFS RCE is also undertaking the role of the leader of the general coordination group of the Joint Special Team for a DEMO design. Since the collaboration among many researchers from NIFS and other institutions and technicians from companies is indispensable for the conceptual design investigations of DEMO reactor, which are spread widely across instruments, equipment and facilities, and the head of the NIFS Rokkasho staff works as a coordinator and provides advice on various design activities.

In summary, the NIFS RCE contributes widely not only to the success of ITER but also to the realization of fusion energy through the continuous efforts mentioned above.

(N. Nakajima)

Large video wall in the REC room showing the video conference and countdown (left), the live data of the main plasma parameter (center), the video of the plasma (right), and so on.

10. International Collaboraiton

Many research activities in NIFS are strongly linked with the international collaborations with institutes and universities around the world. These collaborations are carried out in various frameworks, such as 1) coordination with foreign institutes, 2) bilateral coordination with intergovernmental agreements, and 3) multilateral coordination under the International Energy Agency (IEA).

The coordination with foreign institutes is important as the basis of collaborative research. From 1991, NIFS concluded 29 coordination through FY2017. In FY2018, a new coordination was concluded between NIFS and Huazhong University of Science and Technology (China).

NIFS is the representative institute for the three bilateral coordination with intergovernmental agreements (J-US, J-Korea, and J-China), and for the four multilateral coordination under the IEA (Plasma Wall Interactions (PWI), Stellarator-Heliotron concept, Spherical Tori, and Steady State Operation). For the bilateral coordination, and the multilateral coordination PWI Technology Collaboration Program (TCP), NIFS coordinate the collaborative research not only for NIFS researchers, but also for researchers in universities. The activities of the bilateral and multilateral coordination activities are reported in the following subsections, respectively.

In 2018, the joint meeting of the 27th International Toki Conference on Plasma and Fusion Research and the 13th Asia Pacific Plasma Theory Conference was held on 19 – 22 November in Toki, Japan, and NIFS hosted the meeting. More than 200 researchers from 16 countries participated.

(S. Masuzaki)

Academic Exchange Agreements

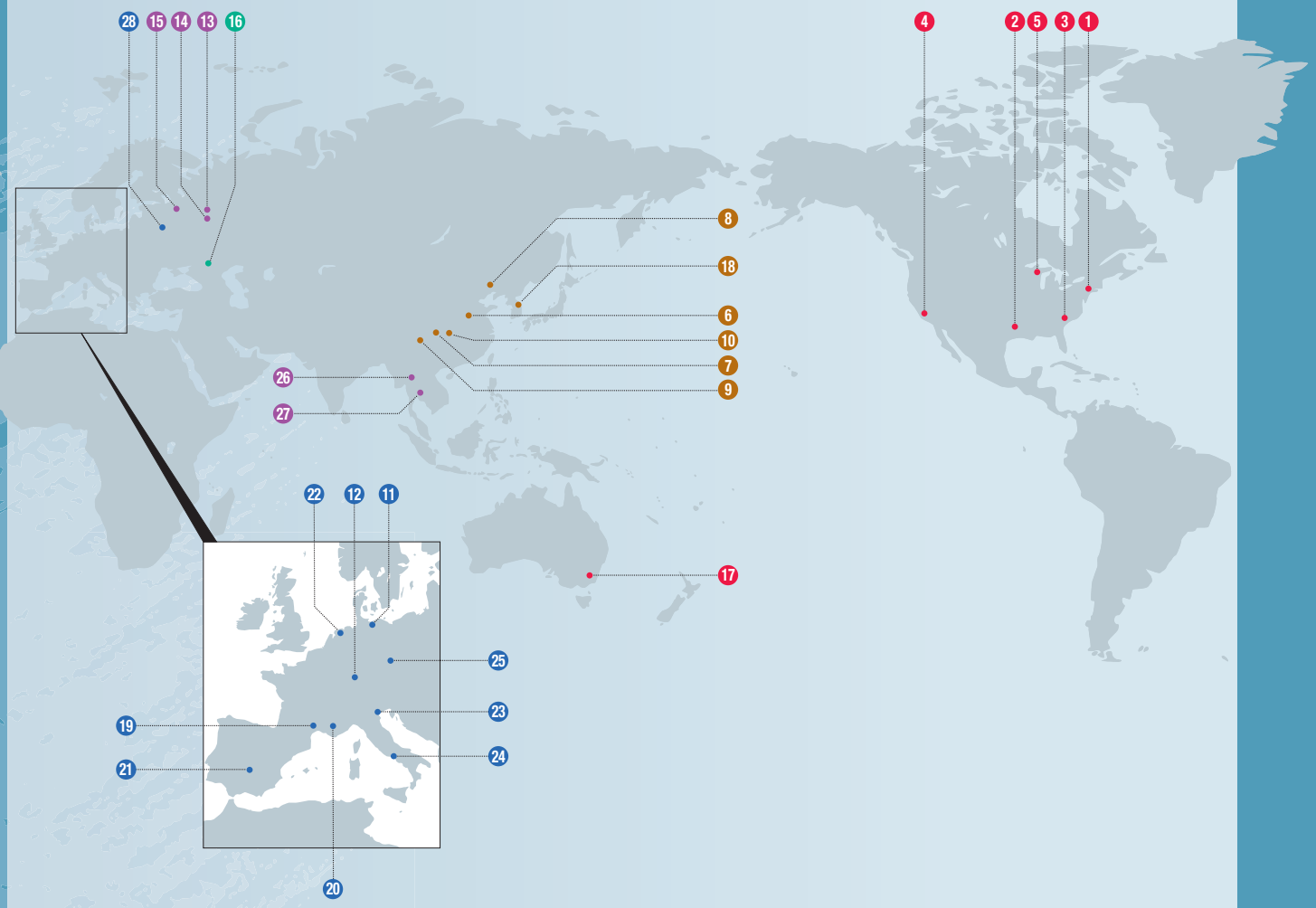

U.S.A. 1 Princeton Plasma Physics Labolatory (PPPL)
2 Institute for Studies, The University of Texas at Austin (IFS)
3 Oak Ridge National Laboratory (ORNL)
4 Center for Energy Science and Technology Advanced Research, University of California, Los Angelse (UCLA)
5 College of Engineering, University of Wisconsin, Madison

China 6 Institute of Plasma Physics, Chinese Academy of Sciences (ASIPP)
7 Southwestern Institute of Physics (SWIP)
8 Peking University
9 Southwest Jiaotong University (SWJTU)
10 Huazhong University of Science and Technology

Germany 11 Max Planck Institute for Plasma Physics (IPP)
12 Karlsruhe Institute of Technology (KIT)

Russia 13 Russian Research Center, Kurchatov Institute (KI)
14 A. M. Prokhorov General Physics Institute, Russian Academy of Sciences (GPI)
15 Peter the Great St. Petersburg Polytechnic University

Ukraine 16 National Science Center of the Ukraine Khar'kov Institute of Physics and Technology Institute of Plasma Physics (KIPT)

Australia 17 Australian National University (ANU)

South Korea 18 National Fusion Research Institute (NFRI)

France 19 Aix-Marseille University (AMU)
20 Commissariat à l'énergie atomique et aux énergies alternatives (CEA)

Spain 21 National Research Center for Energy, Environment and Technology (CIEMAT)

Netherlands 22 Dutch Institute for Fundamental Energy Reseearch (FOM)

Italy 23 CONSORZIO RFX
24 Institute of Lonized Gas (IGI)

Czech 25 HiLASE Center, Institute of Physics CAS (FZU)

Tailand 26 Chiang Mai University
27 Thailand Institute of Nuclear Technology (TINT)

Poland 28 Institute of Plasma Physics and Laser Microfusion (IPPLM)

The ITER International Fusion Energy Organization (ITER)

US – Japan (Universities) Fusion Cooperation Program

The US-Japan Joint Activity has continued from 1977. The 39th CCFE (Coordinating Committee for Fusion Energy) meeting was held on March 7, 2019 via televideo conference system. The representatives from the MEXT, the DOE, universities and research institutes from both Japan and the United States participated. At the meeting, the current research status of both countries were reported together with bilateral technical highlights of the collaborations. The FY 2018 cooperative activities were reviewed, and the FY 2019 proposals were approved. It was noted that both sides have developed significant and mutually valuable collaborations involving a wide range of technical elements of nuclear fusion. Discussion on the bilateral programs and multi-lateral activities also was conducted. Both sides agreed on the usefulness and necessity of the continuation of the Joint Activity.

Fusion Physics Planning Committee (FPPC)

In the area of fusion physics, 7 workshops (6 from JA to US, 1 from US to JA) and 13 personnel exchanges (9 from JA to US, 4 from US to JA) were carried out. Due to the funding limitation and the schedule conflict, 7 personnel exchanges (1 from JA to US, 6 from US to JA) were cancelled or postponed.

Each personnel exchange was performed successfully in the research fields of steady-state operation, high-beta physics, confinement and transport, diagnostics and the high density physics related to the inertial fusion and its application. Fruitful discussions were conducted in the workshops with many participants from both sides. These programs were productive and beneficial for the progress of fusion physics, and were recommended to be continued.

In the category of the high density physics related to the inertial fusion, experiments were performed to obtain the scaling of the laser-generated intense magnetic field towards ignition-scale targets in the OMEGA-EP facility in Laboratory for Laser Energetics in the University of Rochester. In this method, the intense magnetic field is generated by current running along the periphery of the hohlraum wall surface, as shown in Figure 1. Dependencies of the generated magnetic field on laser pulse length and target-size were studied with the proton deflectometry method.

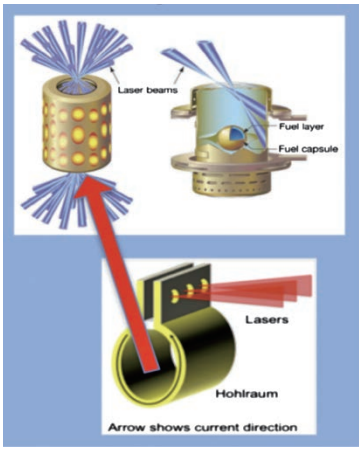

Fig. 1 Schematic of intense magnetic field generation with laser.

Joint Institute for Fusion Theory (JIFT)

Most of the activities in the two categories, workshops and personnel exchanges, that had been scheduled for the 2018–2019 JIFT program were carried out during the past year. Three workshops were successfully held, in addition to the JIFT Steering Committee meeting. In the workshops, multiscale methods in plasma physics, co-designs of fusion simulations for extreme scale computing, and simulation of the high field and high energy density physics were discussed as main topics (Figure 2). In the category of personnel exchanges, two Visiting Professors and eight Visiting Scientists made exchange visits for the purpose of collaborations on theoretical modeling and simulation of magnetic and inertial confinement fusion plasmas. At the JIFT Steering Committee meeting that was held in Portland, on November 7, 2018, the status of JIFT activities for 2018–2019 was reviewed and the recommenda-

Fig. 2 Workshop on "US-Japan collaborations on co-designs of fusion simulations for extreme scale computing" which was held in PPPL from July 30-31, 2018.

tion plans for 2019–2020 were discussed. The JIFT discussion meeting was held at Toki on September 14, 2018, in the Plasma Simulator Symposium.

Fusion Technology Planning Committee (FTPC)

In this category of the US-Japan Collaboration, personnel exchange programs were continued in six research fields, i.e., superconducting magnets, low-activation structural materials, plasma heating related technology, blanket engineering, in-vessel/high heat flux materials and components, and others (power plant studies and related technologies). Of the 14 originally planned items, 10 were completed including 3 workshops/technical meetings and 7 personnel exchanges.

One of the highlights was the joint experiment of a large-current high-temperature superconductor (HTS) as shown in Figure 3. A coiled sample of a Twisted Stacked-Tape Cable (TSTC) HTS conductor was prepared by Massachusetts Institute of Technology (MIT) and installed into the superconducting magnet testing facility at NIFS, equipped with a 13-T magnetic field, 700-mm-bore superconducting solenoid magnet and a temperature control capability at 4.2–50 K for the sample area. A sample current of 9 kA was measured at the bias magnetic field of 5 T with an inlet temperature of ~5 K.

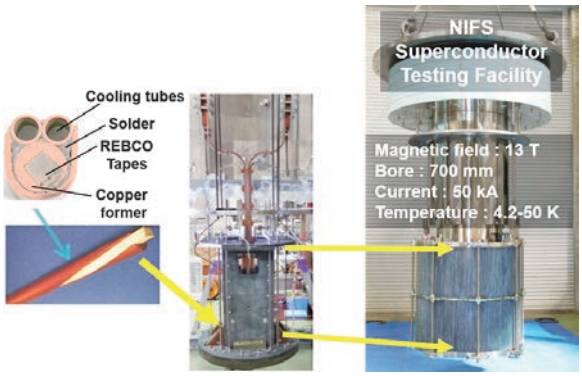

Fig. 3 TSTC-type HTS conductor sample fabricated at MIT and tested at NIFS.

US-Japan Joint Project: PHENIX

FY2018 was the last year of the six-year project of PHENIX. A number of experiments were successfully carried out to reach the project's goals.

Task 1 derived a new and simplified configuration of He-cooled gas divertor, named "flat design", from both results of the high pressure and the high temperature multi-nozzle impinging jet heat transfer experiments conducted in the past five years at the Georgia Institute of Technology with the He loop and of the numerous downselection studies by means of numerical simulation. The fundamental physics for heat flow of the He-cooled divertor was understood, and its cooling performance of each component of He-cooled divertor was demonstrated. Heat load tests were also performed for neutron-irradiated W and K-doped W-3%Re.

Task 2 examined mechanical and thermal properties of W and W alloys irradiated in the RB-19J capsule in the High Flux Isotope Reactor (HFIR), ORNL at around 500°C, 800°C, and 1100°C. K-doped W-3%Re developed during PHENIX project showed good ductility even after neutron irradiation, though significant irradiation embrittlement was observed for pure W.

Task 3 exposed neutron-irradiated W specimens to high flux deuterium (D) plasma and D+He plasma at 400°C in Tritium Plasma Experiment at Idaho National Laboratory. The retention of D was evaluated using thermal desorption spectrometry. The mixing of He in D plasma resulted in orders-of-magnitude decrease in D retention in neutron-irradiated W, as shown in Figure 4. This observation indicates that tritium inventory in W divertor can be significantly reduced by controlling He concentration in edge plasma.

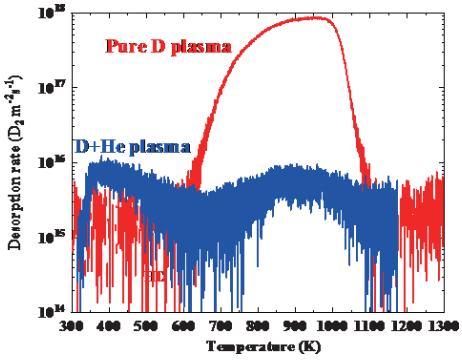

Fig. 4 Thermal desorption spectra of D_2 from neutron-irradiated W exposed to pure D and D+He plasma.

(T. Muroga, S. Okamura, H. Kasahara and K. Yaji)

Plasma Wall Interaction (PWI) Collaboration

This collaboration is based on the IEA Technical Collaboration Programme (TCP) of the "Development and Research on Plasma Wall Interaction Facilities for Fusion Reactors" (in short, PWI TCP). The objective of this TCP is to advance physics and technologies of the plasma-wall interaction research by strengthening cooperation among plasma–wall interaction facilities (in particular, by using dedicated linear plasma devices), to enhance the research and development effort related to the first wall materials and components for fusion reactor. In this fiscal year, collaborations on PWI experiment such as the impact of impurities on tungsten erosion, tritium retention analysis, plasma diagnostics and mechanical examination of tungsten alloys, and edge plasma simulation were conducted. All the collaborations are listed in Table I. Highlight of each activity is described in this report.

Condition of generation of supersonic plasma flows and its effect on impurity transports and radiation losses in advanced divertors

The super-X divertor, one of advanced divertors, has a total flux expansion and, thus, can drive supersonic plasma flows by the magnetic nozzle effect. In this study, we investigate effects of particle recycling on supersonic plasma flows by using a 2D plasma fluid code B2 which is based on the Braginskii's equations.

(S. Togo, University of Tsukuba)

Impact of impurity on tungsten erosion expose to helium plasma

Impact of impurity and incident energy on the surface erosion in helium plasma exposed tungsten has been investigated on the linear device; PSI-2. The typical flux and fluence were 1×10^{22} /m^2/s and 1×10^{26} /m2, respectively. In order to investigate the effect of incident energy on the surface erosion, the incident helium energy was surveyed crossing the threshold energy of the sputtering, namely, within the range 30 eV and 130 eV applying bias on the sample holder. The sample temperature is actively controlled at 773 K by a combination of water cooling and electric heating, based on an infrared (IR) camera temperature measurement. Neon doped plasma exposure experiments are also carried out in order to investigate the effect of impurity on the surface erosion.

(R. Sakamoto)

Collaboration of plasma diagnostic study on Magnum-PSI

The detached plasma conditions are successfully produced in some linear devices and the tandem mirror GAMMA 10/PDX with optimization of background gas pressures and plasma source parameters. In the detachment plasma condition, the strong density fluctuations are observed in the linear plasma devices. We concentrated to study fluctuation in the detachment plasma. A 3-channel frequency multiplied microwave interferometer (MIF) system, which was constructed in GAMMA 10/PDX, was installed to the Magnum-PSI device to measure the electron line densities and their fluctuation.

(M. Yoshikawa, University of Tsukuba)

Evaluation of Damage Formation Mechanism of Doped Tungsten Alloys Under Thermal Shock Loading

To clarify the thermo-mechanical properties of radiation-tolerant W alloys (pure W, K-doped W, W-3%Re, and K-doped W-3%Re), which have been developed by Tohoku university, Japan, thermal shock tests using the JUDITH 1 were carried out at Forschungszentrum Juelich GmbH in 2017 and the evaluation of cracks and defects produced by the thermal shock tests was performed in 2018.

(S. Nogami, Tohoku University)

Tritium Distribution Analysis of Be Limiter Tiles from JET-ITER Like Wall Campaigns using Imaging Plate Technique

In this study, tritium (T) distributions on plasma-facing surfaces and side surfaces of selected Be tiles were examined using imaging plate (IP) technique. Samples were inner-wall guard limiter (IWGL), outer poloidal limiter (OPL) and dump plate (DP) retrieved after ILW-3. The highest T concentration was observed at the central part of plasma-facing surface of the OPL. The T concentrations at the plasma-facing surfaces of IWGL and DP were significantly lower than those on the OPL.

(Y. Hatano, University of Toyama)

Table I. List of collaborations

Subject	Participants	Term	Key persons
Condition of generation of supersonic plasma flows and its effect on impurity transports and radiation losses in advanced divertors	Satoshi Togo (Univ. Tsukuba)	9 – 28 July 2018	Dirk Reiser, Petra Börner, Detlev Reiter (FZJ)
Impact of impurity on tungsten erosion expose to helium plasma	Ryuichi Sakamoto (NIFS)	16 – 23 Sep. 2018	A. Kreter (FZJ)
Collaboration of plasma diagnostic study on Magnum-PSI	Masayuki Yoshikawa (Univ. Tsukuba)	29 Sep. – 7 Oct. 2018	H. V. Meiden (DIFFER)
Evaluation of Damage Formation Mechanism of Doped Tungsten Alloys Under Thermal Shock Loading	Shuhei Nogami (Tohoku Univ.)	18 – 31 Oct. 2018	Jens Reiser (KIT), Gerald Pintsuk (FZJ)
Tritium Distribution Analysis of Be Limiter Tiles from JET-ITER Like Wall Campaigns using Imaging Plate Technique	Yuji Hatano (Univ. Toyama)	26 Jan. – 2 Feb. 2019	J. Likonen (VTT)

(S. Masuzaki)

IEA (International Energy Agency) Technology Collaboration Programme for Cooperation in Development of the Stellarator-Heliotron (SH) Concept ("IEA SH-TCP")

Highlight

Programmatic collaborations have been extending centering on two-flagship experiments, Large Helical Device and Wendelstein 7-X

The SH-TCP's objective is to improve the physics base of the Stellarator-Heliotron concept and to enhance the effectiveness and the productivity of research by strengthening cooperation among member countries. All collaborative activities among worldwide stellarator and heliotron research are combined under the umbrella of this programme, which promotes the exchange of information among the partners, the assignment of specialists to facilities and research groups of the contracting parties, joint planning and coordination of experimental programmes in selected areas, joint experiments, workshops, seminars and symposia, joint theoretical and design and system studies, and the exchange of computer codes. The bi-annual "International Stellarator-Heliotron Workshop" (ISHW) has served as an important forum for scientific exchange within the scientific community. The joint programming and research activities have been organized mainly through the "Coordinated Working Group Meetings" (CWGM).
The second Deuterium experimental campaign of the LHD and the third operation phase (OP 1.2b) of Wendelstein 7-X (W7-X) mark the highlights of 2018.

Major achievements in 2018

The second deuterium campaign (20th campaign) of LHD started on October 23, 2018 and continued until February 21, 2019. The four topical groups (TGs) examined: high-performance plasma, transport and confinement, edge/divertor/atomic and molecular processes, and high-beta/MHD/energetic particles, with the participation of international and domestic collaborators. The 3rd International Program Committee meeting was held on September 19, 2018, to share and discuss the main goals of the 20th campaign such as maximizing and integrating performance, isotope effects, increasing understanding of edge and divertor plasmas to be extrapolated to reactor-relevant regime, extension of high-beta plasmas in low-collisional and high field regime, and further extending the energetic particles physics study.

The NIFS-SWJTU (Southwest Jiaotong University, China) has proceeded with programmatic physics and engineering study on the joint project, CFQS (Chinese First Quasi-axisymmetric Stellarator), of which results were presented on many occasions (EPS, International Toki Conference, etc.). The first plasma is foreseen in 2021.

The third experimental campaign of W7-X (OP 1.2b) took place from July to October 2018. The experiments used electron cyclotron resonance heating (ECRH) with a maximum power of ~7 MW, which is the highest ECRH power ever employed in a fusion experiment. Later in the campaign, neutral beam injection (NBI) with up to 3.6 MW was tested for the first time on W7-X. This included first studies of fast ion confinement and the loss of fast ions. The scientific program focused on the demonstration of stationary, high performance discharges

and the characterization of the inertially cooled test divertor in preparation for operation of the actively cooled high heat-flux divertor in the later campaigns.

Increasing the density in hydrogen plasmas was achieved reliably by improving the wall conditioning using boronization. It was demonstrated that high plasma densities can be reached with a transition of the micro-wave heating power from X2-polarization to full power O2-polarization which is necessary to exceed the X2 cut-off density. At 5 MW heating power discharge lengths could be considerably improved from a few seconds in the previous campaign to a maximum of 25 seconds with stationary conditions. Sustaining a plasma over such a long time without any active divertor cooling was only possible because of the so-called detachment.

Group photo taken at 18th Coordinated Working Group Meeting, Princeton, Courtesy of Dr. David Gates (Princeton Plasma Physics Laboratory.)

47th Executive Committee (ExCo) Meeting

The 47th Executive Committee took place on October 24, 2018 in Ahmedabad, India. The ExCo nominated Alvaro Cappa to replace Axel Könies in the ITPA Energetic Particle Physics Topical Group, confirmed the International Programme Committee for the ISHW 2019 in Madison, discussed and decided on a structure for future CWGM reporting milestones, and received progress reports from the CWGM and the SSOCG. The ExCo also received briefings about the member's domestic stellarator activities. I. Vargas supplied an update on the progress of the accession of Costa Rica and Y. Xu gave a presentation on the Chinese stellarator activities.

18th Coordinated Working Group Meetings (CWGM)

The 18th CWGM was held in Princeton Plasma Physics Laboratory, in April 10–12, 2018. There was a total of 59 presentations from 45 from onsite participants, and 14 from offsite participants. Representatives from 14 institutions and 9 countries gave presentations.

Talks covered a wide range of topics:

- Divertor physics; W7-X scraper elements (section leader: Oliver Schmitz),
- 3D Turbulence; isotope effect (section leader: Motoki Nakata),
- Database Progress and ITPA Links (section leader: Jose Luis Velasco),
- Impurity Transport (section leader: Novimir Pablant),
- Core Electron Root Confinement (section leader: Felix Warmer),
- Plasma Terminating Events by Excess Fuelling and Impurities (section leader: Andreas Dinklage),
- Wall Conditioning (section leader: Paco Tabares), and
- Fuelling and Pellet Injection (section leader: Naoki Tamura).

Numerous joint activities and relevant responsible individuals were identified. The presentations are available at the meeting website located at: https://sites.google.com/a/pppl.gov/cwgm18/.

(Y. Takeiri, T. Morisaki and M. Yokoyama)

Japan-China Collaboration for Fusion Research (Post-CUP Collaboration)

I. Post-CUP collaboration

The post-CUP collaboration is motivated by collaboration on fusion research with institutes and universities in China including Institute of Plasma Physics Chinese Academy of Science (ASIPP), Southwestern Institute of Physics (SWIP), Peking University, Southwestern Jiaotong University (SWJTU), Huazhong University of Science and Technology (HUST) and other universities both in Japan and China. The Post-CUP collaboration is carried out for both studies on plasma physics and fusion engineering. Based on the following implementation system, the Post-CUP collaboration is executed.

Table 1. Implementation system of Japan-China collaboration for fusion research

Category	① Plasma experiment				② Theory and simulation	③ Fusion engineering research
Subcategory	①-1	①-2	①-3	①-4	—	—
Operator	A. Shimizu	S. Kubo	M. Isobe	T. Oishi	Y. Suzuki	T. Tanaka

①-1 : Configuration optimization, transport, and magnetohydrodynamics, ①-2 : Plasma heating, and steady state physics, ①-3 : Energetic particles, and plasma diagnostics, ①-4 : Edge plasma and divertor physics, and atomic process

II. Primary research activities of collaboration in FY 2018

As for the NIFS-SWJTU joint project for CFQS, the 1st steering committee meeting was held on May 30, 2018 at SWJTU in Chengdu, China, as shown in Fig. 1. Physics and engineering design, and the construction of mockup coil of CFQS quasi-axisymmetric stellarator were discussed. Physics design of CFQS was completed and fixed in this meeting [1-3]. The main parameters of CFQS were fixed as follows: the major radius is 1.0 m, the averaged minor radius is 0.25 m, the aspect ratio is 4.0, the toroidal periodic number is 2, and the maximum magnetic field strength is 1.0 T. The modular coil system for CFQS magnetic field configuration was designed by using the NESCOIL code. The main modular coil set consists of 4 different coil types with 4 identical coils, and the total number of modular coils are 16. Construction of mock up coil of the most complicated modular coil in shape was started. The casting blank mould of the mockup coil was made up to February 2019, and the mould fabrication will be continued by computerized numerical control machine until April, 2019. Supporting structure design of coil system and the finite element method analysis are now in progress.

Fig. 1 The 1st steering committee meeting of NIFS-SWJTU Joint project for CFQS.

Energy and pitch angle-resolved measurement of beam ion loss is conducted using scintillator-based fast ion loss detector installed under the Japan-China collaboration onto the EAST tokamak. Prompt loss of beam ions having energy of 45 keV and pitch angle of 55 degrees were clearly seen in NBI2L injection phase [4]. Study of global beam ion confinement is performed by time-dependent analysis of total neutron emission rate (S_n) using the one-dimensional neutron emission calculation code FBURN. Relative time evolution of S_n in plasma discharge with an injection of short pulse neutral beam was successfully reproduced in both LHD and EAST [5].

In the research of the edge and divertor plasmas, spectroscopic diagnostics for tungsten impurities has been progressed using extreme-ultraviolet (EUV) spectrometers developed in LHD. Tungsten density profiles of W^{43+} and W^{45+} were derived from the line emission profiles measured using the space-resolved EUV spectrometers in EAST [6]. A tungsten influx to the edge plasmas was evaluated using the EUV spectroscopy for W^{6+} line emission in HL-2A [7].

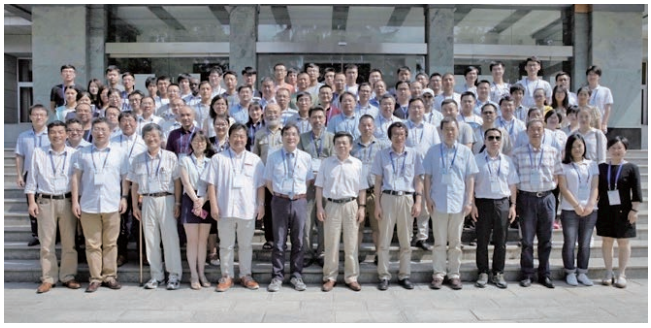

Fig. 2 AMPP2018 hosted by ASIPP, 24–26 July 2018.

In addition, the subcategory ①-4 group had the 7th China-Japan-Korea joint seminar on atomic and molecular processes in plasma (AMPP2018) hosted by ASIPP in July, 2018 as shown in Fig. 2.

In the category ②, EMC3-EIRENE transport modeling of neon-seeded EAST SOL/divertor plasma was performed to study non-axisymmetric impurity transport. This result will be compared with a result by SOLPS package. The simulation of energetic particle-driven instabilities is ongoing. MEGA code was applied to EAST plasma and it was found that the energetic particle-driven mode, which is toroidicity-inducted Alfvén eigenmode or energetic-particle mode, becomes unstable in an EAST plasma. In the J-TEXT tokamak, external resonant magnetic perturbation was used to control the tearing mode. To model the magnetic field, the HINT code is being applied. This result will be compared with NIMROD simulation result.

In the category ③, tritium release kinetics for biphasic Li2TiO3-xLi4SiO4 tritium breeders was studied by tritium-thermal desorption spectroscopy (TDS) method. The tritium release temperature and the shape of TDS spectra are dependent on the phase ratio of Li2TiO3 to Li4SiO4. In the case of Li2TiO3- 2 Li4SiO4, tritium release starts at 400 K, and the tritium migration is mainly controlled by the diffusion process. As increasing Li4SiO4 content, tritium release is influenced by the de-trapping process[8]. Also, the category ③ group had the 14th Japan-China symposium on materials for advanced energy systems and fission & fusion engineering (JCS-14) was held in September, 2018, in Sendai, Japan as seen in Fig. 3.

Fig. 3 JCS-14 hosted by Tohoku University, 25–27 September 2018, Sendai, Japan (100 participants).

[1] A. Shimizu *et al.*, Plasma Fusion Res. **13**, 3403123 (2018).
[2] H. Liu *et al.*, Plasma Fusion Res. **13**, 3405067 (2018).
[3] Y. Xu *et al.*, "*Physics and Engineering Designs for Chinese First Quasi-axisymmetric Stellarator (CFQS)*", 27th IAEA Fusion Energy Conference, Ahmedabad, India, 22–27 October 2018, EX/P5-23.
[4] C.R. Wu *et al.*, Rev. Sci. Instrum. **89**, 10I144 (2018).
[5] K. Ogawa *et al.*, Plasma Phys. Control. Fus. **60**, 095010 (2018).
[6] Ling Zhang *et al.*, Nucl. Instrum. Meth. **A 916**, 169–178 (2019).
[7] C.F. Dong *et al.*, Nucl. Fusion **59** (2019) 016020.
[8] Q. Zhou *et al.*, J. Nucl. Mater. **522**, 286–293 (2018).

(M. Isobe, T. Oishi, Y. Suzuki and T. Tanaka)

Collaboration under implement agreement between MEXT of Japan and the MOST of China for cooperation in the area of magnetic fusion energy research and development and related fields (JWG)

The People's Republic of China-Japan collaboration under the collaboration agreement between the MEXT of Japan and the MOST of the People's Republic of China has been performed following the results of the 11th JWG (Joint Working Group) held in Tianjin, China on July 26–27 2018.

In the meeting, in total collaborative programs (sixteen programs from NIFS and other institutes to the People's Republic of China and twenty-one programs from the People's Republic of China to NIFS and other institutes) are proposed and approved for the fiscal year 2018. The ollowing ten among sixteen approved programs from Japan to the People's Republic of China are performed.

- JC152 KUBO Shin and YANAI Ryoma (NIFS) to SWIP/ASIPP, 24–28 Mar., 2019
  - *ECRH System Optimization and ECRH Experiment in HL-2A,EAST and HL-2M*
- JC153 TSUMORI Katsuyoshi (NIFS) to SWIP, Feb. 24 – Mar. 8, 2016
  - *Development of Cs-Seeded Negative Ion Source for NBI*
- JC155 ISOBE Mitsutaka and OGAWA Kunihiro to ASIPP, Mar. 27–30, 2019
  - *Energetic-particle confinement study in LHD and EAST*
- JC156 YAMADA Ichihiro to SWIP, Feb. 26 – Mar. 1, 2019
  - *Electron temperature profile measurement by the HL-2A/2M Thomson scattering system*
- JC159 OISHI Tetsutaro and KAWAMOTO Yasuko to ASIPP, Feb. 24 – Mar. 2, 2019
  - *Collaboration on EUV spectroscopy in EAST*
- JC160 MORITA Shigeru and KATO Daiji to ASIPP, Jul. 23–27, 2018
  - *The 7th China-Japan-Korea Joint Seminar on Atomic and Molecular Processes in Plasma (AMPP2018)*
- JC163 TODO Yasushi to ASIPP, Jan. 23–27, 2019
  - *Simulation of energetic particle driven instabilities*
- JC165 YANAGI Nagato and MIYAZAWA Junichi to ASIPP/SWIP, Nov. 6–11, 2018
  - *Simulation of energetic particle driven instabilities*
- JC166 SAKAMOTO Yoshiteru and HIWATARI Ryoji to /SWIP, Nov. 7–8, 2018
  - *Discussion of Fusion DEMO Design and R&D in SWIP*
- JC167 SAKAMOTO Yoshiteru and HIWATARI Ryoji to /SWIP, Nov. 9–10, 2018
  - *Discussion of Fusion DEMO Design and R&D in SWIP*

Each program has been performed as substantial collaborations in each field and have benefitted the research progress of both sides as well as making the mutual understanding stronger for the future collaborations.

The following eight (CJ190 divided into three and CJ196 into two) collaborations are executed, eight are postponed and five are cancelled out of the twenty-one approved programs from People's Republic of China to NIFS.

- CJ190A ZHANG Ling (ASIPP) with MORITA Shigeru (NIFS), Jan.6-19, 2019
  - *Impurity radiation and transport Line analysis of EUV spectra and tungsten control in LHD and EAST*

  MORITA Shigeru
- CJ190B DUAN Yanming (ASIPP) with PETERSON Byron (NIFS), June 25 – July 5, 2019
  - *Impurity radiation and transport The EAST Bolometer diagnostics and the LHD IRVB technique*

- CJ190C ZHANG Yang (ASIPP) with ISOBE Mitsutaka and SUZUKI Yasuhiro (NIFS), June 25 – July 2, 2019
  - *Impurity radiation and transport Modeling of FTD experiment with HINT2*
- CJ192 ZHENG Jinxing (ASIPP) with YANAGI Nagato (NIFS) and SAKAMOTO Yoshiteru (QST), July 11–18, 2019
  - *HTS superconducting samples HTS superconductor of CFETR and JA DEMO*
- CJ193 QIN Shijun (ASIPP) with YANAGI Nagato (NIFS) and SAKAMOTO Yoshiteru (QST), July 11–18, 2019
  - *Design, analysis and assessment on CFETR and JA DEMO divertor*
- CJ194 GUO Fei (ASIPP) with CHIKARAISHI Hirotaka (NIFS), Jan. 15–22, 2019
  - *High voltage power supply*
- CJ195 LI Jiang (ASIPP) with CHIKARAISHI Hirotaka (NIFS), Jan. 15–22, 2019
  - *Coil power supply system*
- CJ196A FU Jia (ASIPP) with IDA Katsumi (NIFS), June 9–15, 2019
  - *The motional Stark effect diagnostic on EAST and LHD*
- CJ196B CHANG Jiafeng (ASIPP) with IDA Katsumi (NIFS), June 9–15, 2019
  - *FILD diagnostic development on EAST and Large Helical Device*
- CJ199 JIANG Caichao and WEI Jianglong (ASIPP) with OSAKABE Masaki (NIFS), Nov. 6–12, 2018
  - *N-NBI system*
- CJ200 DONG Chunfeng (SWIP) with OHISHI Tetsutaro (NIFS), July. 15–20, 2019
  - *Comparative study of the edge impurity transport between HL-2A and LHD*
- CJ201 HUANG Mei and ZHANG Feng (SWIP) with KUBO Shin (NIFS), Dec. 5–9, 2018
  - *Comparative study of ECRH transmission line, antenna and system commissioning on HL-2A and LHD*
- CJ202 GENG Shaofei, LIU He, WEI Huilin, YU Peixuan and YANG Xianfu (SWIP) with TSUMORI Katsuyoshi (NIFS), Nov. 25 – Dec.1, 2018
  - *Discuss about the design and control on neutral beam line based on negative ion source*
- CJ204 XU Min, ZHENG Pengfei and CHE Tong (SWIP) with YANAGI Nagato (NIFS), May 12–18, 2019
  - *Testing of HTS conductors for magnets design*
- CJ206 CHEN Jiming and WEI Ran (SWIP) with NAGASAKA Takuya (NIFS) and TANIGAWA Hiroyasu (QST), May 12–18, 2019
  - *Discussion about neutron irradiation testing technology for structural materials*
- CJ207 LIU Yi and ZHANG Yipo (SWIP) with ISOBE Mitsutaka and OGAWA Kunihiro (NIFS), June 23–28, 2019
  - *Developments of neutron diagnostics for HL-2A/LHD and joint experimental studies of energetic particles Physics in LHD*

Next JWG meeting (JWG-12) will be held in Nagoya, Japan near the end of July 2019 to discuss fiscal year 2019 programs.

(S. Kubo)

Japan-Korea Fusion Collaboration Programs

Closer and deeper cooperation in the areas of plasma heating systems, diagnostic systems, and SC toroidal device experiments were essential for physics research. Another important aspect of this collaboration is human resource development for future fusion research.

I. KSTAR collaboration

1 Plasma Heating Systems

The Korea-Japan Workshop on the Physics and Technology of Heating and Current Drive was held in Seoul, Korea in March 2019.

1.1 Radio Frequency Systems

Both Parties continued the collaboration and exchange of personnel and technical knowledge for the development of radio frequency technologies in fusion plasmas.

2 Diagnostic Systems

2.1 Bolometer Systems

Discussions continued regarding the reinstallation of the resistive bolometers on KSTAR as part of the KSTAR upgrade planned for 2021[1,2]. Joint work was done by Japanese and Korean researchers from NIFS and NFRI on the design and the proposal of a future upgrade of the IRVB for disruption mitigation experiments in KSTAR[3].

2.2 Edge Thomson Scattering System

Collaboration regarding the high repetition rate sampling (5 GS/s) DAQ system has been continued. For this collaboration, Japanese researchers from NIFS visited NFRI. NIFS and NFRI continued the collaboration on the 10 Hz YAG Laser.

2.3 Electron Cyclotron Emission (ECE) and Imaging (ECEI) System

The ECE radiometer system was continuously used for the KSTAR experiment. There has been discussion about the information on the ECE imaging systems of KSTAR and LHD. Both parties will continue the discussion regarding how to understand the imaging data and other issues.

2.4 Fast RF Spectrometer System

Collaboration papers have been submitted/published including those by UK collaborators for comparison between nonlinear simulation and KSTAR/LHD data. Based on the experiences from KSTAR and LHD, the design of a new RF radiation measurement system on QUEST has been discussed through a collaboration with Japanese researchers from Kyushu University. This diagnostic is primarily intended to measure RF radiations from runaway electrons.

2.5 Charge Exchange Recombination Spectroscopy

Charge exchange spectroscopy is one of the active spectroscopy using neutral beam to measure ion temperature, plasma rotation velocity, and impurity density. Korean and Japanese researchers continued the collaboration on the three types of CES spectrometers for the advanced KSTAR physics research.

2.6 Neutron and Energetic-ion Diagnostics

Japanese and Korean researchers will cooperate together to enhance temporal resolution of the Fast ion Loss Detector (FILD) system utilizing the fast electronics[4,5,6,7]. In addition, collaborative works on the Lorentz-Orbit (LORBIT) and/or Orbit Following Monte Carlo (OFMC) simulation will be continued to understand beam-ion behaviors in KSTAR.

2.7 Soft X-ray CCD Camera (SXCCD) and VUV Telescope System

Japanese and Korean researchers continued the preparation of the SXCCD camera system to be installed at the B port in KSTAR. A new supporting structure shared with the VUV telescope system has been jointly designed and fabricated. The remaining necessary items (a cooling water chiller and an in-vacuum neutron shield) of the SXCCD camera system will be shipped from NIFS to NFRI in the next scal year.

2.8 EMA Post Data Analysis System

Korean researchers from NFRI and Japanese researchers from NIFS continued the collaboration on data analysis system, EMA, which consists of EG data server, Myview data viewer, and Autoana automatic analysis system. We use Git, a distributed version-control system, to establish remote collaborative development. Also, the latest AutoAna system was installed for the KSTAR project using VPN service.

2.9 The 9th Japan-Korea Seminar on Advanced Diagnostics

The 9th Japan-Korea Seminar on Advanced Diagnostics was held at the National Institute for Fusion Science and at the KKR Hotel in Nagoya from August 7–10, 2018 and was hosted by Prof. K. Ida of NIFS. The purpose of this seminar was as follows: (1) to give young researchers and students from both countries a comprehensive knowledge of diagnostics for steady-state fusion plasmas, (2) to give them the opportunity to present their scientic results and (3) to help them to develop international friendships and collaborations. The number of lectures given was 15 (8 from Japan and 7 from Korea) on a variety of topics related to plasma diagnostics. 34 young researchers attended the seminar (20 from Japan and 14 from Korea) and gave poster presentations of their research.

2.10 SC Toroidal Device Experiments

Korean researchers from NFRI visited NIFS to participate in LHD D-D experiments to study rotation dynamics by external heating beam direction. Japanese researchers participated in the KSTAR experiment to study rotation transport dynamics under the nonaxisymmetric magnetic perturbation field.

II. Human Resource Development

The total number of researchers that were exchanged between Japan and Korea in JFY 2018 were 47 from Japan to Korea and 54 from Korea to Japan. Thirteen Workshops in various fields were held in each country (6 in Japan and 6 in Korea).

- Workshop on Physics validation and control of turbulent transport and MHD in fusion plasmas, Kyoto U., Japan, May 24–26, 2018.
- 4th Japan-Korea Joint Workshop for Fusion Material Technology Integration and Engineering, Otsu, Japan, June 29–30, 2018.
- 14th JCM, Seoul, Korea, July 4–5, 2018.
- Recovery of tritium in fusion reactor and its safety technology (III), Seoul National University, Korea, July 10–13, 2018.
- Workshop on ITER tritium system, Seoul National University, Korea, July 11–12, 2018.
- Modeling and Simulation of Magnetic Fusion Plasmas, Busan, Korea, July 11–14, 2018.
- Physics of fine plasma particles, Kamakura, Japan, July 26, 2018.
- The 9th Korea-Japan Seminar on Advanced Diagnostics, NIFS, Nagoya, Japan, August 7–10, 2018.
- Japan-Korea Blanket Workshop, QST, Japan, November 19–20, 2018.
- 12th Workshop on ITER Diagnostics, QST, Japan, December 13–14, 2018.
- KSTAR Conference, Seoul Korea, February 19, 2019.
- Workshop on Physics and Technology of Heating and Current Drive, SNU, Korea, March 18–21, 2019.

1) Juhyeok Jang *et al.*, Rev. Sci. Instrum. **89**, 10E111 (2018).
2) B. J. Peterson *et al.*, Rev. Sci. Instrum. **89**, 10E115 (2018).
3) Seungtae Oh *et al.*, Rev. Sci. Instrum. **89**, 10E118 (2018).
4) M. Isobe *et al.*, IEEE Trans. Plasma Sci. **46**, 2050 (2018).
5) K. Ogawa *et al.*, Rev. Sci. Instrum. **89**, 10I101 (2018).
6) K. Ogawa *et al.*, Plasma Phys. Control. Fusion **60**, 095010 (2018).
7) Jungmin Jo, et al., Rev. Sci. Instrum. **89**, 10I118 (2018).

(K. Ida)

11. Research Enhancement Strategy Office

The Research Enhancement Strategy Office (RESO) was founded in October 2013, and three University Research Administrators (URAs) were assigned. Under the Research Planning Task Group, the following four Task Groups were organized.

(1) IR(Institutional Research)/Evaluation Task Group
(2) Public Relations Enhancement Task Group
(3) Collaboration Research Enhancement Task Group
(4) Young Researchers Development Task Group

(1) The collaborative research activities

1) Enhancing international collaborative research in the stellarator-heliotron (S-H) plasma, and steady-state operation (SSO) toward a fusion reactor

After the divertor installation to Wendelstein 7-X (W7-X), which is promoted by Max Planck Institute of Plasma Physics (IPP) at Greifswald in Germany, the third helical plasma experiment (OP1.2b) for W7-X was carried out from July to October 2018. In this campaign, the neutral particle injector (NBI) was newly installed to study fast particle physics. A fast particle confinement and verification of local heat load on the divertor was one of the crucial commissions for W7-X. Several scientists in NIFS were assigned to IPP to initiate collaboration using NBI. In order to accelerate the collaborations, the Annexes to the NIFS-IPP Agreements were updated.

Collaborative research was also enhanced with PPPL and the University of Wisconsin in the United States, CIEMAT in Spain, CEA in France, CONSORZIO RFX in Italy, Culham Centre in the United Kingdom, and Peking University and Southwest Jiaotong University (SWJTU) in China.

2) International research network for integrated plasma physics

In addition to the individual MoUs with Princeton University and three Max-Planck institutes (IPP, MPA and MPS), a new MoU for starting the International Research Collaboration Center for Astrofusion Plasma Physics (IRCC-AFP) in NINS was discussed. A postdoctoral fellow employed by NIFS for the integral plasma physics has finished a term of two years with fruitful international collaboration results among Princeton University and many Japanese universities.

3) Promoting establishment of Agreements with Asian institutes to accelerate collaborative research

In order to enhance helical and stellarator research in Asian countries, the Chinese First Quasi-axisymmetric Stellarator (CFQS) project between NIFS and SWJTU and an international research collaboration between NIFS and Peking University has been promoted. The design parameters of plasma experiment in CFQS were completed, and test manufacturing of the magnetic coils has started.

(2) Supporting young researchers

In the activities for supporting young researchers, international collaboration activities of young researchers were encouraged, enforcing their basic research skills. RESO supported the international collaboration plans proposed by young researchers in NIFS. Applications were reviewed by the Young Researchers Development Task Group. One program was supported in FY2018 as follows.

1. Measurement and analysis of ultra-violet spectra emitted from the high-Z atoms of high-energy EBIT(electron beam ion trap).

In addition, RESO supported the basic research plans of young scientists for the purpose of enhancing their fundamental scientific skills. Three programs were supported in FY2018 as follows.

1. Experimental study of recovering cracks on the plasma facing materials using strong electron beam irradiation.
2. Fokker-Planck model analysis for the confinement of energetic ions with MHD instabilities driven by the high energy ions.

3. Transport analysis with collisional radiation model based on the impurity spectroscopic measurement data in Large Helical Device.

RESO also assisted with the applications of young scientists to the 'Grants-in-aid Scientific Research' program. About 70 application documents were reviewed and suggestions were given to the authors for improvement.

(3) Enhancing public relations

1) Dissemination of research achievements through EurekAlert!

Three topics were released: i) "The First Experimental Discovery in the World of the Propagation of Plasma Turbulence: Results of Japan-United States Joint Research," ii) "Developing New Materials for the Fusion Reactor: Success in Developing Vanadium Alloys Strong at High Temperatures and Appropriate for Manufacturing and Welding," and iii) "Fusion Science and Astronomy Collaboration Enables Investigation of the Origin of Heavy Elements". These topics were released to the media in Japan, too. Some topics attracted attention from the international media.

2) Information release about NIFS and fusion science

The NINS director's press conference was held on 21 December 2018 and the state-of-the art plasma and fusion science results were given to the press. RESO participated in the AAAS annual meeting and introduced NIFS and our research results to meeting participants in collaboration with other Japanese institutes, from 14-17 February 2019.

3) Outreach activities based on the fusion community

One of the outreach activities is to join the organization of the ITER/BA Projects annual report meeting. RESO exhibited panels showing NIFS research activities at the meeting. RESO also joined the discussion of the fusion science outreach headquarter.

4) Others

RESO introduced interesting science topics to the public on the occasion of the science café at the Open House of NIFS shown in the Figure 1.

Fig. 1 The science café at the Open House of NIFS.

(4) IR/Evaluation activities

The task group for the IR (Institutional Research) and evaluation continued its role to make systematic analyses of the present research activities of the institute and for providing proposals to improve the research management of the institute. A systematic reviewing was undertaken for recognizing what are important issues in managing efficient research collaborations.

(T. Muroga, S. Okamura, H. Kasahara and K. Yaji)

12. The Division of Health and Safety Promotion

The Division of Health and Safety Promotion is devoted to preventing work-related accidents, to ensuring safe and sound operation of machinery and equipment, and to maintaining a safe and healthful environment for researchers, technical staff, co-researchers, and students. Each division cooperates with each other to ensure health and safety.

As a nationwide activity, we hold an information exchange meeting on health and safety each year, calling on those involved in the health and safety of university related organizations. About 60 people from 19 organizations participated this fiscal year.

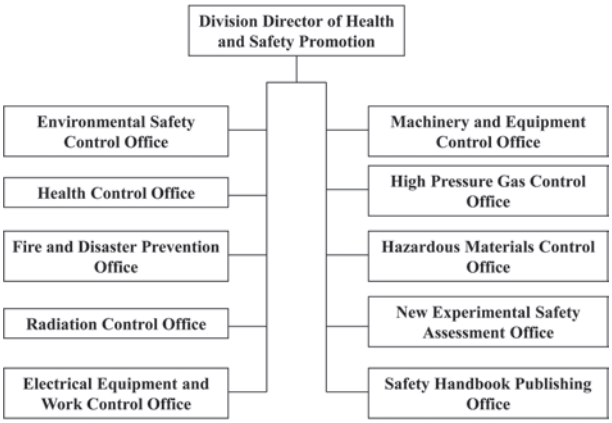

Fig. 1 Division of Health and Safety Promotion

1. Environmental Safety Control Office

This office has the responsibility to maintain a safe work space and environment. Although the other nine offices of the division of health and safety promotion cover most of the risks that exist in the institute, some problems fall wide of them. The role of this office is to cope with such problems. Therefore, this office has a broad range of tasks.

(i) Management to solve the problems pointed out by the safety and health committee.
(ii) Maintenance of the card-key system for the gateways of controlled area.
(iii) Maintenance and management of the vehicle gate at the entrance of the experimental zone.
(iv) Maintenance of the fluorescent signs of the evacuation routes and the caution marks.

2. Health Control Office

The main role of this office is to keep the workers in the institute healthy, including co-researchers and students.

(i) Medical checkups both for general and special purposes and immunization for influenza.
(ii) Mental health care services and health consultation.
(iii) Accompany the inspections of the health administrator and the occupational physician.
(iv) Maintenance of AEDs.

Various lectures were held for physical and mental health. And, an on-line stress-check was held in October.

3. Fire and Disaster Prevention Office

The main role of this office is to prevent or minimize damage caused by various disasters.

(i) Making self-defense plans for fires and disasters, and implementation of various training.
(ii) Promotion of first-aid workshops and the AED class.
(iii) Maintenance of fire-defense facilities and attending on-site inspections by a local fire department.
(iv) Review and update disaster prevention rules and disaster prevention manuals.

All workers have to attend the disaster prevention training held every year.

4. Radiation Control Office

The main role of this office is to maintain radiation safety for researchers and the environment. Legal procedures for radiation safety and regular education for the radiation area workers are also important roles of this office

(i) Maintain radiation safety for the workers
(ii) Registration and dose control of radiation area workers.
(iii) Observation of radiation in the radiation controlled area and the peripheral area.
(iv) Maintenance of the radiation monitor.
(v) Applications for radiation equipment to the agencies and the local government.
(vi) Revise official regulations and establish new rules.

Two educational lectures were held on March 6, 2018 and March 14, 2018 for the radiation area workers. Non-Japanese workers can be educated and trained in English.

5. Electrical Equipment and Work Control Office

The main role of this office is to maintain electrical safety for researchers, technical staffs and students.

(i) Check and control the electric facilities according to the technical standards.
(ii) Safety lecture for the researchers and workers.
(iii) Annual check of the electric equipment during a blackout.

The annual inspection of the academic zone was carried out on May 20, 2018, and that of the experimental zone was carried out on June 2 and June 3, 2018.

6. Machinery and Equipment Control Office

The main role of this office is to maintain the safe operation of cranes. The tasks of this office are summarized as follows.

(i) Inspection and maintenance of cranes.
(ii) Management of the crane license holders and safety lectures for the crane users.
(iii) Schedule management of crane operations.

7. High Pressure Gas Control Office

This office has a very important role in NIFS, because the main experimental machine LHD is the super-conducting machine which requires cooling by liquid helium. Many other machines have cryogenic pumping systems, which also require cooling down. The tasks of this office are summarized as follows.

(i) Safety operation and maintenance of high pressure gas handling facilities in NIFS.
(ii) Daily operation, maintenance, system improvement, and safety education according to the law.
(iii) Safety lectures for researchers and workers.

8. Hazardous Materials Control Office

The main role of this office is the management of the safe treatment of hazardous materials and maintaining safety for researchers against hazardous events.

(i) Research the requests for hazardous materials and the storage status.
(ii) Management to ensure safe storage of the waste.
(iii) Monitoring of discharging water to prevent water pollution.
(iv) Implementation of chemical substance risk assessment.

9. New Experimental Safety Assessment Office

The main role of this office is to check the safety of experimental devices other than LHD. For this purpose, researchers who want to setup new experimental apparatus must apply for the safety review. Two reviewers are assigned from members of this office and other specialists. They check the safety of these devices.

(i) Examine new experiments for safety problems and advise on safety measures. (New experiments in LHD are reviewed by the LHD Experiment Group.)
(ii) Improve safety in each experiment and reinforce the safety culture at NIFS by annual reviews by NIFS employees.

10. Safety Handbook Publishing Office

The tasks of this office are publication of the Safety Handbook in Japanese and in English and to update them as necessary. The regular safety lectures were held on May 9, May 22, and May 24, 2018. All workers including the co-researchers and students must attend this safety lecture every year.

Detailed information is available on our web-site:
http://www.nifs.ac.jp/

(K. Nishimura)

13. Division of Deuterium Experiments Management

The deuterium experiment has been carried out on LHD since March 7th, 2017. Objectives of the deuterium experiments are (1) to Achieve high-performance plasmas by confinement improvement and by the improved heating devices and other facilities, (2) to explore the isotope effect study, (3) to demonstrate the confinement capability of energetic particles (EPs) in the helical system and to explore confinement studies in toroidal plasmas, and (4) to proceed with the extended studies on Plasma-Material Interactions (PMI) with longer time scales.

The division of deuterium experiments management was founded to establish the safety management system and to consolidate experimental apparatus related to the deuterium experiments. After the start of the deuterium experiment on the LHD, the function of this division was shifted to the management of the safe and reliable operation of the deuterium experiment. Under this division, a taskforce named 'Deuterium Experiment Management Assistance Taskforce' was founded. The main jobs of the taskforce are (1) the establishment and improve manuals to operate LHD and peripheral devices safely during deuterium experiments, (2) check and improvement of the regulations related to proceeding with the deuterium experiments safely, (3) the upgrade of LHD, its peripheral devices and the interlock systems for the safe operation during the deuterium experiments, (4) upgrade and optimization of heating devices and diagnostic systems for the deuterium experiments, and (5) remodeling the LHD building and related facilities, and other matters. These jobs proceed with the cooperation of the LHD board meeting and the division of health and safety promotion. In addition, the necessary tasks related to the safety evaluation committee founded by NIFS and those related to the safety inspection committee for the National Institute for Fusion Science (NIFS) founded by local government bodies are advanced in this division. The publication of an annual report for the radiation management of the LHD deuterium experiment is another important task of this division.

During the fiscal year 2018, the safety evaluation committee met three times. The main topics of the committee are the evaluation of the annual report for radiation management in the deuterium experiment and the evaluation of the safety operation of the deuterium experiment in the experimental campaign of 2018. In addition, the reduction of night and weekend duty was discussed by the committee. The suggestion to increase the number of staff, who are engaged in this duty was made by the committee.

The cooperation with the safety inspection committee at NIFS is an important task for the division of the deuterium experiments management. The environmental neutron dose monitoring at NIFS and the tritium concentration monitoring in the environmental water around the NIFS has been performed by the committee since 2015. In FY 2017, these monitoring activities were performed twice as scheduled with the cooperation of the division of deuterium experiment management.

a)

b)

c)

d)

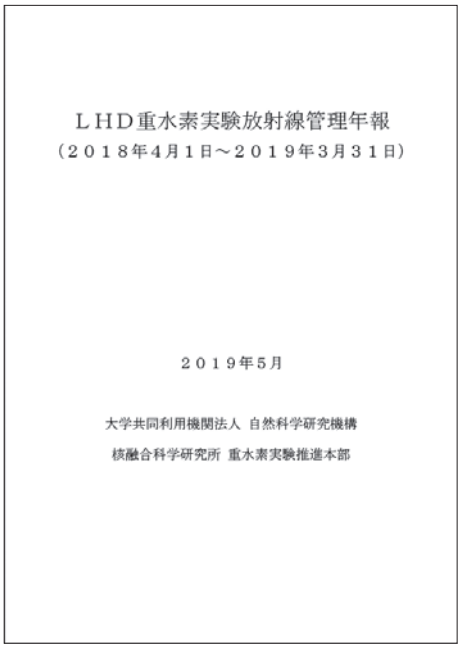

(a) Photographs at the environmental water sampling with the secretariat of the safety inspection committee. (b) The real-time radiation monitoring post where the cooperative environmental neutron monitoring is performed with the secretariat. (c) Additional neutron dosimeters placed by the secretariat of the safety inspection committee (left) and by the division of deuterium experiment management (right) near the radiation monitoring post for the cooperative environmental neutron monitoring with the secretariat. (d) The front cover of the annual report for the radiation management at the first LHD deuterium experiment (in Japanese).

(M. Osakabe)

14. Division of Information and Communication Systems

The Department of Information and Communication System (ICS) was founded in 2014 in order to develop and maintain the information and network systems of NIFS efficiently. All of the information system experts in NIFS belong to the ICS. There are five TASK groups which correspond to the job classifications in NIFS. The Network Operation task group manages and maintains the communication systems in NIFS, such as the E-mail system including security issues. The Experimental Data System task group performs operation and development of data acquisition systems for the LHD experiment. The Institutional Information Systems task group carries out the maintenance and development of the management systems for collaboration research and its output. The Atomic and Molecule Database task group maintains the atom and molecule database which is open to researchers around the world. The Integrated ID Management and Authentication System task group manages integrated ID and authentication systems.

The ICS works as follows: the request for the maintenance, improvement, and development of the information and communication system from each section is submitted to the ICS. The deputy division directors of ICS check all the requests, establish the priority among them, and assign them to the appropriate Task Group. Because all the experts belong to the Technical Service Section of ICS, each Task Group Leader asks the Section Leader to allot the required number of experts for a prescribed period of time so as to finish the job.

In NIFS, three research projects extend across the research divisions. It can be said that the ICS is another "project" which lies across all the divisions in the institute for keeping the information and communication systems stable, secure, and up-to-date.

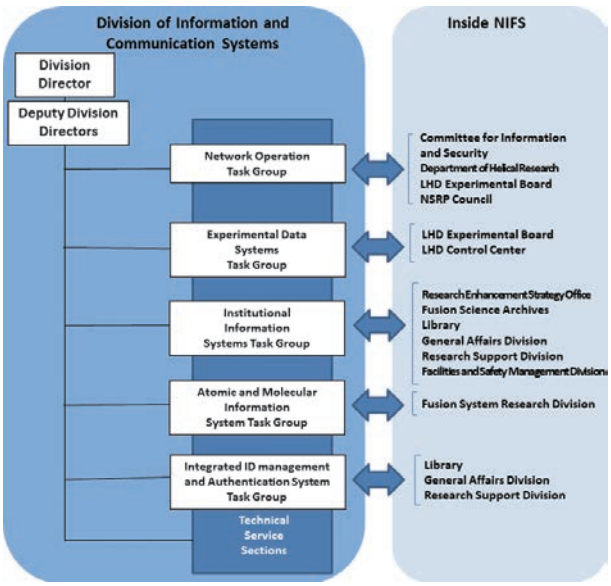

Fig. 1 Structure of Division for Information and Communication Systems.

Information Network Task Group

The information network is a foundation for research activity. The Information Network Task Group operates the advanced NIFS campus information network named "NIFS-LAN," which contributes to the development of fusion research, with strong security systems.

Notable activities in FY 2018 by the Information Network Task Group:

- The backup system for the virtual foundation system of the Research Information Cluster has been

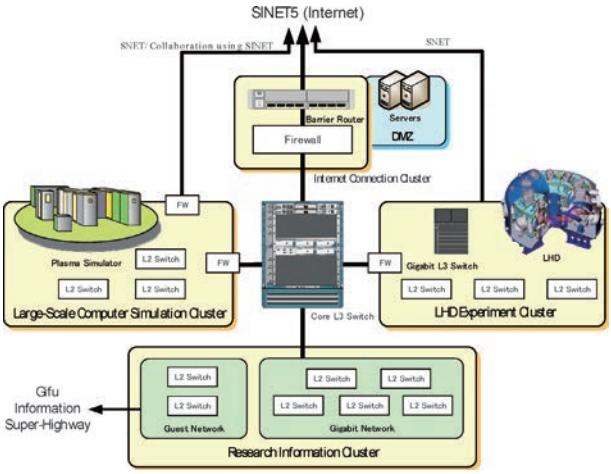

Fig. 2 Block diagram of the NIFS campus information network, which consists of three autonomous clusters that have their own purposes and usages.

upgraded. The malware detection appliance has been upgraded. New appliance has virtual PC running not only Windows OS but also Mac OS X to detect malware.

- The core switch of the LHD control LAN on the LHD Experiment Cluster has been upgraded. Before the LHD experiment campaign, the security condition of each PC was checked in order to keep the safety network free of malware.
- Security incidents were treated with a malware detection appliance and the firewall. Lectures were held regarding the information network and its security. An informational system audit held by NINS was also accomplished.

Experimental and Institutional Information Systems Task Groups

The objective of these Task Groups (TGs) is to promote the research activities in both the LHD experiment and the NIFS institutional aspects by providing better computational services for research and official work.

Regarding the experimental information systems (EIS), a number of LHD-related computer subsystems were successfully operated in the 20th campaign until February 2019. It had more than 9000 plasma discharge experiments (shot no. 144105–153366). The accumulated raw data amount is approximately 683 TB. Since the beginning of the 20th campaign, a pair of fast SSD arrays has been installed as the preceding part of the main HDD storage. Two SSD storages are directly connected via 40 Gbps Ethernet and provides 11 and 9 GB/s read/write speeds. They are one-digit faster than HDDs and therefore suitable for I/O rush after every discharge end.

Another innovation in the institutional information systems (IIS) is a new version 3.5 of NIFS Article Information System (NAIS). Figure 3 shows the brand-new user interface of the article search. It has been equipped with the new "free-word" search, which can be switched over to the advanced search. Almost all the related bibliographic variables can be set in search conditions. The free-word search and the advanced search are expected to improve the usability for novice and professional users, respectively.

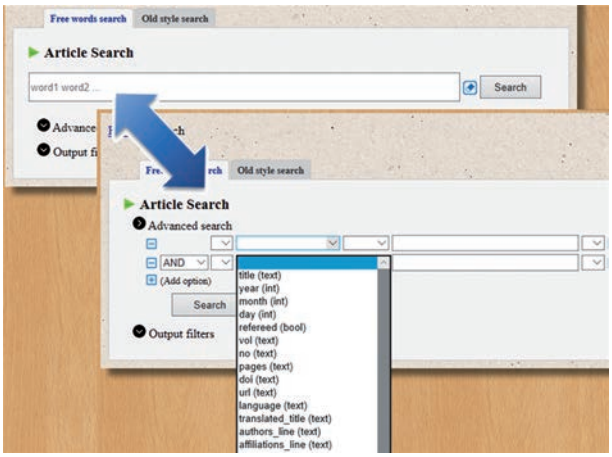

Fig. 3 New user interface for article search in NAIS: New free-words search can be switched over with the advanced search where any number of search conditions can be set. Quick searches and conditional searches are enabled respectively.

(S. Ishiguro)

15. Division of External Affairs

The Division of External Affairs has been focusing on the following six activities with a view to increasing societal recognition of the necessity of nuclear fusion research and also NIFS's scientific achievements.

- Planning and conducting the NIFS Tour
- Participation in local events and festivals
- Publication of the PR magazine "NIFS NEWS"
- Creation of showpieces and booklets to make PR efforts more attractive and effective
- Update of the NIFS website
- Educational tie-ups with national high schools/Educational programs for local communities (e.g., work experience, scientific demonstrations, and workshops)

Fig. 1 A photo of the Tajimi Festival in Tajimi City

Below are details of the PR efforts made by the Division of External Affairs.

• NIFS Tour
  - Handling requests, coordinating schedules, and conducting tours of the institute: A total of 3,470 visitors participated in the NIFS Tour.
  - Development of various materials and devices for scientific demonstrations/attractions during the tour
  - Upgrading of the scientific exhibit space "Kids Corner"

• Publications
  - Design, publication, and distribution of the PR magazine "NIFS NEWS"
  - Design, publication, and distribution of the PR booklets: "NIFS 2018-2019," "Fusion – Energy to Pave the Way for the Future," "NIFS Performs Research Aimed at Extracting Energy from Sea Water," and "Introduction to NIFS and the NIFS Tour"
  - Design, publication, and distribution of the PR leaflet "Plasma-kun Dayori"

- Web
  - Release of information through Web pages, mailing lists, and SNS (Twitter and Facebook)
  - Design of signs and other advertising materials
  - Creation of special website featuring scientific events, symposia, and conferences
  - Creation of frames for research division homepages
  - Upgrading of various on-line application forms
  - Expansion of in-house contents

- Educational contributions
  - Educational partnership activities of Super Science High School (SSH): Thirteen high schools and 493 students participated.
  - Special alumnus lectures and other visiting lectures: Eight high schools were visited.
  - Internship and working experiment programs for junior high school and high school students: Four schools were accepted.
  - Internship programs for college and technical college students: Sixteen students were accepted.
  - Science handicraft workshops for local communities: Thirty-three workshops were organized and a total of 1,088 participants attended.

Fig. 2 Working experiment for junior high school students

Fig. 3 Science handicraft activity at community center

(K. Takahata)

16. Department of Engineering and Technical Services

The Department of Engineering and Technical Services covers a wide range of work in the design, fabrication, construction, and operation of experimental devices in the fields of software and hardware.

The department consists of the following five divisions. The Fabrication Technology Division oversees the construction of small devices and quality control of parts for all divisions. The Device Technology Division works on the Large Helical Device (LHD) and its peripheral devices except for heating devices and diagnostic devices. The Plasma Heating Technology Division supports the ECH system, the ICRF system, and the NBI system. The Diagnostic Technology Division supports plasma diagnostic devices and radiation measurement devices, and takes charge of radiation control. Finally, the Control Technology Division concentrates on the central control system, the cryogenic system, the current control system, and the NIFS network.

The engineering department welcomed five newcomers in April and October. The total number of staff is 57 (2018.10). We are in charge of the development, the operation, and the maintenance of the LHD and its peripheral devices together with approximately 57 operators.

1. Fabrication Technology Division

The main work of this division is the fabrication of experimental equipment. We also take care of technical consultation and experimental parts supplies related to the LHD experiment. In addition, we manage the administrative procedures of the department.

The number of requests for machining was 144, and the total number of produced parts was 369 in this fiscal year (FY). The number of electronic engineering requests was 14, and the total number of produced electric articles was 77. The details of some of this division's activities follow below.

(1) Injection pipe for TESPEL

We have fabricated injection pipe for TESPEL. (Fig. 1) The injection pipe consists of two kinds of pipes. One is an outer pipe, which is a stainless steel pipe with an outer diameter of 11mm. The other is an inner pipe with an outer diameter of 3mm and a thickness of 1mm. The inner pipe is welded to the tip part. The welding is TIG welding. We placed a guide block at the center of the pipe to prevent the inner pipe from bending.

(2) 56GHz ECH power monitor

We have fabricated power monitor (Fig. 2) for ECH. Power monitor has 21 small diameter holes on the reflection surface of the microwave. The small diameter holes are five different sizes in DIA 0.75mm to 0.87mm. The microwave passed through the small diameter holes is transmitted to the detector by the sub waveguide. The sub waveguide is rectangular in cross section, whose size is 1.88 mm length and 3.78 mm width.

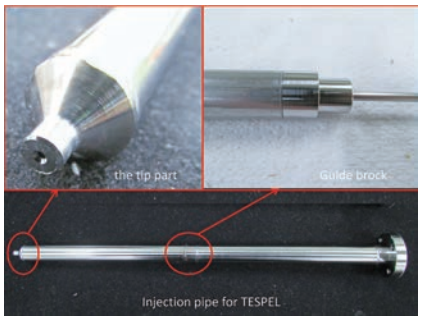

Fig. 1 Injection pipe for TESPEL

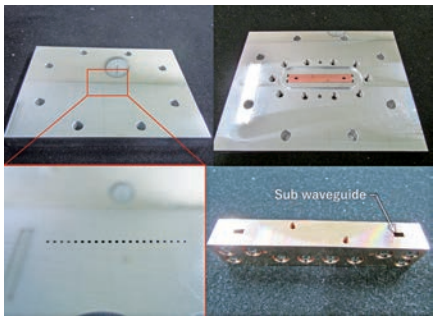

Fig. 2 56 GHz ECH Power monitor

(3) 35ch PIN photo diode amplifier

The amplifier circuit of the 35 channels PIN photo diode array for a fast spectroscope, which detects a visible light from the high-density plasmoid, is shown in Fig. 3. The voltage gain of the amplifier is from 20 to 40 dB and frequency bandwidth is DC to 2 MHz. The upper three layers of the board are the 35 channels PIN photo diode array and fixed gain preamplifiers, and the lower two boards are variable gain main amplifiers.

(4) Wire bonding

Wire bonding is a technique of electrically connecting among MMICs and a printed circuit board by using thin gold wires. We applied the technique to making our original antenna of the ECEI (electron cyclotron emission imaging) system. Fig. 4 shows the wire-connecting-MMICs of active frequency multipliers and mixers on our receiver board. This technique has made it possible to reduce the size and the cost of our microwave circuits, and has contributed to the development of multichannel imaging system.

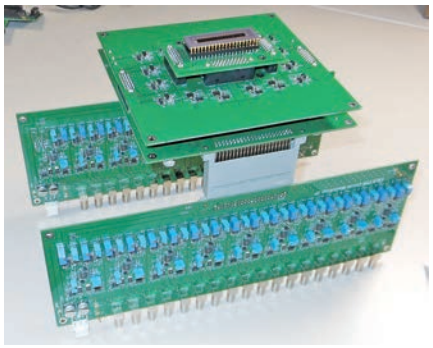

Fig. 3 35ch PIN photo diode amplifier

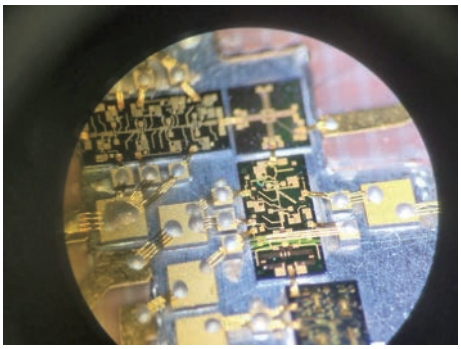

Fig. 4 Wire Bonding

2. Device Technology Division

The Division supports the operation, the improvement, and the maintenance of LHD.

(1) Operation of LHD

We started pumping of the cryostat vessel for cryogenic components on August 23, 2018 and pumping of the plasma vacuum vessel on August 24. Subsequently, we checked air leaking from the flanges of the plasma vacuum vessel. The number of checked flanges was 54. As a result, we found leaks in 4 flanges and repaired those flanges.

The pressure of the cryostat vessel reached the adiabatic condition ($< 2 \times 10^{-2}$ Pa) on August 25 and the pressure of the plasma vacuum vessel reached below 1×10^{-5} Pa on September 4.

The LHD experiment of the 20th experimental campaign began on October 11, 2018 and was implemented continuously until February 21, 2019. The number of days of the plasma experiment was 63 in total.

During this experimental campaign, the vacuum pumping systems could eliminate air from both vessels without trouble. In addition, the utilities (compressed air system, water cooling system, GN2 supply system, etc.) of LHD, and Exhaust detritiation system did not report any major problems. The LHD operation was completed on March 15, 2019.

(2) Engineering analysis in the fields of electromagnetic and structural development

A magnetic shielding is widely used to protect sensitive equipment from magnetism in magnetic field. We tried to develop some existing magnetic shields by ANSYS using finite element method software. To design the magnetic shield with higher shielding performance, both the analysis and the measurement of the magnetic shield are needed. Therefore, we introduced the Helmholtz coils which create a uniform magnetic field between two coils, and investigated the property of the magnetic shield. The magnetic shield is composed of the multi-layer structure as shown in Fig. 5, and these materials are stainless (SUS316) and aluminum (A5052). Based on the results of ANSYS analysis and measurement by using the Helmholtz coils, it was shown that both distributions of magnetic field became almost uniform.

CFQS device is going to be built as a part of a joint project conducted by NIFS in Japan and Southwest Jiaotong University (SWJTU) in China. We concluded the MoU in 2017 on NSJP (NIFS and SWJTU Joint Project) for CFQS experiment. In addition, we are working together with Keye Electro Physical Equipment Manufacturing Co., Ltd. in Hefei with their contribution in engineering design and manufacture of the device. In advance of manufacturing, the Department of Engineering in NIFS has contributed to this project with analysis work. Fig. 6 shows one example, the stress analysis of vacuum vessel. In order to ensure the reliability of the CFQS vacuum vessel, stress analysis has been performed using ANSYS, FEM software by ANSYS, Inc. The result was reported to the project member in China at the 2nd steering committee meeting in May, 2019.

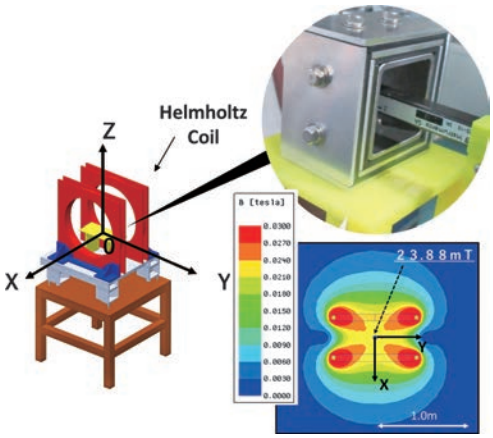

Fig. 5 Arrangement of the Helmholtz coil system, a mockup of magnetic shield, and distribution of magnetic flux density.

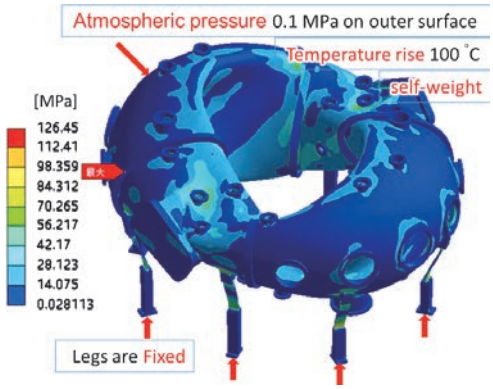

Fig. 6 The stress distribution on vacuum vessel

(3) A water bubbler system

To monitor tritium in the exhaust gas from LHD, we designed and constructed a water bubbler system. A flow diagram of the water bubbler system is shown in Fig. 7.

This system can distinguish chemical forms of tritium. In addition, this system can also change to a simplified sampling line without the distinction of chemical forms in order to reduce the load on an operator and the number of tritium water samples.

The evaporation from sample water was controlled by a cold bath using aluminum beads.

To verify the consistency of the date from this system, we compared this with the measuring result by a commercially available bubbler system (MARC7000, SDEC France).

As a result, the tritium concentration measured by this system was almost the same as the tritium concentration measured by MARC7000.

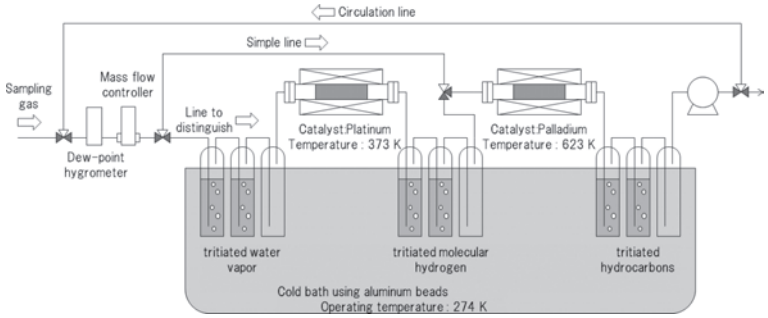

Fig. 7 Water bubbler system flow chart

3. Plasma Heating Technology Division

The main tasks of this division are the operation and the maintenance of individual three different types of plasma heating devices and their common facilities. We have also performed technical support for improving, developing, and newly installing these devices. In this fiscal year, we mainly carried out device improvement and modification for a deuterium plasma experiment. The details of these activities are as follows.

(1) ECH

(a) Gyrotron Operation & LHD experiment

During the 20th experimental campaign, we injected the power of 5 MW to assist plasma experiments. That contributed to accomplish the plasma with 10 keV of high ion temperature, and before that, operated by long pulse discharge to clean the wall of vacuum vessel with low power. Some trouble occurred but they did not affect experiments. ECH technical staff of LHD experimental group achieved to contributing to the various plasma experiments.

(b) Support to cooperative research (Optical Vortex)

We improved some parts of our experimental device for achieving high vacuum, because we could not achieve the working vacuum which could operate the electron gun. The improvements include expanded MOU connecting new transmission line and relocation of the 82.7 GHz Gyrotron.

(2) ICH

In order to increase the injection power per antenna, we developed a power combination system and installed it in the Heating Power Equipment Room. The system was inserted in the transmission line for the 4.5L antenna and connected with the #6A and the #6B oscillator. We successfully injected the power of more than 2MW for 6 seconds and 1MW for 10 minutes in an injection test using a dummy load.

(3) NBI

(a) The operation and maintenance of NBI in the 20th campaign of LHD experiments

In the 20th campaign, approximately 8,000 beam shots were injected into the LHD plasmas with three

negative-NBIs (BL1, BL2, and BL3). The injection history of the total injection power for the negative-NBIs is shown in Fig. 8. The maximum injection power in this campaign was 14MW. As for the positive-NBIs (BL4 and BL5), about 4,500 beam shots were injected into the LHD plasmas. The maximum total injection power of positive-NBI was 12MW by hydrogen beam, 18MW by deuterium beam.

NBIs had several problems. BL1 had air leak in the ion source. BL3 had cold leak at LN2 piping in the cryo-pump system. BL3 and BL5 had failures of the power supply unit in the arc power supply system and filament power supply system, respectively. These troubles lowered the injection power a little, but did not lead to serious problems in the plasma experiments. These troubles are now under repair for the next campaign.

(b) A vacuum-vessel inspection for NBI beamline

After every experimental campaign, we have inspected the vacuum vessel of the NBI beamline. In the deuterium experiment, some devices inside the beamline are activated with neutrons, and radioactive tritium is generated via deuterium-deuterium reactions in the vacuum vessel. Thus we first measured the concentration of radioactivity and radiation dose in the vacuum vessel and confirmed that there are no problems in the inspection work.

A small room is prepared outside the vessel entrance to avoid leakage of tritium. Inspection work is carried out with wearing dust protection clothing and a mask. At the end of the work, we surveyed the dust protection clothing to ensure that there was no contamination using both a scintillation survey meter and a tritium/C-14 survey meter (Fig. 9).

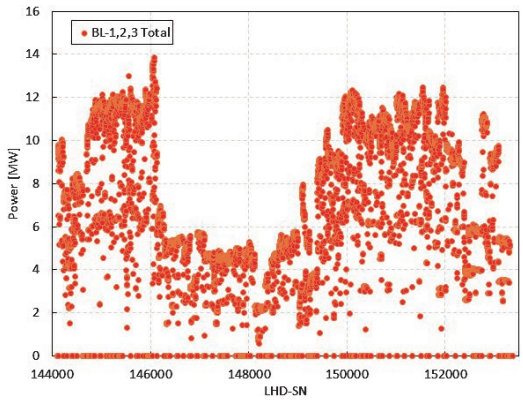

Fig. 8 History of the total injection power for the negative-NBIs

Fig. 9 Dust protective clothing

(4) Motor-Generator (MG)

The MG is used to supply the pulsed power to the NBI and the ECH for LHD. The MG has supplied power for 22,648 shots in this fiscal year and 636,663 shots since its construction. The operation time was 1,195 hours. We updated the excitation control panel and the PLC of speed control panel before the 20th experimental campaign (fig. 10, Fig. 11).

Fig. 10 The updated excitation control panel

Fig. 11 The updated PLC of speed control panel

4. Diagnostics Technology Division

This division mainly supports the development, the operation, and the maintenance for plasma diagnostic devices and radiation measurement devices for LHD. In addition, we also are in charge of radiation control.

(1) Plasma diagnostic device

Fig. 12 shows diagnostics racks installed where some intelligence controller units are located. In order to shield those racks from neutron radiation, we surrounded those racks by 10 cm thick high density borated polyethylene blocks, as shown in Fig. 13. Because total weight of the polyethylene blocks is about 800 kg, we reinforced the rack by using some nonmagnetic angles, and fixed the polyethylene blocks in the angle.

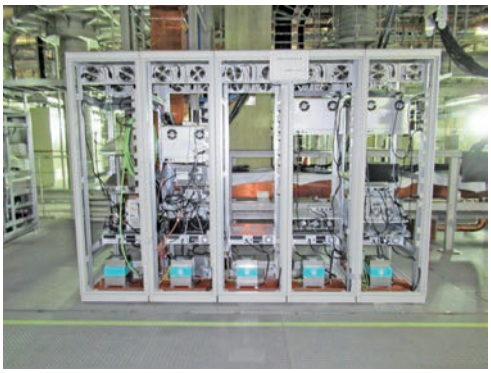

Fig. 12 Diagnostics racks installed with some intelligence controller units

Fig. 13 Radiation shielding by high density borated polyethylene blocks

Some plasma diagnostics devices have worked for about 20 years, and require maintenance. For the Nd:YAG Thomson scattering system and the far-infrared (FIR) interferometer, we carried out the replacement of cooling system for lasers. Those cooling systems are a water-cooled chiller refrigeration unit with the cooling capacity of 10 kW as shown in Fig. 14 and an air-cooled chiller refrigeration unit with 10 kW, respectively.

For the LHD Data Acquisition (DAQ) System, we have added SSD storage system in front of the existing HDD storage system as shown in Fig. 15. We have also applied 40GbE network. Consequently, the throughput of the DAQ system has increased significantly in the situation of accessing 'Hot Data'.

Fig. 14 Water cooled refrigeration type chiller for YAG Thomson scattering system

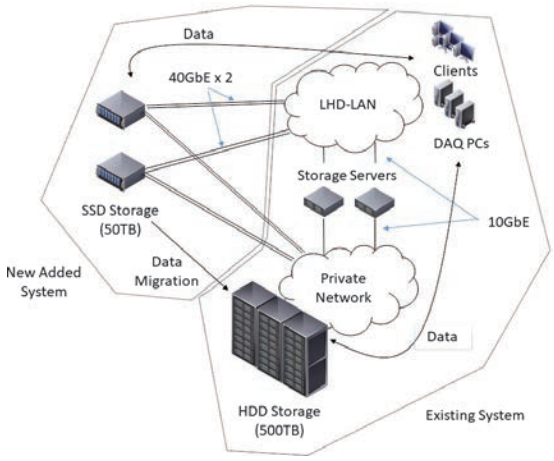

Fig. 15 New DAQ system added SSD storage

(2) Radiation measurement and radiation control

In order to control the safety of radioactivity, we carry out the operation and the maintenance for three high-purity germanium (HPGe) detectors, seven liquid scintillation counters, three stack tritium monitoring systems, two gas monitor systems and the drain water monitor. In particular, two gas monitor systems have been installed to measure gas in the torus hall and the stack of the LHD building, respectively. However, because the gas monitor system for the torus hall, which is installed in the LHD basement, is affected by radiation of the deuterium experiments, we installed the 3rd gas monitor in the air conditioning room. This monitor is isolated with concrete wall of 2 m thick from the torus hall (Fig. 16). The gas is sampled from a circulating air duct for the torus hall.

In order to exit paper-based system for radiation worker registration, we are now developing the WWW registration system to apply, update, approve, and manage radiation workers in NIFS. Fig. 17 shows the front page of WWW registration system.

Fig. 16 3rd gas monitor in air conditioning room

Fig. 17 The front page of WWW registration system (in Japanese)

5. Control Technology Division

The Control Technology Division is in charge of the important engineering tasks in the LHD project, such as operation, management, and development, which are mainly targeted to central control system, cryogenic system, coil power supply, and super-conducting coils.

We are also responsible for the IT infrastructures, e.g., LHD experiment network, NIFS campus information

network and internet servers, in every phase of the project including requirements analysis, design, implementation, operation, and user support.

The essential topics of the activities for the last fiscal year are described below.

(1) The operation of the LHD cryogenic system

The completion of the cooling operation in the 20th experimental campaign was delayed by 4 days due to a cooling failure at the final stage. The cause of the cooling failure was vacuum degradation in the adiabatic vacuum chamber of the superconducting bus line H2-I system. Then, sufficient vacuum evacuation could not be carried out. The vacuum evacuation could be successful by several opening and closing operations. Consequently, the cooling operation could be completed.

During the steady operation period (129 days, 3097 hours), the monitoring system was improved by monitoring the vacuum degree in the adiabatic vacuum chamber and the surface temperature on the bus line by the IR camera. As a result, the 20th cycle operation could be finished without any trouble for one year.

(2) Development of Velocity-measuring Pulse Generator

A new idea to electromagnetically accelerate an object is investigated using high-temperature superconductors and magnetic coils, which is called the "superconducting linear catapult". In the Summer Student Program of SOKENDAI held in August, 2018, a program regarding this technique was prepared. In the program, a magnetically levitated small vehicle equipped with high-temperature superconducting bulk materials was accelerated using magnetic coils (Fig. 18). For this acceleration, the timing when the magnetic field is applied is important. Therefore, to precisely control the timing, we developed a pulse generator system using Arduino (an open-source electronics platform) (Fig. 19). The generator can trigger TTL signals to switch on electrical currents to magnetic coils by measuring the velocity of the vehicle using laser optical sensors. It was successfully demonstrated to accelerate the vehicle by using the generator, with the result that the velocity of the vehicle became approximately doubled compared to that obtained without using the generator (by manual control). The superconducting linear catapult may become a good tool for ice pellet injection in fusion plasmas and for the study of space debris.

Fig. 18 Accelerating system

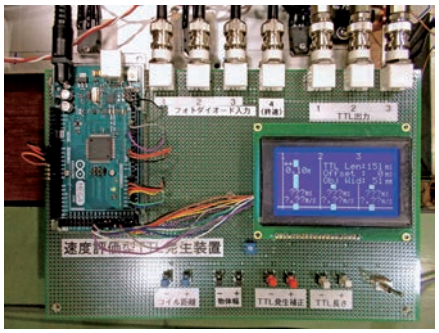

Fig. 19 Pulse generator

(3) Network management for NIFS-LAN and LHD-LAN

The NIFS campus information networks consist of several clusters, i.e., Research Information Cluster (NIFS-LAN) and LHD Experiment Cluster (LHD-LAN).

New contributions in FY 2018 are as follows:

(a) Renewal of the backup system for the virtual server system

A backup system for the virtual server system has been upgraded with Veeam Backup & Replication.

(b) Renewal of the targeted attack detection system

A targeted attack detection system has been replaced with FireEye NX 4500. This system can detect malware and unknown threats.

(c) Update of the core switch of the LHD control LAN

The core switch of the LHD control LAN on the LHD experimental cluster has been updated by configuring a virtual router using VRF (Virtual Routing and Forwarding), which is a function of the existing LHD-LAN core switch (Nexus 7009). There were no failures after upgrade and it resulted in a cost reduction.

(4) Development of the Helmholtz Coil Operation System for Magnetic Shielding Tests

This project was conducted as the technical training program for 6 new members of the department of technical service and technology. Fig. 20 is the overall view of the Helmholtz coil operation system and a control panel of coil operation program developed by LabVIEW (Fig. 21).

The operation system consists of a Helmholtz coil, a chiller for coil cooling, DC power sources with up to DC200A (maximum magnetic flux density: 23.5mT) and a Note PC for coil energization control, and operational parameters monitoring. The operational parameters, i.e., the coil energizing duration and sampling frequency are variable, and the initial settings are 10s and 1Hz, respectively. Interlock programs for coil energization are implemented as well. They are triggered in case the surface temperature of the coolant outlet tube exceeds the limit value. The Helmholtz coil device was built not only for the magnetic shielding tests, but also for a summer student program in NIFS.

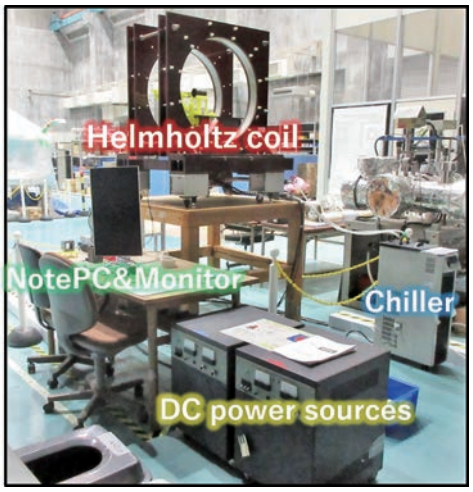

Fig. 20 Overall view of the Helmholtz coil operation system

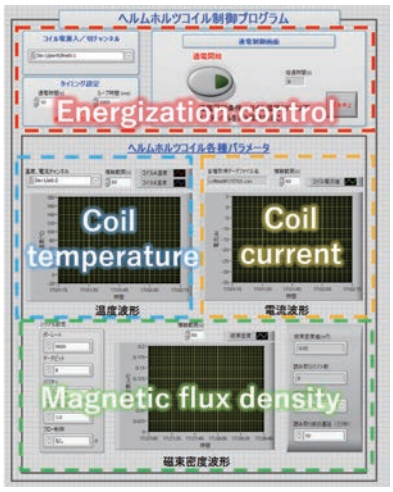

Fig. 21 Control panel of coil operation program

6. Exchange activity on the analysis technology using the finite element method

We are holding technical exchange meetings that have contributed to future technological improvements over the past few years. The purpose is sharing knowledge obtained in the field of design and manufacture of equipment and technical information in control program development by the technical staff of each university/ research institution.

On March 1st, 2019, the 2nd exchange meeting (Fig. 22) on the structural analysis technology using the finite element method was held in NIFS. A total of 38 guests attended the meeting including the participants by using the ZOOM (communications software for online meetings). The breakdown of the participants was as follows: High Energy Accelerator Research Organization (7), National Institutes for Quantum and Radiological Science and Technology (1), Institute for Molecular Science (6), National Astronomical Observatory of Japan (5), NIFS (14), and private enterprises: Kurihalant CO., LTD. (5). The special lecture regarding a utilization of the finite element method in a fusion reactor conceptual design was given by Associate Professor Tamura at the beginning of the meeting. Then, six speakers introduced each analysis case and its difficulties. After each presentation, fruitful and active questions and answers were held. Through this exchange meeting, it was possible to build a human network of engineers involved in analysis technology.

On 3–7 Dec 2018 and 24–27 Jan 2019, a student from Kyoto University stayed at NIFS to carry out electromagnetic analysis in the framework of technical cooperation (Fig. 23). The analysis target was the ECH microwave of Heliotron J, and the electric field strength distribution in the vacuum vessel was calculated. It is planned to calculate the orbit of electrons based on this result.

Fig. 22 Technical exchange meeting

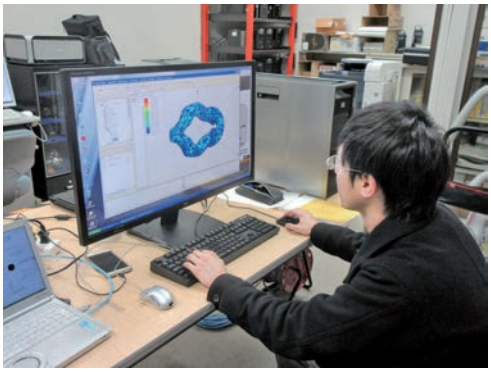

Fig. 23 Technical cooperation

17. Department of Administration

The Department of Administration handles planning and external affairs, general affairs, accounting, research support, and facility management work.

The major operations of this department are to support the promotion of the Institute's regular research and the development of the collaborative research.

The department consists of the following four divisions, namely, the General Affairs Division, the Financial Affairs Division, the Research Support Division, and the Facilities and Safety Management Division. Details of these divisions are described below.

General Affairs Division

The General Affairs Division handles administrative work and serves as the contact point with the outside. This Division consists of four sections. The General Affairs Section is in charge of secretarial work for the Director General and the Deputy Director General, support for the Advisory Committee meetings, and enacting rules and regulations. The Planning and Evaluation Section is in support for assessment of the institution's performance including scientific achievement and management efficiency. The Personnel and Payroll Section is in charge of general personnel affairs, salary, and public welfare. And the Communications and Public Affairs Section focuses on outreach and publicity activities.

Number of Staff Members (※ This list was compiled as of March 31, 2019.)

Director General	1
Professors	34
Associate Professors	41
Assistant Professors	51
Administrative Staff	45
Technical and Engineering Staff	45
Employee on Annual Salary System	14
Center of Excellence Researcher	3
Research Administrator Staff	2
Visiting Scientists	15
Total	251

Financial Affairs Division

The Financial Affairs Division consists of six sections: The Audit Section, the Financial Planning Section, the Accounts and Properties Administration Section, the Contracts Section, the Procurement Section, and the Purchase Validation Section.

The major responsibilities of the division are to manage and execute the budget, to manage corporate property, revenue/expenditure, and traveling expenses of staff, and to purchase supplies and receive articles.

(JFY 2018)

Settlement (in million of Yen)

Salaried Wages	2,097
Operating Costs	7,054
Equipment	0
Site and Buildings	150
Grant-in-Aid for Scientific Research	149
Total	9,450

Research Support Division

The Research Support Division consists of four sections and one center. These are the Graduate Student Affairs Section, the Academic Information Section which includes the Library at NIFS (since Feb. 2014), the Research Support Section and the International Collaboration Section, which is in charge of inter-university coordination and arranging international cooperation. The Visitor Center assists collaborating researchers and visitors.

Collaboration Research Programs (JFY 2018)

	Applications Applied	Applications Accepted	Researchers Accepted
LHD Project Collaboration Research	25	24	296
Joint Research	249	247	1,854
Joint Research Using Computers	134	132	373
Workshops	31	31	643
Bilateral Collaboration Research	101	101	1,304
Total	540	535	4,470

Number of Graduate School Students
(SOKENDAI: The Graduate University for Advanced Studies) (As of March 31, 2019)

Doctoral Course					
Grade 1	Grade 2	Grade 3	Grade 4	Grade 5	Total
1	2	5	1	6	15

(The Joint Program of Graduate Education)

Graduate course education is given in NIFS apart from SOKENDAI in joint programs with the Department of Energy Science and Engineering of the Graduate School at Nagoya University, Division of Particle and Astrophysical Science of the Graduate School of Science at Nagoya University, Division of Quantum Science of the Graduate School of Engineering at Hokkaido University, Department of Energy Science of the Graduate School of Science and Engineering at University of Toyama, Interdisciplinary Graduate School of Engineering Science in Kyushu University and the Graduate School of Engineering at Tohoku University. In total, 19graduate students are involved in the programs as of March 31, 2018.

The Special Research Collaboration Program for Education (As of March 31, 2019)

Degree / Affiliation	Master's Course	Doctoral Course	Total
National Graduate School	31	4	35
Public Graduate School	0	0	0
Private Graduate School	0	1	1
Total	31	5	36

Foreign Researchers to NIFS (JFY 2018)

P.R. China	Rep. of Korea	Philippines	U.S.A.	Germany	Thailand	Italy	Spain	Others	Total
76	37	19	18	16	16	4	4	25	215

NIFS Researchers to Foreign Countries (JFY 2018)

U.S.A.	P.R. China	Rep. of Korea	Germany	France	Italy	Taiwan	Czech Rep.	Spain	Others	Total
62	54	41	37	18	16	15	15	11	45	314

Books and Journals (JFY 2018)

Books in Japanese	19,320
Books in Other Languages	50,354
Total (volumes)	69,674
Journals in Japanese	272
Journals in Other Languages	816
Total (titles)	1,088

Facilities and Safety Management Division

The Facilities and Safety Management Division consists of three sections: The Safety and Health Management Section, the Facilities Planning Section, and the Facilities Maintenance Section. They are in charge of planning, designing, making contracts, supervising the construction and maintenance of all facilities at NIFS, such as buildings, campus roads, electricity, telephone, power station, air conditioning, water service, gas service, elevators, and cranes. The Facilities and Safety Management Division submits a budget request and administers the budget for those facilities.

The Safety and Health Management Section also arranges medical examination and disaster drills. These three sections promote facilities' environment better for all staff.

Site and Buildings (JFY 2018)

Toki	
Site	464,445 m^2
Buildings	
Total Building Area	39,557 m^2
Total Floor Space	71,830 m^2

APPENDIX

APPENDIX 1. Organization of the Institute

NATIONAL INSTITUTE for FUSION SCIENCE

Organization

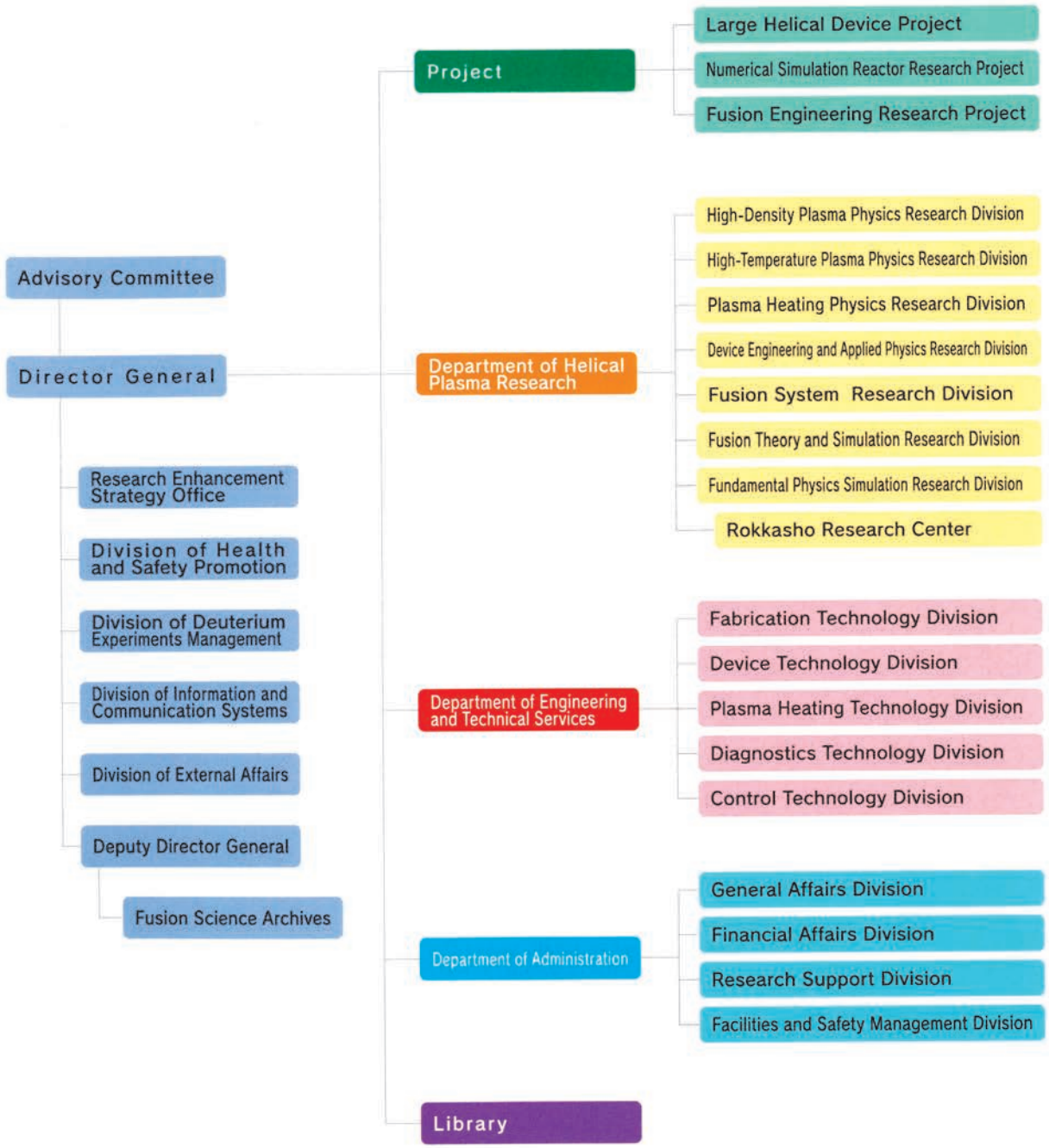

APPENDIX 2. Members of Committees

Advisory Committee

Advisory Committee

ANDO, Akira	Professor, Graduate School of Engineering, Tohoku University
USHIGUSA, Kenkichi	Managing Director, Fusion Energy Research and Deveropment Directorate, National Institutes for Quantum and Radiological Science and Technology
OHNO, Noriyasu	Director, Graduate School of Engineering, Nagoya University
OGAWA, Yuichi	Professor, Graduate School of Frontier Science, The University of Tokyo
KODAMA, Ryousuke	Director, Institute of Laser Engineering, Osaka University
NAGASAKI, Kazunobu	Professor, Institute of Advanced Energy, Kyoto University
NAKASHIMA, Yousuke	Director, Plasma Research Center, University of Tsukuba
HANADA, Kazuaki	Director, Resarch Institute for Applied Mechanics, Kyushu University
WATANABE, Tomohiko	Professor, Depaertment of Physics , Nagoya University
WADA, Motoi	Professor, Faculty of Science and Engineering, Doshisha University
MUROGA, Takeo	Deputy Director General, NIFS and Executive Director of Fusion Engineering Research Project, NIFS
MORISAKI, Tomohiro	Executive Director of Large Helical Device Project (on Science), NIFS
OSAKABE, Masaki	Executive Director of Large Helical Device Project (on Device), NIFS
SUGAMA, Hideo	Executive Director of Numerical Simulation Research Project, NIFS
YANAGI, Nagato	Executive Director of Fusion Engineering Research Project, NIFS
KUBO, Shin	Director of Plasma Heating Research Division, NIFS
MITO, Toshiyuki	Director of Device Engineering and Applied Physics Research Division, NIFS
MURAKAMI, Izumi	Director of Fusion Systems Research Division, NIFS
TODO, Yasushi	Director of Fusion Theory and Simulation Research Division, NIFS
ISHIGURO, Seiji	Director of Fundamental Physics Simulation Research Division, NIFS
NISHIMURA, Kiyohiko	Division Director for Health and Safety Promotion, NIFS

※ This list was compiled as of March 31, 2019

APPENDIX 3. Advisors, Fellows, and Professors Emeritus

Advisors

Michael Tendler	Professor Royal Institute of Technology Alfvèn Laboratory

Fellows

YAMADA, Hiroshi

Professors Emeritus

ICHIKAWA, Yoshihiko (1993)
MIZUNO, Yukio (1994)
OBAYASHI, Haruo (1995)
FUJITA, Junji (1996)
KURODA, Tsutomu (1997)
AMANO, Tsuneo (1998)
MOMOTA, Hiromu (1998)
IIYOSHI, Atsuo (1999)
HATORI, Tadatsugu (1999)
TANAHASHI, Shugo (2000)
KAWAMURA, Takaichi (2000)
SATO, Tetsuya (2001)
FUJIWARA, Masami (2002)
TODOROKI, Jiro (2003)
KAMIMURA, Tetsuo (2003)
OHKUBO, Kunizo (2005)
HAMADA, Yasuji (2007)
KATO, Takako (2007)
NODA, Nobuaki (2008)
WATARI, Tetsuo (2008)
MOTOJIMA, Osamu (2009)
SATOH, Kohnosuke (2010)
OHYABU, Nobuyoshi (2010)
MATSUOKA, Keisuke (2010)
TOI, Kazuo (2012)
NARIHARA, Kazumichi (2012)
KUMAZAWA, Ryuhei (2012)
UDA, Tatsuhiko (2012)
SATO, Motoyasu (2012)
YAMAZAKI, Kozo (2013)
KAWAHATA, Kazuo (2013)
OKAMURA Shoichi (2014)
KOMORI, Akio (2015)
SUDO, Shigeru (2015)
SKORIC, Milos (2015)
MUTO, Takashi (2016)
NAGAYAMA, Yoshio (2017)
NAKAMURA, Yukio (2017)
SAGARA, Akio (2017)
ITOH, Kimitaka (2017)
HORIUCHI, Ritoku(2017)
HIROOKA, Yoshihiko (2018)
MORITA, Shigeru (2019)
NISHIMURA, Arata (2019)

※ This list was compiled as of March 31, 2019

APPENDIX 4. List of Staff

Director General

TAKEIRI, Yasuhiko

Deputy Director General

MUROGA, Takeo

Department of Helical Plasma Research

Prof. MUROGA, Takeo (Director)

High-Density Plasma Physics Research Division

Prof. MORISAKI, Tomohiro (Director)
Prof. YAMADA, Hiroshi
Prof. WATANABE, Kiyomasa
Prof. MORITA, Shigeru
Prof. SAKAMOTO, Ryuichi
Assoc. Prof. YOSHIMURA, Shinji
Assoc. Prof. OHDACHI, Satoshi
Assoc. Prof. SHOJI, Mamoru
Assoc. Prof. TOKUZAWA, Tokihiko
Assoc. Prof. KOBAYASHI, Masahiro
Assoc. Prof. MOTOJIMA, Gen
Asst. Prof. NARUSHIMA,Yoshiro
Asst. Prof. TAKEMURA, Yuki
Asst. Prof. TSUCHIYA, Hayato
Asst. Prof. OISHI, Tetsutaro
Asst. Prof. NISHIMURA, Shin
Asst. Prof. HAYASHI, Yuki
Asst. KAWAMOTO, Yasuko
Specially Asst. Prof. OHTSUBO, Yohko

High-Temperature Plasma Physics Research Division

Prof. SAKAKIBARA, Satoru (Director)
Prof. TANAKA, Kenji
Prof. ISOBE, Mitsutaka
Prof. IDA, Katsumi
Prof. PETERSON, Byron Jay
Assoc. Prof. GOTO, Motoshi
Assoc. Prof. AKIYAMA, Tsuyoshi
Assoc. Prof. YAMADA, Ichihiro
Assoc. Prof. OZAKI, Tetsuo
Assoc. Prof. NAKANISHI, Hideya
Asst. Prof.OGAWA, Kunihiro
Asst. Prof. KOBAYASHI, Tatsuya
Asst. Prof. MUTO, Sadatsugu
Asst. Prof. TAMURA, Naoki
Asst. Prof. FUNABA, Hisamichi
Asst. Prof. YASUHARA, Ryo
Asst. Prof. YOSHINUMA, Mikirou
Asst. Prof. SUZUKI, Chihiro
Asst. Prof. SHIMIZU, Akihiro
Asst. Prof. EMOTO, Masahiko
Asst. Prof. MUKAI, Kiyofumi
Asst. Prof. UEHARA, Hiyori
Specially Appointed Prof. NISHITANI, Takeo

Plasma Heating Physics Research Division

Prof. KUBO, Shin (Director)
Prof. SIMOZUMA, Takashi
Prof. OSAKABE, Masaki
Prof. TSUMORI, Katsuyoshi
Assoc. Prof. YOSHIMURA, Yasuo
Assoc. Prof. IGAMI, Hiroe
Assoc. Prof. SAITO, Kenji
Assoc. Prof. SEKI, Tetsuo
Assoc. Prof. NAGAOKA, Kenichi
Asst. Prof. TSUJIMURA, Toru
Asst. Prof. NAKANO, Haruhisa
Asst. Prof. MAKINO, Ryohhei
Asst. Prof. KAMIO, Shuji
Asst. Prof. IKEDA, Katsunori
Asst. Prof. KISAKI, Masashi
Asst. Prof. TAKAHASHI, Hiromi
Asst. Prof. SEKI, Ryosuke
Asst. Prof. FUJIWARA, Yutaka
Asst. Prof. NUGA, Hideo
Asst. Prof. YANAI, Ryohma

Device Engineering and Applied Physics Research Division

Prof. MITO, Toshiyuki (Director)
Prof. TAKAHATA, Kazuya
Prof. IMAGAWA, Shinsaku
Prof. YANAGI, Nagato
Prof. NISHIMURA, Kiyohiko
Assoc. Prof. IWAMOTO, Akifumi
Assoc. Prof. HAMAGUCHI, Shinji
Assoc. Prof. CHIKARAISHI, Hirotaka
Assoc. Prof. TAKAYAMA, Sadatsugu
Assoc. Prof. TANAKA, Masahiro
Assoc. Prof. SAZE, Takuya
Asst. Prof. TAKADA, Suguru
Asst. Prof. OBANA, Tetsuhiro
Asst. Prof. KOBAYASHI, Makoto

Fusion Systems Research Division

Prof. MURAKAMI, Izumi (Director)
Prof. MUROGA, Takeo
Prof. MIYAZAWA, Jun-ichi
Prof. HIROOKA, Yoshihiko
Prof. NISHIMURA, Arata
Prof. MASUZAKI.Suguru
Prof. NAGASAKA, Takuya
Assoc. Prof. TANAKA, Teruya
Assoc. Prof. TAMURA, Hitoshi
Assoc. Prof. HISHINUMA, Yoshimitsu
Assoc. Prof. KATO, Daiji
Assoc. Prof. TOKITANI, Masayuki
Asst. Prof. GOTO, Takuya
Asst. Prof. YAGI, Juro
Asst. Prof. ASHIKAWA, Naoko
Asst. Prof. NOTO, Hiroyuki
Asst. Prof. SAKAUE, Hiroyuki
Asst. Prof. HAMAJI.Yukinori
Specially Asst. Prof. YAJIMA, Miyuki

Fusion Theory and Simulation Research Division

Prof. TODO, Yasushi (Director)
Prof. SUGAMA, Hideo
Prof. NAKAJIMA, Noriyoshi
Prof. ICHIGUCHI, Katsuji
Prof. ITOH, Kimitaka
Prof. YOKOYAMA, Masayuki
Assoc. Prof. MIZUGUCHI, Naoki
Assoc. Prof. TODA, Shin-ichiro
Assoc. Prof. SATAKE, Shinsuke
Assoc. Prof. KANNO, Ryutaro
Assoc. Prof. SUZUKI, Yasuhiro
Assoc. Prof. NUNAMI, Masanori
Asst. Prof. YAMAGISHI, Osamu
Asst. Prof. NAKATA, Motoki
Asst. Prof. WANG, Hao
Asst. Prof. KAWAMURA, Gakushi
Asst. Prof. SATO, Masahiko
Asst. Prof. YAMAGUCHI, Hiroyuki

Fundamental Physics Simulation Research Division

Prof. ISHIGURO, Seiji (Director)
Prof. HORIUCHI, Ritoku
Prof. MIURA, Hideaki
Prof. NAKAMURA, Hiroaki
Prof. SAKAGAMI, Hitoshi
Assoc. Prof. OHTANI, Hiroaki
Assoc. Prof. ITO, Atsushi M.
Assoc. Prof. TOIDA, Mieko
Assoc. Prof. USAMI, Shunsuke
Asst. Prof. HASEGAWA, Hiroki
Asst. Prof. MORITAKA, Toseo
Asst. Prof. ITO, Atsushi
Asst. Prof. TAKAYAMA, Arimichi

Rokkasho Research Center

Prof. NAKAJIMA, Noriyoshi (Director, Additional Post)
Prof. NISHIMURA, Arata (Additional Post)
Asst. Prof. SATO, Masahiko (Additional Post)

Project

Large Helical Device Project

Prof. MORISAKI, Tomohiro (Executive Director (on Science))
Prof. OSAKABE, Masaki (Executive Director (on Device))

Numerical Simulation Reactor Research Project

Prof. SUGAMA, Hideo (Executive Director)

Fusion Engineering Research Project

Prof. MUROGA, Takeo (Executive Director)
Prof. YANAGI, Nagato (Executive Director)

Research Enhancement Strategy Office

Prof. MUROGA, Takeo (Director)
Specially Appointed Prof. MATSUOKA, Keisuke
Specially Appointed Prof. OKAMURA, Shoichi
Assoc. Prof. KASAHARA, Hiroshi

Division of Health and Safety Promotion

Prof. NISHIMURA, Kiyohiko (Division Director)

Division for Deuterium Experiments Management

Prof. OSAKABE, Masaki (Division Director)

Division of Information and Communication Systems

Prof. ISHIGURO, Seiji (Division Director)
Assoc. Prof. YAMAMOTO, Takashi

Division of External Affairs

Prof. TAKAHATA, Kazuya (Division Director)

Fusion Science Archives

Prof. KUBO, Shin (Director)

Library

Prof. MURAKAMI, Izumi (Director)

※ This list was compiled as of March 31, 2019

Guest Professor

Prof. GAIGALAS, Gediminas	Vilnius University	May 7, 2018-June 7, 2018
Prof. VLADIMIR, Alimov	National Research Nuclear University	May 14, 2018- Nov. 9, 2018
Prof. COOPER, Wilfred Anthony	Swiss Federal Institute of Technology in Lausanne	May 1, 2018-Oct. 31, 2018
Prof. TSISAR, Valentyn	KIT, Karlsruher Institut für Technologie	Oct. 1, 2018-Mar. 1, 2019
Prof. SERGEEV, Valdimir	Peter the Great St. Petersburg Polytechnic University	Sept. 29, 2018-Dec. 1, 2018
Prof. SLEZAK, Ondrej	Czech Academy of Sciences	Sept. 26, 2018-Oct. 31, 2018
Prof. TOKAR, Mikhail Zelmanovistsch	Jülich Research Centre	Jan. 6, 2019-Apr. 6, 2019
Prof. LI, Bowen	Lanzhou University	Jan. 15, 2019-Feb. 15, 2019
Prof. O'SULLIVAN, Gerard Daniel	University College Dublin, UCD	Jan. 15, 2019-Feb. 22, 2019
Prof. WANG, Weixing	Princeton Plasma Physics Lab	Mar. 22, 2019- Apr. 21, 2019

COE Research Fellows

ZHOU, Qilai
TERASAKI, Yoshiro
YONEDA, Ryota
BO, Huang

Research Fellow (Science research)

(none)

Research Fellow (Industrial-Academic coordination)

(none)

JSPS Research Fellow

(none)

Depertment of Administration

NISHIYAMA, Kazunori	Department Director

General Affairs Division

TAKEUCHI, Shohji	Director
ICHIOKA, Akihiro	Senior Advisor
ARAI, Masanori	Chief/General Affairs Section
SHIMIZU, Kazuma	Chief/Planning and Evaluation Section
MAEDA, Yoshikazu	Chief/Employee Section
SUGIMOTO, Michiyasu	Chief/Personnel and Payroll Section
TAKAHASHI, Nobuhiro	Chief/Communications and Public Affairs Section

Financial Affairs Division

NISHIYAMA Kazunori	Director (Additional Post)
TSUDA, Makoto	Deputy Director
IKEDA, Katsumi	Specialist
KAWAI, Sanae	Chief/Financial Planning Section
IWASHIMA, Itsuki	Chief/Accounts and Properties Administration Section
FUJII, Kazuki	Chief/Audit Section
FUKUOKA, Miwa	Chief/Contracts Section
MATSUBARA, Tomohisa	Chief/Procurement Section
TSUDA, Makoto	Leader/Purchase Validation Section (Additional Post)

Research Support Division

KUWABARA, Hiroaki	Director
TERUMOTO, Naoki	Deputy Director
FUKAYA, Yosuke	Chief/Research Support Section
SOGA, Shihoko	Chief/International Collaboration Section
URUSHIHARA, Satona	Chief/Graduate Student Affairs Section
OHTA, Masako	Chief/Academic Information Section
TERUMOTO, Naoki	Leader/Visitor Center (Additional Post)
KONDO, Takahiko	Chief/Visitor Center

Facilities and Safety Management Division

KAWASE, Yasuaki	Director
NITTA, Haruki	Senior Specialist.
NITTA, Haruki	Chief/Facilities Section (Additional Post)
MIYATA, Kazuaki	Chief/Equipment Section

Department of Engineering and Technical Services

KOBAYASHI, Sakuji	Department Director
HAYASHI, Hiromi	Deputy Department Director

Fabrication Technology Division

BABA, Tomosumi	Director
KATOH, Akemi	Chief/Parts and Material Section
ITO, Yasuhiko	Chief/Electronic Engineering Section
OKADA, Kohji	Chief/Mechanical Engineering Section
SEKIGUCHI, Haruo	Chief/Device Maintenance Engineering Section

Device Technology Division

HAYASHI, Hiromi	Director
TSUCHIBUSHI, Yasuyuki	Chief/Device System Engineering Section
SUZUKI, Naoyuki	Chief/Vacuum Engineering Section
YASUI, Koji	Chief/Power Supply Engineering Section
MURASE, Takanori	Chief/Experimental Application Engineering Section

Plasma Heating Technology Division

KONDO, Tomoki	Director
MIZUNO, Yoshinori	Chief/Heating System Engineering Section
SATO, Mamoru	Chief/Particle Heating Engineering Section
ITO, Satoshi	Chief/Electron Heating Engineering Section
NOMURA, Goro	Chief/Ion Heating Engineering Section

Diagnostics Technology Division

HAYASHI, Hiroshi	Director
SHIBUYA, Masayuki	Chief/Radiation Measurement System Engineering Section
KOBUCHI, Takashi	Chief/Experimental Radiation Measurement Engineering Section
YOKOTA, Mitsuhiro	Chief/Environmental Radiation Measurement Engineering Section
OHSUNA, Masaki	Chief/Radiation Measurement Device Control Engineering Section

Control Technology Division

MORIUCHI, Sadatomo	Director
TAKAMI, Shigeyuki	Chief/Control System Engineering Section
INOUE, Tomoyuki	Chief/Information Infrastructure Engineering Section
OBA, Koki	Chief/Low Temperature Control Engineering Section
OGAWA, Hideki	Chief/Control Information Engineering Section

※ This list was compiled as of March 31, 2019

APPENDIX 5. List of Publications I (NIFS Reports)

NIFS-PROC-113 Edited by Koichi Takaki and Tetsuo Ozaki
Pulsed Power and High-Density Plasma and Applications
Feb. 6, 2019

NIFS-PROC-112 Edited by E. Kikutani (KEK) and S. Kubo (NIFS)
Proceedings of the meetings on Archives in Fields of Natural Sciences in FY 2017
Oct. 16, 2018

NIFS-PROC-111 Edited by Liqun HU, Shigeru MORITA and Yeong-Kook OH
Proceeding of A3 Foresight Program Seminar on Critical Physics Issues Specific to Steady State Sustainment of High- Performance Plasmas 12–15 December, 2017, Chongqing, China
June 11, 2018

NIFS-MEMO-85 Radiation Control Office/Division of Health and Promotion National Institute for Fusion Science
Report on Administrative Work for Radiation Safety From April 2017 to March 2018
Jan. 28, 2019

NIFS-MEMO-84 T. Yamamoto and members of information Network Task Group
The Division of Information and Communication Systems, National Institute for Fusion Science
Construction of the Campus Information Network with Information Security Measures on NIFS
Oct. 05, 2018

NIFS-MEMO-83 Kazuyoshi Yoshimura
Nonlinear Wave Propagations in Binary-Gas Mixture
May 14, 2018

※ This list was compiled as of March 31, 2019

APPENDIX 6. List of Publications II (Journals, etc.)

1 Akata N., Iwata C., Miyake H., Tanaka M.

Expiratory Testing as a Simple and Effective Bioassay Method for Screening Workers for Tritium Exposure in Fusion Test Facilities
Plasma and Fusion Research 13 Regular Issue 1305076

2 Akata N., Kakiuchi H., Shima N., Tamari T., Kovacs T.

Determination of Non-Exchangeable Organically Bound Tritium concentration in reference material of pine needles (NIST 1575a)
Journal of Radioanalytical and Nuclear Chemistry 319 3 1359-1363

3 Akata N., Kakiuchi H., Tanaka M., Shima N., Shiroma Y., Tokonami S., Hosoda M., Ishikawa Y., Furukawa M., Sanada T.

Development of rapid sampling system of atmospheric water vapor for tritium measurement
Plasma and Fusion Research 13 Special Issue 2 3405064

4 Auriemma F., Lopez-Bruna D., Lorenzini R., Momo B., Predebon I., Suzuki Y., Lopez-Fraguas A., Narushima Y., Sattin F., Terranova D., Zhang Y.

A novel approach to studying transport in plasmas with magnetic islands
Nuclear Fusion 58 9 96037

5 Bando T., Ohdachi S., Isobe M., Suzuki Y., Toi K., Nagaoka K., Takahashi H., Seki R., Du X., Ogawa K., Ido T., Shimizu A., Ozaki T., LHD experiment group.

Excitation of helically-trapped-energetic-ion driven resistive interchange modes with intense deuterium beam injection and enhanced effect on beam ions/bulk plasmas of LHD
Nuclear Fusion 58 8 82025

6 Bando T., Ohdachi S., Zhou R., Zhong G., Yi Y., Hu L., Ling B.

Experimental examination of a method to estimate temporal effect by neutrons and γ-rays on scintillation light in scintillator-based soft x-ray diagnostic of experimental advanced superconducting tokamak and large helical device
Review of Scientific Instruments 90 1 13507

7 Berkel M., Kobayashi T., Vandersteen G., Zwart H., Igami H., Kubo S., Tamura N., Tsuchiya H., Baar M.

Heat flux reconstruction and effective diffusion estimation from perturbative experiments using advanced filtering and confidence analysis
Nuclear Fusion 58 96036 96036

8 Bierwage A., Shinohara K., Todo Y., Aiba N., Ishikawa M., Matsunaga G., Takechi M., Yagi M.

Simulations tackle abrupt massive migrations of energetic beam ions in a tokamak plasma
Nature Communications 9 3282

9 Bussiahn R., Tamura N., McCarthy K., Burhenn R., Hayashi H., Laube R., Klinger T., LHD Experimental Group.

Tracer-Encapsulated Solid Pellet (TESPEL) Injection System for Wendelstein 7-X
Review of Scientific Instruments 89 10 10K112

10 Chikada T., Fujita H., Engels J., Houben A., Mochizuki J., Horikoshi S., Matsunaga M., Tokitani M., Hishinuma Y., Kondo S., Yabuuchi K., Schwarz-selinger T., Terai T., Oya Y.

Deuterium permeation behavior and its iron-ion irradiation effect in yttrium oxide coating deposited by magnetron sputtering
Journal of Nuclear Materials 511 560-566

11 Chikada T., Fujita H., Tokitani M., Hishinuma Y., Terai T., Oya Y.

Deuterium permeation through monoclinic erbium oxide coating
Fusion Engineering and Design 133 121-124

12 Chikada T., Kimura K., Mochizuki J., Horikoshi S., Matsunaga M., Fujita H., Okitsu K., Tanaka T., Hishinuma Y., Sakamoto Y., Someya Y., Nakamura H.

Surface oxidation effect on deuterium permeation in reduced activation ferritic/martensitic steel F82H for DEMO application
Fusion Engineering and Design 146 Part A 450-454

13 Chikaraishi H.

Dc Power system for LHD Superconducting Coils
Journal of the Cryogenic Society of Japan 53 3 122-129

14 Dai S., Oishi T., Kawamura G., Kobayashi M., Morita S., Feng Y., Wang D.

Three-dimensional simulations of edge impurity flow obtained by the vacuum ultraviolet emission diagnostics in the Large Helical Device with EMC3-EIRENE
Nuclear Fusion 58 9 96024

15 Emika A., Terasaka K., Yoshimura S., Aramaki M., Tanaka M.

Observation of Axial Neutral-Gas Flow Reversal in an ECR Plasma
Plasma and Fusion Research 14 Regular Issue 1201066

16 Emoto M., Nakanishi H., Yoshida M., Ohsuna M., Ogawa H., Imazu S., Maeno H., Ito T., Yokota M., Nonomura M.

Inter-Application Communication during LHD Consecutive Short Pulse Discharge Experiment
Fusion Engineering and Design 129 190-195

17 Emoto M., Suzuki C., Yokoyama M., Yoshinuma M., Seki R., Ida K.

Improvement of Automatic Physics Data Analysis Environment for the LHD Experiment
Fusion Science and Technology 74 1-2 161-166

18 Fox W., Wilder F., Eriksson S., Jara-almonte J., Pucci F., Yoo J., Ji H., Yamada M., Ergun R., Oieroset M., Phan T.

Energy Conversion by Parallel Electric Fields During Guide Field Reconnection in Scaled Laboratory and Space Experiments
Geophysical Research Letters 45 12 12677-12684

19 Fujii K., Yamada I., Hasuo M.

Machine Learning of Noise in LHD Thomson Scattering System
Fusion Science and Technology 74 1-2 57-64

20 Fujita H., Chikada T., Mochizuki J., Horikoshi S., Matsunaga M., Tanaka T., Terai T.

Deuterium permeation through metals under γ-ray irradiation
Fusion Engineering and Design 133 95-98

21 Fujita H., Mochizuki J., Horikoshi S., Matsunaga M., Tanaka T., Terai T., Oya Y., Chikada T.

The effect of γ-ray irradiation on deuterium permeation through reduced activation ferritic steel and erbium oxide coating
Nuclear Materials and Energy 17 78-82

22 Fujiwara S., Nakamura H., Li H., Miyanishi H., Mizuguchi T., Yasunaga T., Otsuka T., Hatano Y., Saito S.

Computational strategy for studying structural change of tritium-substituted macromolecules by a beta decay to helium-3
Journal of Advanced Simulation in Science and Engineering 6 1 94-99

23 Fujiwara S., Yoshiki I., Tsutsui T., Mizuguchi T., Hashimoto M., Tamura Y., Nakamura H.

Dissipative Particle Dynamics Simulation for Self-Assembly of Symmetric Bolaamphiphilic Molecules in Solution
Plasma and Fusion Research 13 Special Issue 2 3401095

24 Furukawa M., Watanabe T., Morrison P., Ichiguchi K.

Calculation of large-aspect-ratio tokamak and toroidally-averaged stellarator equilibria of high-beta reduced magnetohydrodynamics via simulated annealing
Physics of Plasmas 25 8 82506

25 Goto Y., Kubo S., Tsujimura T.

Development of the Grating Mirror for the High Power Transmission System and its General Theory
Plasma and Fusion Research 13 Special Issue 2 3405089

26 Haba Y., Nagaoka K., Tsumori K., Kisaki M., Nakano H., Ikeda K., Fujiwara Y., Kamio S., Yoshimura S., Osakabe M.

Development of a dual beamlet monitor system for negative ion beam measurements
Review of Scientific Instruments 89 12 123303

27 Hamaguchi S., Imagawa S., Obana T., Yanagi N., Mito T.

Operations of the Helium Subcooling System for the LHD Helical Coils during Ten Plasma Experimental Campaigns
Plasma and Fusion Research 13 Special Issue 2 3405057

28 Hamaji Y., Tokitani M., Kreter A., Sakamoto R., Sagara A., Tamura H., Masuzaki S.
Influence of Thermal Shocks on the He Induced Surface Morphology on Tungsten
Nuclear Materials and Energy 18 321-325

29 Horikoshi S., Matsunaga M., Mochizuki J., Fujita H., Hishinuma Y., Oya Y., Chikada T.
Microstructure change and deuterium permeation behavior of ceramic-metal multi-layer coatings after immersion in liquid lithium-lead alloy
Nuclear Materials and Energy 16 66-70

30 Horiuchi R.
The Role of Magnetic Islands in Collisionless Driven Reconnection: A Kinetic Approach to Multi-Scale Phenomena
Plasma 1 1 68-77

31 Horiuchi R., Moritaka T., Usami S.
PIC simulation study of merging processes of two spheromak-like plasmoids
Plasma and Fusion Research 13 Special Issue 2 3403035

32 Ida K.
Pioneering work before becoming mainstream research
AIP conference proceedings 1933 1 20001

33 Ida K., Kobayashi T., Ono M., Evans T., McKee G., Austin M.
Hysteresis relation between turbulence and temperature modulation during the heat pulse propagation into a magnetic island in DIII-D
Physical Review Letters 120 24 245001

34 Ida K., Kobayashi T., Tokuzawa T., Akiyama T., Tanaka H., Yoshinuma M., Itoh K.
Exhaust of turbulence cloud at the tongue shaped deformation event
Nuclear Fusion 58 11 112008

35 Ido T.
Period doubling bifurcation of geodesic acoustic mode in high tmeperature plasmas
Parity 34 1 29

36 Ikeda K., Tsumori K., Kisaki M., Nakano H., Nagaoka K., Osakabe M., Kamio S., Fujiwara Y., Haba Y., Takeiri Y.
First Results of Deuterium Beam Operation on Neutral Beam Injectors in the Large Helical Device
AIP conference proceedings 2011 60002

37 Imagawa S.
Study on wind-react-transfer method for helical coils wound from Nb_3Sn cable-in-conduit conductors
Plasma and Fusion Research 13 Special Issue 2 3405027

38 Imagawa S., Kajitani H., Obana T., Takada S., Hamaguchi S., Chikaraishi H., Takahata K., Matsui K., Hemmi T., Koizumi N.
Test of ITER-TF Joint Samples with NIFS Test Facilities
IEEE Transactions on Applied Superconductivity 28 3

39 Isobe M., Ogawa K., Nishitani T., Miyake H., Kobuchi T., Pu N., Kawase H., Takada E., Tanaka T., Li S., Yoshihashi S., Uritani A., Jo J., Murakami S., Osakabe M., LHD experiment group.
Neutron Diagnostics in the Large Helical Device
IEEE Transactions on Plasma Science 46 6 2050-2058

40 Isobe M., Ogawa K., Nishitani T., Pu N., Kawase H., Seki R., Nuga H., Takada E., Murakami S., Suzuki Y., Yokoyama M., Osakabe M., LHD experiment group.
Fusion neutron production with deuterium neutral beam injection and enhancement of energetic-particle physics study in the Large Helical Device
Nuclear Fusion 58 8 82004

41 Ito A.
Special Topic Articles: Fuzzy Nano-Structures on Metal Surfaces Induced by Exposure to Helium Plasma 4. Numerical Identification for Physical Mechanism of Fuzzy Nanostructure Growth on Material Surface
Journal of Plasma and Fusion Research 94 6 306-310

42 Ito A., Nakajima N.

Erratum: “Analytic Equilibria of High-Beta Tokamaks with Toroidal and Poloidal Flows and Pressure Anisotropy Associated with Parallel Heat Flux” [J. Phys. Soc. Jpn. 82, 064502 (2013)]
Journal of the Physical Society of Japan 88 2 28001

43 Ito A., Nakajima N.

Corrigendum: Analytic high-beta tokamak equilibria with poloidal-sonic flow (2009 Plasma Phys. Control. Fusion 51 035007)
Plasma Physics and Controlled Fusion 61 2 29501

44 Ito A., Takayama A., Nakamura H.

Triple Hybrid Simulation Method for Tungsten Fuzzy Nanostructure Formation
Plasma and Fusion Research 13 Special Issue 2 3403061

45 Kamio S., Seki R., Seki T., Saito K., Kasahara H., Sakakibara S., Nomura G., Mutoh T.

Third harmonic ICRF heating in LHD hydrogen experiments
Nuclear Fusion 58 12 126004

46 Kasuya N., Nunami M., Tanaka K., Yagi M.

Numerical diagnostics of fluctuation spectrum in 3D magnetic configurations
Nuclear Fusion 58 10 106033

47 Kawamura G., Miyazawa J., Goto T., Shoji M., Masuzaki S., Suzuki Y., Feng Y.

Application of EMC3-EIRENE to Estimation of Influence of a Liquid Metal Limiter on an LHD-Type Fusion Plasma
Plasma and Fusion Research 13 Special Issue 2 3403034

48 Kawamura G., Tanaka H., Mukai K., Peterson B., Dai S., Masuzaki S., Kobayashi M., Suzuki Y., Feng Y., LHD Experiment Group.

Three-dimensional impurity transport modeling of neon-seeded and nitrogen-seeded LHD plasmas
Plasma Physics and Controlled Fusion 60 8 84005

49 Kawase H., Ogawa K., Nishitani T., Pu N., Murakami S., Isobe M., LHD Experiment Group.

Initial results of neutron emission profile measurements in LHD deuterium plasmas
Plasma and Fusion Research 13 Special Issue 2 3402122

50 Kenmochi N., Nishiura M., Yoshida Z., Yamada I., Funaba H., Sugata T., Nakamura K., Katsura S.

Nd:YAG laser Thomson scattering diagnostics for a laboratory magnetosphere
Review of Scientific Instruments 89 10 10C101

51 Kin F., Itoh K., Fujisawa A., Kosuga Y., Sasaki M., Yamada T., Inagaki S., Itoh S., Kobayashi T., Nagashima Y., Kasuya N., Arakawa H., Yamasaki K., Hasamada K.

Extraction of nonlinear waveform in turbulent plasma
Physics of Plasmas 25 6 25-6, 62304

52 Kisaki M., Ikeda K., Nakano H., Tsumori K., Fujiwara Y., Haba Y., Kamio S., Nagaoka K., Osakabe M.

Demonstration of Beam Optics Optimization Using Plasma Grid Bias in a Negative Ion Source
Plasma and Fusion Research 13 Regular Issue 1205110

53 Kobayashi M., Masuzaki S., Tanaka K., Tokuzawa T., Yokoyama M., Narushima Y., Yamada I., Ido T., Seki R., The LHD Experimental Group.

Core plasma confinement during detachment transition with RMP application in LHD
Nuclear Materials and Energy 17 137-141

54 Kobayashi M., Nishitani T., Kato A., Saze T., Tanaka T., Yoshihashi S., Ogawa K., Isobe M.

Evaluation of imaging plate measurement for activated indium as fast-neutron detector in large radiation field
Progress in Nuclear Science and Technology 6 58-62

55 Kobayashi M., Oya Y.

Development of the Tritium Transport Model for Pebbles of Li_2TiO_3
Plasma and Fusion Research 13 Special Issue 2 3405048

56 Kobayashi M., Tanaka T., Nishitani T., Ogawa K., Isobe M., Kato A., Saze T., Yoshihashi S., Osakabe M., LHD experiment group.

First measurements of thermal neutron distribution in the LHD torus hall generated by deuterium experiments
Fusion Engineering and Design 137 191-195

57 Kobayashi T.
On the turbulence interface in magnetically confined plasmas
AIP conference proceedings 1993 20003

58 Kobayashi T., Ida K., Tsujimura T., Inagaki S., Tokuzawa T., Tsuchiya H., Tamura N., Igami H., Yoshimura Y., Itoh S., Itoh K.
Density dependence of transient electron thermal transport property in LHD
Nuclear Fusion 58 12 126031

59 Kobayashi T., Kobayashi M., Iwama N., Kuzmin A., Goto M., Kawamura G., The LHD Experimental Group.
Single field-of-view tomographic imaging of 3D impurity emission distribution in magnetized edge plasma of LHD
Review of Scientific Instruments 89 12 123502

60 Kobayashi T., Kobayashi M., Kuzmin A., Goto M., Tanaka H., Kawamura G., Peterson B., Iwama N.
Measurement of Impurity Emission Intensity Distribution in the Edge Region of LHD and Its Relation with Magnetic Field Structure
Plasma and Fusion Research 13 Special Issue 2 3402030

61 Koike S., Takahashi T., Mizuguchi N., Mitarai O.
Simulation study on a merging core fueling technique for an advanced fuel fusion spherical tokamak reactor
Fusion Engineering and Design 136 PartA 111-115

62 Kumagai K., Tanaka T., Nagasaka T., Yagi J., Watanabe T., Yamazaki G., Sato F., Tamaki S., Murata I., Fukada S., Katayama K., Sagara A.
Tritium Release from Molten FLiNaBe under Low Flux Neutron Irradiation
Plasma and Fusion Research 14 Regular Issue 1405044

63 Kumagai K., Tanaka T., Yagi J., Watanabe T., Sato F., Tamaki S., Murata I., Sagara A.
Tritium release from molten salt FLiNaK under low flux neutron irradiation with an AmBe neutron source
Fusion Engineering and Design 136 PartB 1269-1272

64 Kumagai K., Tanaka T., Yagi J., Watanabe T., Sato F., Tamaki S., Murata I., Sagara A.
Control of Chemical Forms of Tritium in FLiNaK under Low Flux Neutron Irradiation
Plasma and Fusion Research 13 Special Issue 2 3404071

65 Kuzmin A., Kobayashi M., Nakano T., Hasuo M., Fujii K., Goto M., Shikama T., Morisaki T.
Measurements of the impurity flow velocity and temperature in Deuterium and Hydrogen plasmas in the divertor legs of the stochastic layer in LHD
Plasma and Fusion Research 13 3402058 3402058

66 Kuzmin A., Kobayashi M., Nakano T., Kawamura G., Hasuo M., Fujii K., Morisaki T., The LHD Experimental Group.
Analysis of the impurity flow velocity in a wide plasma parameter range for Deuterium and Hydrogen plasmas in the divertor legs of the stochastic layer in LHD
Nuclear Materials and Energy 17 217

67 Liu Y., Morita S., Murakami I., Oishi T., Goto M., Huang X.
Density evaluation of tungsten W^{24+}, W^{25+}, and W^{26+} ions using unresolved transition array at 27–34 Å in Large Helical Device
Japanese Journal of Applied Physics 57 10 106101-1-9

68 Liu Y., Morita S., Oishi T., Goto M.
Effect of neutron and γ-ray on charge-coupled device for vacuum/extreme ultraviolet spectroscopy in deuterium discharges of large helical device
Review of Scientific Instruments 89 10 10I109-1-5

69 Liu Y., Morita S., Oishi T., Goto M., Huang X.
Observation of Tungsten Line Emissions in Wavelength Range of 10–500 Å in Large Helical Device
Plasma and Fusion Research 13 Special Issue 2 3402020

70 Lopez-Bruna D., Momo B., Predebon I., Lopez-Fraguas A., Auriemma F., Suzuki Y., Lorenzini R.
Flux-surface averaged radial transport in toroidal plasmas with magnetic islands
Nuclear Fusion 58 10 106031

71 Maeda T., Kenta T., Yamoto S., Hatayama A., Hasegawa H., Ishiguro S.

Analysis of the plasma blob formation/transport and its effects on impurity transport in the scrape-off layer regions
Contributions to Plasma Physics 58 6-8 505-510

72 Maeyama S., Watanabe T., Idomura Y., Nakata M., Nunami M.

Implementation of a gyrokinetic collision operator with an implicit time integration scheme and its computational performance
Computer Physics Communications 235 9

73 Mase A., Kogi Y., Kuwahara D., Nagayama Y., Ito N., Maruyama T., Ikezi H., Wang X., Inutake M., Tokuzawa T., Kohagura J., Yoshikawa M., Shinohara S., Suzuki A., Sakai F., Yamashika M., Tobias B., Muscatello C., Ren X., Chen M., Domier C., Luhmann jr. N.

Development and Application of Radar Reflectometer Using Micro to Infrared Waves
Advances in Physics: X 3 1 1472529, 633-675

74 Masuzaki S., Tanaka H., Kobayashi M., Kawamura G.

Effects of drifts on divertor plasma transport in LHD
Nuclear Materials and Energy 18 281-284

75 Matsunaga M., Horikoshi S., Mochizuki J., Fujita H., Hishinuma Y., Isobe K., Hayashi T., Terai T., Oya Y., Chikada T.

Lithium-lead corrosion behavior of erbium oxide, yttrium oxide and zirconium oxide coatings fabricated by metal organic decomposition
Journal of Nuclear Materials 511 537-543

76 McCarthy K., Panadero N., Combs S., Tamura N., Ascasibar E., Calvo M., Chmyga A., Estrada T., FONTDECABA M., García R., Hernández Sánchez J., Khabanov P., Liners M., Melnikov A., Pastor I., Rojo B., Team T., LHD experiment group.

The impact of fast electrons on pellet injection in the stellarator TJ-II
Plasma Physics and Controlled Fusion 61 1 14013

77 Michael C., Tanaka K., Akiyama T., Ozaki T., Osakabe M., Sakakibara S., Yamaguchi H., Murakami S., Yokoyama M., Shoji M., Vyacheslavov L., LHD Experiment Group.

Role of Helium-Hydrogen ratio on energetic interchange mode behaviour and its effect on ion temperature and micro-turbulence in LHD
Nuclear Fusion 58 4 46013

78 Minami T., Ohtani Y., Ohshima S., Nagasaki K., Ito Y., Nakanishi H., Yasuhara R., Funaba H., Yamada I., Akiyama T.

Development of a high-speed full digital processing phase detector for interferometry
Review of Scientific Instruments 89 10 10K108

79 Mito T., Iwamoto A., Hamaguchi S., Moriuchi S., Oba K., Takami S., Noguchi H., Takahata K., Yanagi N., Imagawa S., Kumaki T., Obara K., Nobutoki M., Nakamura K., Nakashima T., Kuwahara S.

Reexamination of Refrigeration Power of the LHD Cryogenic System After Fire and Restart of Operation
IEEE Transactions on Applied Superconductivity 28 4 4206004

80 Miura H.

Extended magnetohydrodynamic simulations of decaying, homogeneous, approximately-isotropic and incompressible turbulence
Fluids 4 1 46

81 Miyazawa J., Goto T., Tamura H., Tanaka T., Yanagi N., Murase T., Sakamoto R., Masuzaki S., Ohgo T., Sagara A.

Maintainability of the Helical Reactor FFHR-c1 Equipped with the Liquid Metal Divertor and Cartridge-type Blankets
Fusion Engineering and Design 136 Part B 1278-1285

82 Mochizuki J., Horikoshi S., Fujita H., Matsunaga M., Hishinuma Y., Oya Y., Chikada T.

Preparation and characterization of Er_2O_2-ZrO_2 multi-layer coating for tritium permeation barrier by metal organic decomposition
Fusion Engineering and Design 136 219-222

83 Mollen A., Landreman M., Smith H., Garcia-regana J., Nunami M.

Flux-surface variations of the electrostatic potential in stellarators: impact on the radial electric field and neoclassical impurity transport
Plasma Physics and Controlled Fusion 60 8 84001

84 Mori Y., Nishimura Y., Ishii K., Hanayama R., Kitagawa Y., Sekine T., Takeuchi Y., Satoh N., Kurita T., Kato Y., Kurita N., Kawashima T., Komeda O., Hioki T., Motohiro T., Sunahara A., Sentoku Y., Miura E., Iwamoto A., Sakagami H.

1-Hz Bead-Pellet Injection System for Fusion Reaction Engaged by a Laser HAMA Using Ultra-Intense Counter Beams
Fusion Science and Technology 75 36-48

85 Morita S., Hu L., Oh Y., Ashikawa N., Isobe M., Kato D., Kishimoto Y., Ohdachi S., Sakakibara S., Todo Y., Kamada Y., Raju D., Xu M.

Fusion research and international collaboration in the Asian region
Plasma and Fusion Research 13 Special Issue 2 3502046-1-10

86 Mukai K., Abe R., Peterson B., Takayama S.

Improvement of infrared imaging video bolometer for application to deuterium experiment on the large helical device
Review of Scientific Instruments 89 10 10E114

87 Mukai K., Nagaoka K., Takahashi H., Yokoyama M., Murakami S., Nakano H., Ida K., Yoshinuma M., Seki R., Kamio S., Fujiwara Y., Oishi T., Goto M., Morita S., Morisaki T., Osakabe M.

Carbon impurities behavior and its impact on ion thermal confinement in high-ion-temperature deuterium discharges on the Large Helical Device
Plasma Physics and Controlled Fusion 60 7 74005

88 Mukai K., Nishitani T., Ogawa K., Peterson B.

Neutron Shielding Design of Infrared Imaging Video Bolometer for LHD Deuterium Experiment
IEEE Transactions on Plasma Science 47 1 18-21

89 Murakami A., Iwamoto A., Noudem J.

Effects of SPS pressure on the mechanical properties of high packing ratio bulk MgB_2 superconductor
Journal of Physics: Conference Series 1054 12051

90 Muroga T., Noto H., Hishinuma Y., Huang B.

Technical Advancement in Fabricating Dispersion Strengthened Copper Alloys by Mechanical Alloying and Hot Isostatic Pressing for Application to Divertors of Fusion Reactors
Materials Science Forum 941 778-783

91 Nagaoka K., Takahashi H., Nakata M., Tanaka K., Mukai K., Yokoyama M., Murakami S., Nakano H., Ida K., Yoshinuma M., Ohdachi S., Bando T., Nunami M., Seki R., Yamaguchi H., Osakabe M., Morisaki T.

Transport characteristics of deuterium and hydrogen plasmas with ion internal transport barrier in LHD
Nuclear Fusion 59 10

92 Nakagawa S., Hochin T., Nomiya H., Nakanishi H.

Estimation of Plasma Emission Transition Using Hidden Markov Model
Plasma and Fusion Research 13 Special Issue 2 3405117

93 Nakamura K., Nishiura M., Takahashi N., Yoshida Z., Kenmochi N., Sugata T., Katsura S., HOWARD J.

Coherence-imaging spectroscopy for 2D distribution of ion temperature and flow velocity in a laboratory magnetosphere
Review of Scientific Instruments 89 10 10D133

94 Nakanishi H., Yokota M., Aoyagi M., Ohsuna M., Ito T., Imazu S., Nonomura M., Ogawa K., Isobe M., Akata N., Tanaka M., Saze T., Nishimura K., Hayashi H., Miyake H., Ogawa H., Maeno H., Emoto M., Yoshida M., Kawamura T., Sakakibara S., Ishiguro S., Osakabe M.

Integrated radiation monitoring and interlock system for the LHD deuterium experiments
Fusion Engineering and Design 129 259-262

95 Nakasone S., Ishizu Y., Ikemoto N., Shiroma Y., Akata N., Tanaka M., Furukawa M.

Tritium Concentration of Inland Water in Okinawa Island, Southwestern Part of Japan
Japanese Journal of Health Physics 53 2 65-71

96 Namba S., Shikama T., Sasano W., Tamura N., Endo T.

Characteristics of an under-expanded supersonic flow in arcjet plasmas
Japanese Journal of Applied Physics 57 6 66101

97 Nishimura A.
Several Considerations on Construction Site of Fusion DEMO
Plasma and Fusion Research 13 Special Issue 2 3405023

98 Nishimura S.
On the anisotropic velocity distribution of fast ions in NBI-heated toroidal plasmas
Physics of Plasmas 25 4 42509

99 Nishitani T., Matsuura H., Pu N., Ogawa K., Kawase H., Isobe M., LHD Experiment Group.
Estimation of the Fast-Ion Anisotropy Effect on the Neutron Source Intensity Measurement and the Experimental Observation
IEEE Transactions on Plasma Science 47 1 12-17

100 Nishitani T., Ogawa K., Isobe M., Kawase H., Pu N., Kashchuk Y., Krasilnikov V., Jo J., Cheon M., Tanaka T., Yoshihashi S., Li S., Osakabe M.
Calibration Experiment and the Neutronics Analyses on the LHD Neutron Flux Monitors for the Deuterium Plasma Experiment
Fusion Engineering and Design 136 PartA 210-214

101 Nishitani T., Ogawa K., Pu N., Kawase H., Murakami S., Isobe M., Osakabe M., The LHD Experimental Group.
Fast ion confinement study by neutron emission rate measurement after short pulse NB injection in the Large Helical Device
Plasma and Fusion Research 13 Special Issue 2 3402024

102 Nuga H., Seki R., Kamio S., Ogawa K., Isobe M., Osakabe M., Yokoyama M.
Analysis of beam slowing-down process in large helical device based on Fokker-Planck operator including beam-beam Coulomb collision effect
Nuclear Fusion 59 1 16007

103 Nunami M., Nakata M., Toda S., Ishizawa A., Kanno R., Sugama H.
Simulation studies on temperature profile stiffness in ITG turbulent transport of helical plasmas for flux-matching technique
Physics of Plasmas 25 8 82504

104 Obana T., Takahata K., Hamaguchi S., Chikaraishi H., Imagawa S., Mito T., Murakami H., Natsume K., Kizu K.
Effect of electromagnetic force on a quad-pancake coil wound with a Nb3Sn CIC conductor
Journal of Physics: Conference Series 1054 12067

105 Obana T., Takahata K., Hamaguchi S., Chikaraishi H., Takada S., Iwamoto A., Imagawa S., Mito T., Murakami H., Natsume K., Kizu K.
Investigation of long time constants of magnetic fields generated by the JT-60SA CS1 module
Fusion Engineering and Design 137 274-282

106 Ogawa K., Isobe M., Kawase H., Nishitani T., LHD Experiment Group.
Neutron Flux Measurement Using a Fast-Neutron Scintillation Detector with High Temporal Resolution on the Large Helical Device
Plasma and Fusion Research 13 Special Issue 2 3402068

107 Ogawa K., Isobe M., Kawase H., Nishitani T., Seki R., Osakabe M., LHD Experiment Group.
Observation of Enhanced Radial Transport of Energetic Ion due to Energetic Particle Mode Destabilized by Helically-trapped Energetic Ion in the Large Helical Device
Nuclear Fusion 58 4 44001

108 Ogawa K., Isobe M., Kawase H., Nishitani T., Seki R., Osakabe M., LHD Experiment Group.
Effect of the helically-trapped energetic-ion-driven resistive interchange modes on energetic ion confinement in the Large Helical Device
Plasma Physics and Controlled Fusion 60 4 44005

109 Ogawa K., Isobe M., Nishitani T., Kobuchi T., LHD Experiment Group.
The large helical device vertical neutron camera operating in the MHz counting rate range
Review of Scientific Instruments 89 113509 113509

110 Ogawa K., Isobe M., Nishitani T., Murakami S., Seki R., Nuga H., Pu N., Osakabe M.

Study of first orbit losses of 1 MeV tritons using the Lorentz orbit code in the LHD
Plasma Science and Technology 21 2 25102

111 Ogawa K., Isobe M., Nishitani T., Seki R., Nuga H., Murakami S., Nakata M., Kawase H., Pu N., Osakabe M., Jo J., Cheon M., Kim J., Zhong G., Xiao M., Hu L.

Time dependent neutron emission rate analysis for neutral-beam-heated deuterium plasmas in a helical system and tokamaks
Plasma Physics and Controlled Fusion 60 9 95010

112 Ogawa K., Isobe M., Nishitani T., Takada E., Kawase H., Amitani T., Pu N., Jo J., Cheon M., Kim J., Miwa M., Matsuyama S., Murata I.

High detection efficiency scintillating fiber detector for time-resolved measurement of triton burnup 14 MeV neutron in deuterium plasma experiment
Review of Scientific Instruments 89 10 10I101

113 Oishi T., Morita S., Huang X., Liu Y., Goto M.

Response of plasmas to tungsten pellet injection in neutral beam heated discharges in Large Helical Device
Plasma and Fusion Research 13 Special Issue 2 3402031

114 Osakabe M., Isobe M., Tanaka M., Motojima G., Tsumori K., Yokoyama M., Morisaki T., Takeiri Y.

Preparation and commissioning for the LHD deuterium experiment
IEEE Transactions on Plasma Science 46 6 2324–2331

115 Pei Y., Xiang N., Shen W., Hu Y., Todo Y., Zhou D., Huang J.

Simulations of toroidal Alfven eigenmode excited by fast ions on the Experimental Advanced Superconducting Tokamak
Physics of Plasmas 25 5 52503

116 Peterson B., Oh S., Seo D., Jang J., Park J., Mukai K., Choe W.

Signal to noise ratio of upgraded imaging bolometer for KSTAR
Review of Scientific Instruments 89 10E115

117 Pinon J., Todo Y., Wang H.

Effects of fast ions on interchange modes in the Large Helical Device plasmas
Plasma Physics and Controlled Fusion 60 7 75007

118 Pu N., Nishitani T., Ogawa K., Isobe M.

Scintillating fiber detectors for time evolution measurement of the triton burnup on the Large Helical Device
Review of Scientific Instruments 89 10 10I105

119 Pu N., Nishitani T., Ogawa K., Isobe M., Murakami S., LHD Experiment Group.

Initial results of triton burnup study in the Large Helical Device
Plasma and Fusion Research 13 Special Issue 2 3402121

120 Pucci F., Usami S., Ji H., Guo X., Horiuchi R., Okamura S., Fox W., Jara-almonte J., Yamada M., Yoo J.

Energy transfer and electron energization in collisionless magnetic reconnection for different guide-field intensities
Physics of Plasmas 25 12 122111

121 Purohit G., Kato D., Murakami I.

Electron impact ionization cross sections of tungsten atoms and tungsten ions
Plasma and Fusion Research 13 Special Issue 2 3401026

122 Purohit S., Suzuki Y., Ohdachi S., Yamamoto S.

Improved design for Heliotron J Soft X-ray diagnostic for tomographic reconstruction studies
Review of Scientific Instruments 89 10 10G102

123 Putra A., Tachibana Y., Tanaka M., Suzuki T.

Lithium isotope separation using displacement chromatography by cation exchange resin with high degree of cross-linkage
Fusion Engineering and Design 136 PartA 377-380

124 Roidl B., Todo Y., Takase Y., Tsujii N., Ejiri A., Yoshida Y., Yajima S., Shinya T.

A simulation environment to simulate lower-hybrid-wave-driven plasmas efficiently
Computer Physics Communications 230 38-49

125 Saito K., Igami H., Toida M., Akiyama T., Kamio S., Seki R., LHD experiment group.

RF wave detection with high-frequency magnetic probes in LHD
Plasma and Fusion Research 13 Special Issue 2 3402043

126 Sakagami H.

Electromagnetic Particle Code Simulations to Analyze Formation Mechanisms of Laser Induced Periodic Nano-structures
Japan Laser Processing Society 25 2 8-14

127 Sakata S., Lee S., Morita H., Johzaki T., Sawada H., Iwasa Y., Matsuo K., Law K., Yao A., Hata M., Sunahara A., Kojima S., Abe Y., Kishimoto H., Syuhada A., Shiroto T., Morace A., Yogo A., Iwata N., Nakai M., Sakagami H., Ozaki T., Yamanoi K., Norimatsu T., Nakata Y., Tokita S., Miyanaga N., Kawanaka J., Shiraga H., Mima K., Nishimura H., Bailly-grandvaux M., Santos J., Nagatomo H., Azechi H., Kodama R., Arikawa Y., Sentoku Y., Fujioka S.

Magnetized fast isochoric laser heating for efficient creation of ultra-high-energy-density states
Nature Communications 9 3937

128 Sasaki M., Itoh K., Ido T., Shimizu A., Kobayashi T., Arakawa H., Kasuya N., Fujisawa A., Itoh S.

Evaluation of Measurement Signal of Heavy Ion Beam Probe of Energetic-Particle Driven Geodesic Acoustic Modes
Plasma and Fusion Research 13 Special Issue 2 13, 3403040

129 Sasaki M., Itoh K., Kobayashi T., Kasuya N., Fujisawa A., Itoh S.

Propagation direction of geodesic acoustic modes driven by drift wave turbulence
Nuclear Fusion 58 11 58-11, 112005

130 Sasao M., Roba M., Dmitry K., James E., Gilles C., Wada M., Tsumori K., Hosono H.

Negative-hydrogen-ion production from a nanoporous 12CaO·7Al2O3 electride surface
Applied Physics Express 11 6 66201

131 Saze T., Miyake H., Sakama M.

Verification of the Thermal Neutron Shielding Effect of the Shielding Door of the LHD Experimental Hall
Plasma and Fusion Research 13 Regular Issue 1205101

132 Seguineaud G., Motojima G., Narushima Y., Goto M.

Spatially-Resolved Electron Density Measurement in Hydrogen Pellet Ablation Cloud
Atoms 6 2 34

133 Sharov I., Sergeev V., Miroshnikov I., Kuteev B., Tamura N., Sudo S.

Electron Temperature Distribution Measurements in Clouds of Polystyrene Pellets Ablating in LHD Heliotron Plasma
Technical physics letters 44 5 384-387

134 Shimizu A., Fujisawa A., Ohshima S., Nakano H., Minami T., Isobe M., Okamura S., Matsuoka K.

Density profile measurement with a heavy ion beam probe in a toroidal plasma of the compact helical system
Review of Scientific Instruments 89 11 89-11, 113507

135 Shimizu A., Liu H., Isobe M., Okamura S., Nishimura S., Suzuki C., Xu Y., Zhang X., Liu B., Huang J., Wang X., Liu H., Tang C.

Configuration property of the Chinese First Quasi-Axisymmetric Stellarator
Plasma and Fusion Research 13 3403123

136 Shimozuma T., Kobayashi S., Ito S., Ito Y., Okada K., Yoshimura Y., Igami H., Takahashi H., Tsujimura T., Mizuno Y., Kubo S.

Analysis Technique of Millimeter-Wave Propagating Modes in an Oversized Corrugated Waveguide Using Developed Beam Profile Monitors
Plasma and Fusion Research 13 Special Issue 2 3405036-1-4

137 Shoji M., Kawamura G., Masuzaki S., Morisaki T., LHD experiment group.

Impurity transport simulation in the peripheral plasma in the Large Helical Device with tungsten closed helical divertor
Nuclear Materials and Energy 17 188-193

138 Sugama H., Nunami M., Satake S., Watanabe T.

Eulerian variational formulations and momentum conservation laws for kinetic plasma systems
Physics of Plasmas 25 10 102506

139 Suzuki C., Koike F., Murakami I., Tamura N., Sudo S.

Systematic observation of EUV spectra from highly charged lanthanide ions in the Large Helical Device
Atoms 6 2 24

140 Tachibana Y., Putra A., Hashimoto S., Suzuki T., Tanaka M.

Lithium Isotope Fractionation in Weak Basic Solution Using Cation Exchange Chromatography
Journal of Ion Exchange 29 3 41-47

141 Takahashi H., Nagaoka K., Mukai K., Yokoyama M., Murakami S., Ohdachi S., Bando T., Narushima Y., Nakano H., Osakabe M., Ida K., Yoshinuma M., Seki R., Yamaguchi H., Tanaka K., Nakata M., Warmer F., Oishi T., Goto M., Morita S., Tsujimura T., Kubo S., Kobayashi T., Yamada I., Suzuki C., Emoto M., Ido T., Shimizu A., Tokuzawa T., Nagasaki K., Morisaki T., Takeiri Y.

Realization of high T_i plasmas and confinement characteristics of ITB plasmas in the LHD deuterium experiments
Nuclear Fusion 58 10 106028

142 Takahata K., Moriuchi S., Ooba K., Takami S., Iwamoto A., Mito T., Imagawa S.

Lessons learned from twenty-year operation of the Large Helical Device poloidal coils made from cable-in-conduit conductors
Cryogenics 91 1-6

143 Takeiri Y.

Advanced Helical Plasma Research towards a Steady-State Fusion Reactor by Deuterium Experiments in Large Helical Device
Atoms 6 4 69

144 Takeiri Y.

The Large Helical Device: Entering Deuterium Experiment Phase Toward Steady-State Helical Fusion Reactor Based on Achievements in Hydrogen Experiment Phase
IEEE Transactions on Plasma Science 46 7 1-6

145 Takeiri Y.

Prospect Toward Steady-State Helical Fusion Reactor Based on Progress of LHD Project Entering the Deuterium Experiment Phase
IEEE Transactions on Plasma Science 46 5 1141–1148

146 Takemura Y., Watanabe K., Sakakibara S., Ohdachi S., Suzuki Y., Ida K., Yoshinuma M., Yamada I.

Comparison of Rotation of Interchange Mode in Large Helical Device Plasmas with Various Ion Species
Plasma and Fusion Research 13 Special Issue 2 3402037

147 Takeno H., Ichimura K., Nakamoto S., Nakashima Y., Matsuura H., Miyazawa J., Goto T., Furuyama Y., Taniike A.

Recent Advancement of Research on Plasma Direct Energy Conversion
Plasma and Fusion Research 14 Special Issue 1 2405013

148 Tanaka H., Masuzaki S., Kawamura G., Kobayashi M., Suzuki Y., Motojima G., Murase T., Morisaki T., Ohno N.

Characterized divertor footprint profile modification with the edge pressure gradient in the Large Helical Device
Plasma Physics and Controlled Fusion 60 12 125001

149 Tanaka M.

Control of dehumidification using polymer permeable membrane and its application to tritium removal system design
Fusion Engineering and Design 136 PartA 141-145

150 Tanaka M., Kato H., Suzuki N., Iwata C., Akata N.

Determination of tritium activity and chemical forms in the exhaust gas from a large fusion test device
Journal of Radioanalytical and Nuclear Chemistry 318 Issue2 877-885

151 Tanaka M., Yamamoto Y., Iwata C., Akata N.

Monitoring of Tritium Concentration by Simplified Active Sampler in a Fusion Test Facility
Plasma and Fusion Research 13 Special Issue 2 3405038

152 Terasaka K., Yoshimura S., Tanaka M.

Observation of high-temperature bubbles in an ECR plasma
Physics of Plasmas 25 5 52113

153 Toda S., Nakata M., Nunami M., Ishizawa A., Watanabe T., Sugama H.

Modeling of turbulent particle and heat transport in helical plasmas based on gyrokinetic analysis
Physics of Plasmas 26 1 12510

154 Todo Y.

Introduction to the interaction between energetic particles and Alfven eigenmodes in toroidal plasmas
Reviews of Modern Plasma Physics 3 1 (33 pages)

155 Toida M., Saito K., Igami H., Akiyama T., Kamio S., Seki R.

Simulation study of high-frequency magnetosonic waves excited by energetic ions in association with ion cyclotron emission
Plasma and Fusion Research 13 Special Issue 2 3403015

156 Tokitani M.

Commentary:Development of the Divertor Heat Removal Component with W and ODS-Cu by the Advanced Brazing Technique
Journal of Plasma and Fusion Research 94 8 385-393

157 Tokitani M., Masuzaki S., Murase T., LHD experiment group.

Demonstration of suppression of dust generation and partial reduction of the hydrogen retention by tungsten coated graphite divertor tiles in LHD
Nuclear Materials and Energy 18 23-28

158 Tokitani M., Miyamoto M., Masuzaki S., Sakamoto R., Oya Y., Hatano Y., Otsuka T., Oyaidzu M., Kurotaki H., Suzuki T., Hamaguchi D., Isobe K., Asakura N., Widdowson A., Heinola K., Rubel M.

Plasma-Wall Interaction on the Divertor Tiles of JET ITER-Like Wall from the Viewpoint of Micro/Nanoscopic Observations
Fusion Engineering and Design 136 PartA 199-204

159 Tokuzawa T., Tsuchiya H., Tsujimura T., Emoto M., Nakanishi H., Inagaki S., Ida K., Yamada H., Ejiri A., Watanabe K., Oguri K., Akiyama T., Tanaka K., Yamada I., LHD Experiment Group.

Microwave frequency comb Doppler reflectometer applying fast digital data acquisition system in LHD
Review of Scientific Instruments 89 10 10H118

160 Tsuchiya H., Iwama N., Yamaguchi S., Takenaka R., Koga M.

Feasibility Study of Holography using Reflectometry Microwave
Plasma and Fusion Research

161 Tsuchiya H., Kuwahara D., Tokuzawa T., Nagayama Y., Takemura Y., LHD Experiment Group.

Installation of New Electron Cyclotron Emission Imaging in LHD
Plasma and Fusion Research 13 Special Issue 2 3402063

162 Tsujimura T.

Front Runner:Optimization of incident electron cyclotron wave polarization in the LHD
Journal of Plasma and Fusion Research 95 3 139-144

163 Tsujimura T., Mizuno Y., Tokuzawa T., Ito Y., Kubo S., Shimozuma T., Yoshimura Y., Igami H., Takahashi H., Ejiri A.

Real-time control of electron cyclotron wave polarization in the LHD
Fusion Engineering and Design 131 130-134

164 Ueda Y., Omori K., Ibano K., Ito A.

Special Topic Articles: Fuzzy Nano-Structures on Metal Surfaces Induced by Exposure to Helium Plasma 7. Formation of He Induced Nano-Structure of Period 6 & 5 Transition Metals Research
Journal of Plasma and Fusion Research 94 6 320-324

165 Usami S., Horiuchi R., Ohtani H., Den M.

Improvement of the Multi-Hierarchy Simulation Model Based on the Real-Space Decomposition Method
Plasma 1 1 9

166 Usami S., Horiuchi R., Ohtani H., Ono Y., Tanabe H.

Effective proton heating through collisionless driven reconnection in the presence of guide field
Plasma and Fusion Research 13 Special Issue 2 3401025

167 Wang H., Todo Y., Ido T., Suzuki Y.

Chirping and Sudden Excitation of Energetic-Particle-Driven Geodesic Acoustic Modes in a Large Helical Device Experiment
Physical Review Letters 120 17 175001

168 Watanabe T., Sagara A., Yagi J., Tsujimura T., Yamazaki G., Kumagai K., Tanaka T.

Hydrogen recovery from metal particle dispersed salt by selective microwave heating
Fusion Engineering and Design 136 PartB 1396-1399

169 Yamagishi O.

Non-isomorphic radial wavenumber dependencies of residual zonal flows in ion and electron Larmor radius scales, and effects of initial parallel flow and electromagnetic potentials in a circular tokamak
Plasma Physics and Controlled Fusion 60 4 45009

170 Yamanaka K., Nakanishi H., Ozeki T., Nakajima N., Farthing J., Manduchi G., Robin F., Abe S., Urushidani S.

High-Performance Data Transfer for Full Data Replication between ITER and the Remote Experimentation Centre
Fusion Engineering and Design 138 202-209

171 Yamasaki K., Ida K., Yoshinuma M., Kobayashi T.

Observation of the spatial profile of deuterium/hydrogen ratio using bulk charge exchange emission
Plasma and Fusion Research 13 Regular Issue 1202103

172 Yamazaki G., Yagi J., Tanaka T., Watanabe T., Sagara A.

Sacrificial effect of titanium powder on the corrosion by hydrogen fluoride in LiF-NaF-KF
Fusion Engineering and Design 136 PartA 394-397

173 Yamazaki G., Yagi J., Tanaka T., Watanabe T., Sagara A.

Corrosion mitigation of ferritic steels in HF-containing FLiNaK by titanium sacrificial anodes
Plasma and Fusion Research 13 Special Issue 2 3405079

174 Yanagi N., Goto T., Miyazawa J., Tamura H., Terazaki Y., Ito S., Tanaka T., Hashizume H., Sagara A.

Progress in the Conceptual Design of the Helical Fusion Reactor FFHR-d1
Journal of Fusion Energy 38 1 147-161

175 Yanagihara K., Kubo S., Tsujimura T.

Numerical description of mode coupled waves in inhomogeneous magnetized plasmas
EPJ Web of Conferences 203 1011

176 Yasuhara R.

Progress of the transparent magneto-optic ceramics
Photonics 4 1

177 Yoshimura Y., Ejiri A., Seki R., Sakamoto R., Nagaoka K., Shimozuma T., Igami H., Takahashi H., Tsujimura T., Warmer F., Yanagihara K., Goto Y., Ida K., Yoshinuma M., Kobayashi T., Kubo S., Osakabe M., Morisaki T.

Effect of Electron Cyclotron Current Drive on the Ion Temperature in the Plasma Core Region of the Large Helical Device
Plasma and Fusion Research 13 Regular Issue 1402124

※ This list was compiled as of March 31, 2019

National Institute for Fusion Science

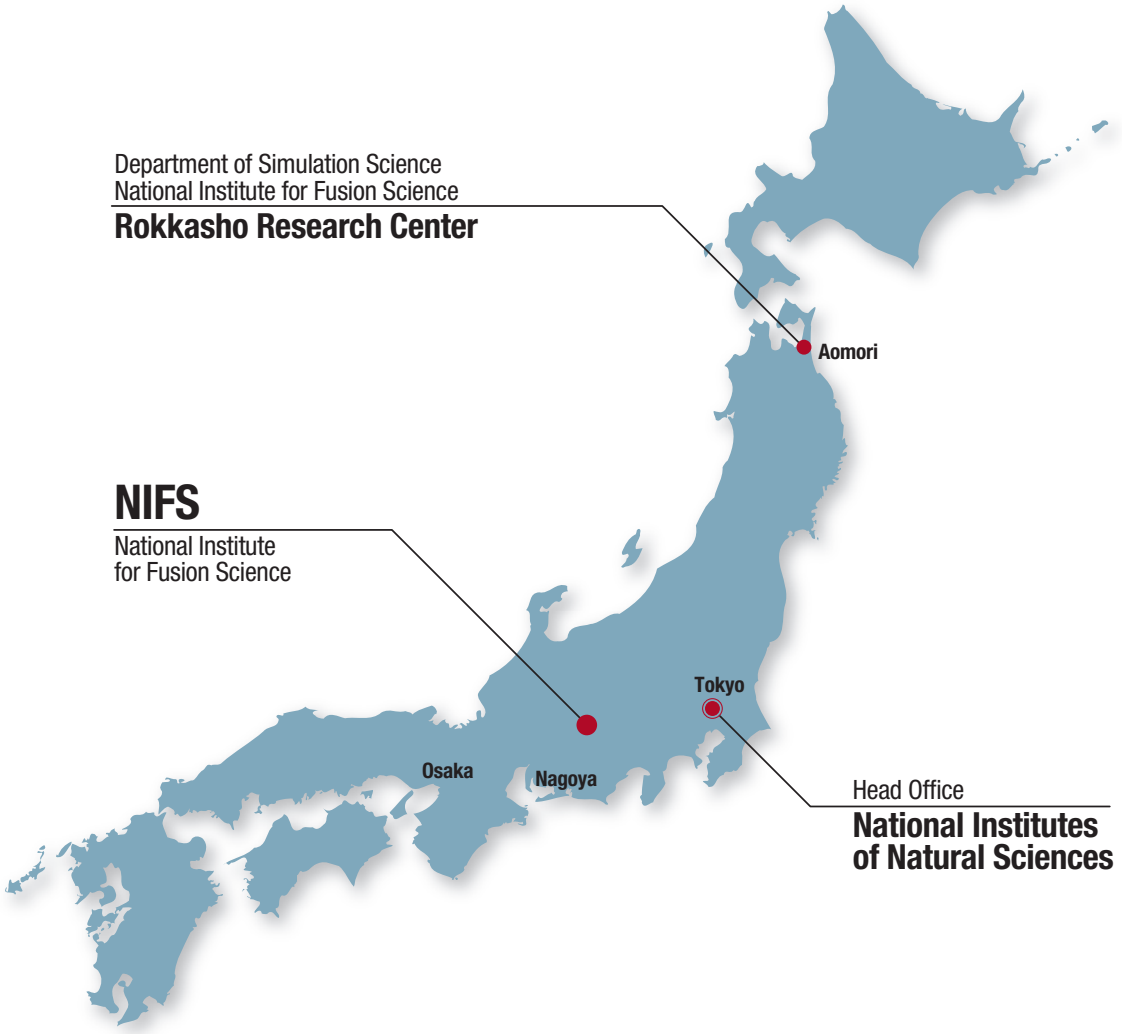

National Institute for Fusion Science
National Institutes of Natural Sciences
(TOKI Area)

322-6 Oroshi-cho
Toki-city, GIFU
509-5292

TEL: 0572-58-2222 FAX: 0572-58-2601

Rokkasho Research Center
Department of Helical Plasma Research
Located in the Aomori Research and Development Center
Japan Atomic Energy Agency

2-166 Oaza-Obuchi-Aza-Omotedate,
Rokkasho-mura, Kamikita-gun,
AOMORI
039-3212

TEL/FAX: 0175-73-2151

How to Reach National Institute for Fusion Science

☐ACCESS

When you use the public transportation facility

◇from Centrair (Central Japan International Airport)

Centrair – (μ-sky) – Meitetsu Kanayama Sta. (36km)
about 25min

JR Kanayama Sta. – (JR Chuo Line) – JR Tajimi Sta. (33km)
about 33min (express)

JR Tajimi Sta. – (Totetsu Bus) – Kenkyuugakuentoshi (7km)
about 15min

◇from JR Nagoya Sta.

JR Nagoya Sta. – (JR Chuo Line) – JR Tajimi Sta. (36km)
about 22min (limited express) / about 30min (lapid) / about 40min (local)

JR Tajimi Sta. – (Totetsu Bus) – Kenkyuugakuentoshi (7km)
about 15min

◇from Nagoya Airport

(Obihiro•Akita•Yamagata•Niigata•Kouchi• Matsuyama•Fukuoka•Kumamoto•Nagasaki)

Nagoya Airport – (Taxi) – JR Kachigawa Sta. (4km)
about 10min

Nagoya Airport – (Meitetsu Bus) – JR Kachigawa Sta. (4km)
about 19min

JR Kachigawa Sta. – (JR Chuo Line) – JR Tajimi Sta. (21km)
about 20min

JR Tajimi Sta. – (Totetsu Bus) – Kenkyuugakuentoshi (7km)
about 15min

When you use a car

from Chuo Expressway Toki I.C. or Tajimi I.C. (8km)
about 20min

from Tokai-Kanjo Expressway Tokiminami Tajimi I.C. (2km)
about 5min

How to Reach Rokkasho Research Center

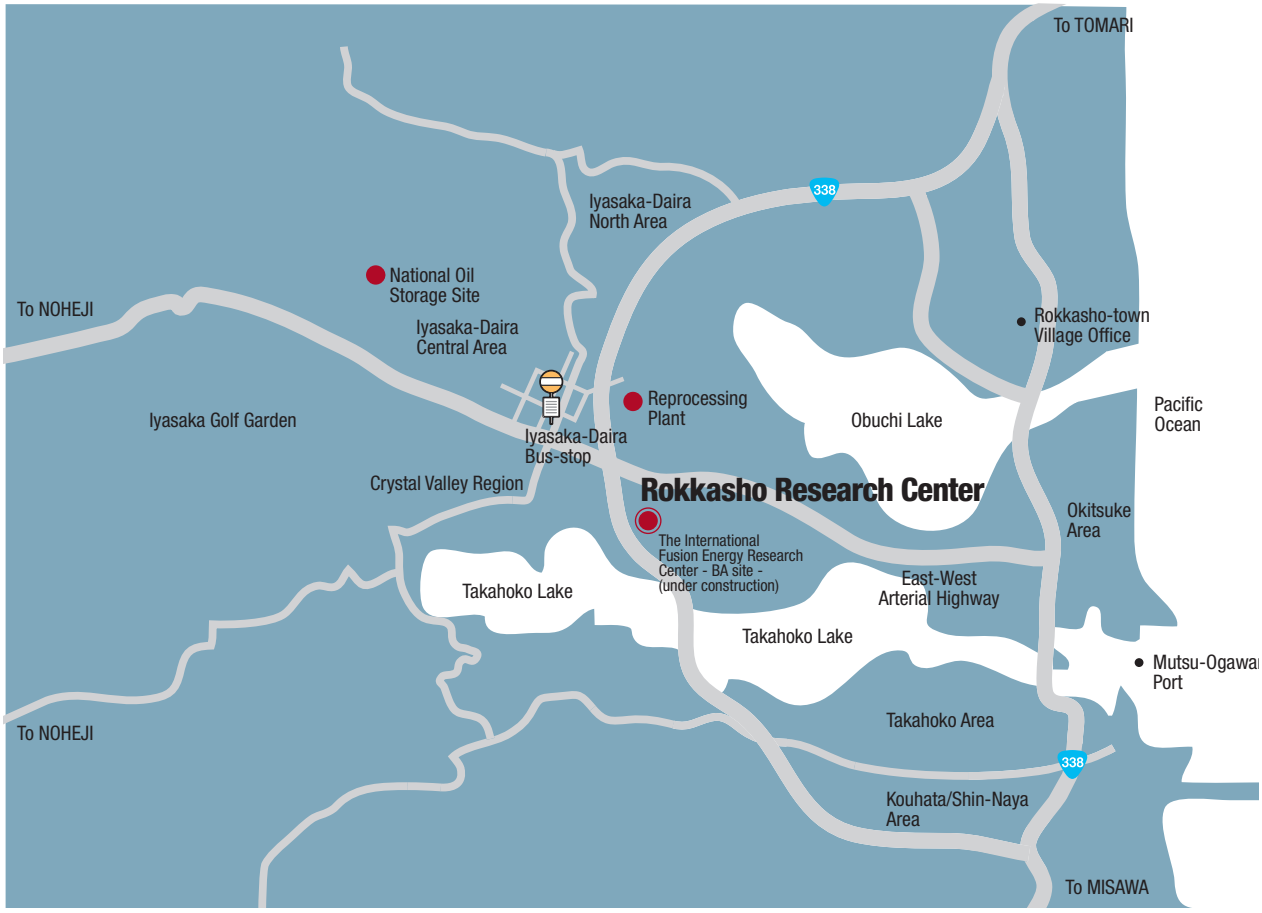

□ACCESS

When you use the public transportation facility

◇from Tokyo

Tokyo – (Tohoku-Shinkansen) – Hachinohe Sta. (630km)
about 3hr

Hachinohe Sta. – (JR Tohoku Limited Express) – Noheji (51km)
about 30min

Noheji – (Shimokita Koutsu Bus) – Iyasaka-Daira (10km)
about 40min

Iyasaka-Daira .....on foot..... Rokkasho Research Center (0.7km)
about 8min

◇from Misawa Airport

Misawa Airport – (Bus) – Misawa (2km)
about 13min

Misawa – (JR Tohoku Limited Express) – Noheji (30km)
about 20min

Noheji – (Shimokita Koutsu Bus) – Iyasaka-Daira (10km)
about 40min

Iyasaka-Daira .....on foot..... Rokkasho Research Center (0.7km)
about 8min

◇from Aomori Airport

Aomori Airport – (Bus) – Aomori (12km)
about 40min

Aomori – (JR Tohoku Limited Express) – Noheji (45km)
about 30min

Noheji – (Shimokita Koutsu Bus) – Iyasaka-Daira (10km)
about 40min

Iyasaka-Daira .....on foot..... Rokkasho Research Center (0.7km)
about 8min

National Institute for Fusion Science

Building Arrangement

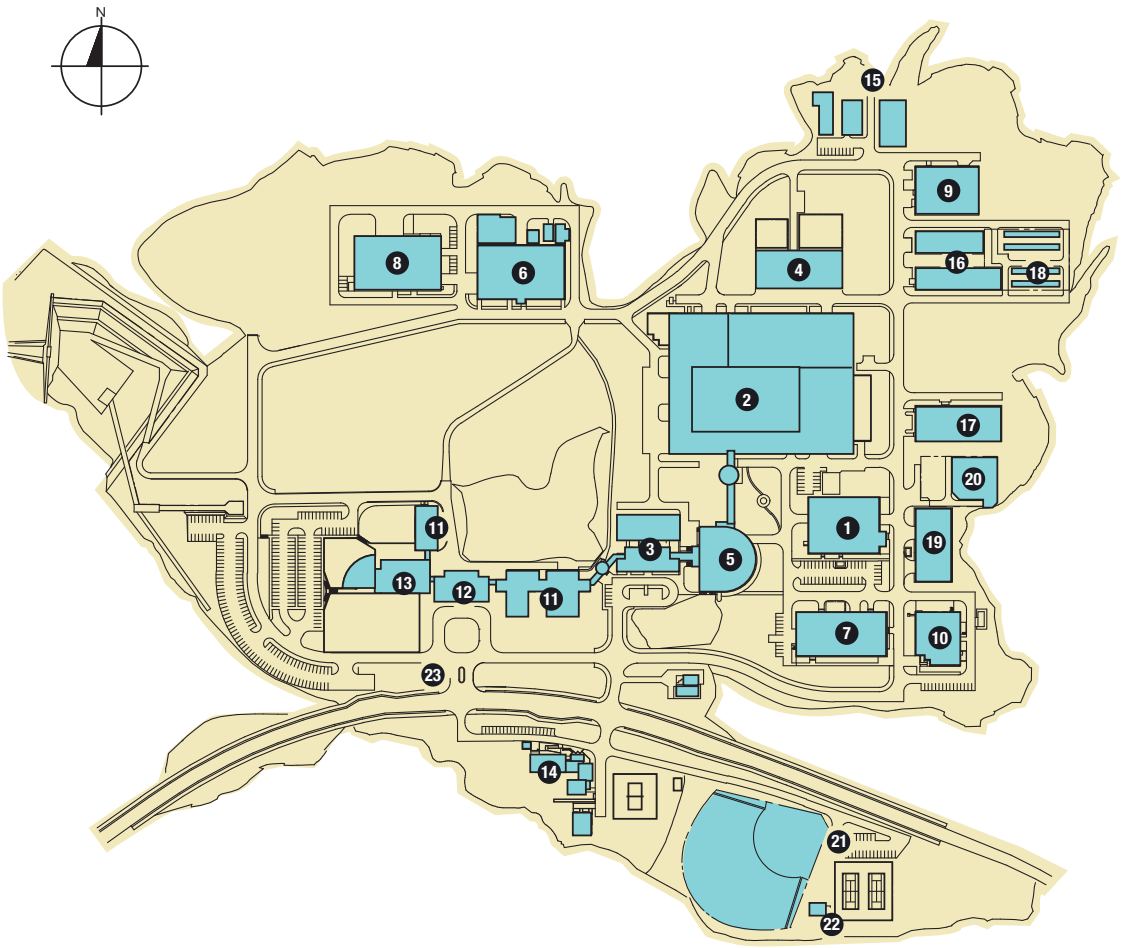

NIFS plot plan

1. Superconducting Magnet System Laboratory
2. Large Helical Device Building
3. Simulation Science Research Laboratory
4. Heating and Power Supply Building
5. LHD Control Building
6. Fusion Engineering Research Laboratory
7. Plasma Diagnostics Laboratories
8. R & D Laboratories
9. Motor-Generator Building
10. Central Workshops
11. Research Staff Building
12. Library Building
13. Administration Building
14. Helicon Club (Guest Housing)
15. High-Voltage Transformer Station
16. Cooling Water Pump Building
17. Helium Compressor Building
18. Cooling Tower
19. Equipments Room
20. Helium Tank Yard
21. Recreation Facilities
22. Club House
23. Guard Office